

ESSENTIALITY AND REGULATION OF DEOXYHYPUSINATION
IN *TRYPANOSOMA BRUCEI*

APPROVED BY SUPERVISORY COMMITTEE

Margaret A. Phillips, PhD

Kim Orth, PhD

Joel M. Goodman, PhD

Jef K. De Brabander, PhD

DEDICATION

I dedicate this work to Justin Sobrino
for all of his love, support, and encouragement
during the course of this work and beyond.

ACKNOWLEDGMENTS

This work would not be possible without the support and guidance of many people. First and foremost, I thank my thesis advisor Meg Phillips for her incredible mentorship over the past five years. She has taught me to be a better scientist in teaching me how to logically approach problems and how to rigorously design and conduct experiments. More than that, she has been an unwavering source of encouragement and motivation in helping me achieve my broader career goals. I also thank my committee members, Kim Orth, Joel Goodman, and Jef De Brabander, for lending their time and expertise to help me overcome the challenges that arose. Next, I thank the members of the Phillips lab, past and present. In particular, Savitha Kalidas and Jessie Xiao taught me everything related to culturing and working with trypanosomes. Xiaoyi Deng very patiently taught me how to express and purify recombinant proteins. Everyone else has been invaluable for discussion, sharing common lab burdens, commiserating over problems, and celebrating the successes. Additionally, I thank the following people at UTSW for providing me with tools beyond our expertise to further my research: Lisa Kinch and Nick Grishin for bioinformatics analyses, Kate Phelps and Abhijit Bugde for fluorescence imaging, Angie Mobley for flow cytometry, and Chad Brautigam for analytical ultracentrifugation. Finally, I thank Carla Childers and Robin Downing for helping me navigate the graduate and MST programs.

ESSENTIALITY AND REGULATION OF DEOXYHYPUSINATION

IN *TRYPANOSOMA BRUCEI*

by

SUONG THU NGUYEN

DISSERTATION

Presented to the Faculty of the Graduate School of Biomedical Sciences

The University of Texas Southwestern Medical Center at Dallas

In Partial Fulfillment of the Requirements

For the Degree of

DOCTOR OF PHILOSOPHY

The University of Texas Southwestern Medical Center at Dallas

Dallas, Texas

April 2014

Copyright

by

Suong Thu Nguyen, 2014

All Rights Reserved

ESSENTIALITY AND REGULATION OF DEOXYHYPUSINATION
IN *TRYPANOSOMA BRUCEI*

Suong Thu Nguyen, PhD

The University of Texas Southwestern Medical Center at Dallas, 2014

Supervising Professor: Margaret A. Phillips, PhD

Human African trypanosomiasis is caused by protozoan parasite *Trypanosoma brucei*. *T. brucei* and other trypanosomatids require spermidine for the formation of trypanothione, a unique thiol-redox factor. In other eukaryotes, spermidine is essential for the (deoxy)hypusination of eukaryotic initiation factor 5A (eIF5A). Hypusination, a post-translational modification, occurs via two enzymatic reactions. First, deoxyhypusine synthase (DHS) transfers the aminobutyl moiety of spermidine onto the eIF5A-lysine generating deoxyhypusine which is then hydroxylated by deoxyhypusine hydroxylase to yield the final

modification, hypusine. Modified eIF5A has been shown to alleviate ribosome stalling on polyproline tracts.

Human and yeast encode two isoforms of eIF5A but only one gene was identified in *T. brucei* (Tb927.11.740). Herein, I show that *TbeIF5A* and its modified lysine are essential for parasite growth by gene knockdown and complementation experiments. I have also identified potential proteins whose translation is regulated by eIF5A using proteomic profiling for proline-rich *T. brucei* proteins. Interestingly, unlike most eukaryotes, trypanosomatids encode two divergent paralogs of DHS (DHSp: Tb927.1.870 and DHSc: Tb927.10.2580), only one of which (DHSc) contains the key catalytic lysine. I showed that both DHS genes are essential for growth of bloodstream-form *T. brucei* using conditional gene knockouts, further establishing the requirement for deoxyhypusine in these parasites. My biochemical characterization of *TbDHS* showed that the two *T. brucei* paralogs form a heterotetrameric complex and that DHSp enhances the activity of recombinant DHSc by 3000-fold.

While the essentiality of eIF5A and DHS is consistent with other eukaryotes, the finding that the functional DHS complex is composed of an impaired catalytic subunit (DHSc) and a catalytically dead paralog (termed a prozyme) is novel. This mechanism reiterates the activation and regulation of S-adenosylmethionine decarboxylase by a catalytically dead paralog (AdoMetDC prozyme) in the trypanosomatids, and remarkably, it has independently evolved for two enzymes within the trypanosomatid spermidine biosynthetic pathway. *T. brucei* seemingly lack several classical eukaryotic transcriptional regulation mechanisms which creates selective pressure to evolve novel strategies to regulate

enzyme function. We postulate that many additional examples of ‘prozymes’ remain to be discovered in the trypanosomatid parasites.

TABLE OF CONTENTS

Summary	vi
Table of Contents	ix
Prior Publications	xi
List of Figures	xii
List of Tables	xiv
List of Appendices	xv
List of Abbreviations	xvi
CHAPTER ONE. Introduction	
I: Human African Trypanosomiasis	1
Pathogenesis of disease	1
Current Therapies	2
Polyamine metabolism in <i>T. brucei</i>	3
A nonpathogenic model for study of <i>T. brucei</i>	4
II: The Hypusination Pathway	5
III: Dissertation Focus	7
CHAPTER TWO. Experimental Methods	
Multiple sequence alignment	10
Generation of transgenic <i>T. brucei</i>	10
Expression of recombinant proteins	15
Other methods for cell and protein characterization	18
CHAPTER THREE. eIF5A is an essential protein in <i>T. brucei</i>	
I: Introduction	25
II: Identification of <i>T. brucei</i> EIF5A	26
III: Spermidine-dependent modification of eIF5A lysine	26
IV: Essentiality of eIF5A	27
V: Discussion	32
CHAPTER FOUR. Exploring the requirement for hypusination	

I: Introduction	48
II: Polyproline tracts in <i>T. brucei</i>	49
III: Discussion	50
CHAPTER FIVE. <i>T. brucei</i> Deoxyhypusine Synthase	
I: Introduction	54
II: Identification of DHS	55
III: Essentiality of DHS paralogs in <i>T. brucei</i>	56
IV: Functional characterization of DHS	59
V: Inhibition of DHS activity	61
VI: Discussion	62
CHAPTER SIX. Identification of potential prozymes	
I: Introduction	77
II: Homologous enzyme pairs	78
III: Discussion	78
CHAPTER SEVEN. Discussion and future directions	
81	
APPENDICES	
Appendix 1. Full sequence alignment of eukaryotic DHS sequences	87
Appendix 2. Cloning primers	92
BIBLIOGRAPHY	94

PRIOR PUBLICATIONS

Pratt, C., **Nguyen, S.**, and Phillips, M.A. (2014) Genetic validation of *Trypanosoma brucei* glutathione synthetase as an essential enzyme. *Eukaryotic Cell*, 7 March 2014. [epub ahead of print]

Xiao, Y., **Nguyen, S.**, Kim, S. H., Volkov, O. A., Tu, B. P., and Phillips, M. A. (2013) Product feedback regulation implicated in translational control of the *Trypanosoma brucei* S-adenosylmethionine decarboxylase regulatory subunit prozyme. *Molecular Microbiology* **88(5)**, 846-61.

Nguyen, S., Jones, D. C., Wyllie, S., Fairlamb, A. H., and Phillips, M. A. (2013) Allosteric activation of trypanosomatid deoxyhypusine synthase by a catalytically dead paralog. *The Journal of Biological Chemistry* **288(21)**, 15256-67.

Oh, J. H., Baum, D. D., Pham, S., Cox, M., **Nguyen, S. T.**, Ensor, J., and Chen, I. (2007) Long-term complications of platinum-based chemotherapy in testicular cancer survivors. *Medical Oncology* **24**, 175-181.

LIST OF FIGURES

FIGURE 1.1. Spermidine and hypusine metabolic pathway in <i>T. brucei</i>	8
FIGURE 1.2. Reaction mechanism of deoxyhypusine synthase	9
FIGURE 2.1. Schematic of generation of cKO cell lines	23
FIGURE 2.2. Schematic of RNAi stem-loop construct.....	24
FIGURE 3.1. ^{14}C -Putrescine labeling of procyclic-form cells	34
FIGURE 3.2. Knockdown of <i>EIF5A</i> in bloodstream-form cells	35
FIGURE 3.3. Cell cycle analysis of BSF <i>EIF5A</i> RNAi cells	36
FIGURE 3.4. Complementation with <i>Hs</i> eIF5A in BSF cells	37
FIGURE 3.5. Overexpression of <i>Hs</i> eIF5A in BSF cells	38
FIGURE 3.6. Complementation with <i>Hs</i> eIF5A ^{K50A} in BSF cells.....	39
FIGURE 3.7. Overexpression of <i>Hs</i> eIF5A ^{K50A} in BSF cells	40
FIGURE 3.8. Knockdown of <i>EIF5A</i> in bloodstream-form cells	41
FIGURE 3.9. Imaging of PF <i>EIF5A</i> RNAi cells	42
FIGURE 3.10. Cell cycle analysis of PF <i>EIF5A</i> RNAi cells.....	43
FIGURE 3.11. Complementation with <i>Hs</i> eIF5A in PF cells.....	44
FIGURE 3.12. Overexpression of <i>Hs</i> eIF5A in PF cells	45
FIGURE 3.13. Complementation with <i>Hs</i> eIF5A ^{K50A} in PF cells	46
FIGURE 3.14. Overexpression of <i>Hs</i> eIF5A ^{K50A} in PF cells.....	47
FIGURE 4.1. Proline composition of <i>T. brucei</i> proteins	52
FIGURE 4.2. Frequency of polyproline tracts in the <i>T. brucei</i> proteome	53
FIGURE 5.1. Reaction scheme for deoxyhypusine synthase	65
FIGURE 5.2. Phylogenetic analysis of DHS genes in eukaryotes	66
FIGURE 5.3. Partial Sequence alignment of DHS from select eukaryotes.....	67
FIGURE 5.4. Knockdown of DHSc	68
FIGURE 5.5. Knockdown of DHSp	69
FIGURE 5.6. Effects of DHSc knockout on growth on and survival.....	70
FIGURE 5.7. Effects of DHSp knockout on growth and survival.....	71

FIGURE 5.8. Biochemical characterization of <i>T. brucei</i> DHS.....	72
FIGURE 5.9. Detection of the enzyme-imine intermediate	73
FIGURE 5.10. Inhibition of DHS and <i>T. brucei</i> growth by GC7	74
FIGURE 6.1. Identification of homologous enzyme pairs	80

LIST OF TABLES

TABLE 5.1. Comparison of specific activity between DHS homo- and heterotetramers	68
TABLE 5.2. Steady-State kinetic parameters of <i>T. brucei</i> heterotetrameric DHS	69

LIST OF APPENDICES

APPENDIX 1. Full sequence alignment of eukaryotic DHS.	86
APPENDIX 2. Cloning primers.....	91

LIST OF ABBREVIATIONS (in alphabetical order)

AdoMetDC.....	S-adenosylmethionine decarboxylase
β-ME	beta-mercaptoethanol
BSF	bloodstream-form
cKO	conditional knockout
CP	cysteine peptidase
d	days
DHS	deoxyhypusine synthase
Dox	doxycycline
EF-P	elongation factor P
eIF5A	eukaryotic initiation factor 5A
EP	procyclins
FBS	fetal bovine serum
GC7	N1-guanyl-1,7-diaminoheptane
h	hours
<i>H.s.</i>	<i>Homo sapiens</i>
HAT	human African Trypanosomiasis
IV	intravenous
LB	Luria broth
min	minutes
mg	milligrams
ml	milliliters
ODC	ornithine decarboxylase
PAGE	polyacrylamide gel electrophoresis
PBS	phosphate buffered saline
PVDF	polyvinylidene fluoride
PF	procyclic-form
PI	propidium iodide
s	seconds
SDS	sodium dodecyl sulfate
SM	single marker
SUMO	small ubiquitin-like modifier
<i>T.b.</i>	<i>Trypanosoma brucei</i>
TBS	tris buffered saline
Tet	tetracycline
VSG	variant surface glycoprotein
μg	micrograms
μL	microliters

CHAPTER ONE

Introduction

I. HUMAN AFRICAN TRYPANOSOMIASIS

Pathogenesis of Disease

Human African trypanosomiasis (HAT) is caused by the protozoan parasite *Trypanosoma brucei*. Infections are perpetuated in a cycle between the tsetse fly vector and the human host. Domestic and wild animals can also serve as a reservoir for the parasite (1). Infection starts when parasite-carrying tsetse flies inoculate the parasites into the human bloodstream during a blood meal. The parasites then differentiate into bloodstream trypomastigotes and continue proliferating, inciting the host immune system and eventually crossing the blood brain barrier to lead to the descriptive symptoms of sleeping sickness. A naive tsetse fly can ingest parasites from the infected host during a blood meal as well. The parasites move to the fly midgut where they replicate as the procyclic-form before migrating to the salivary glands, poised to infect the next victim.

The distribution of the disease is limited to the habitat of the tsetse fly and as such, the disease is endemic to sub-Saharan Africa. In central and western sub-Saharan Africa, the subspecies *T.b. gambiense* is the predominant cause of HAT, and the disease is typically slow-progressing and chronic, lasting for years. It is estimated gambiense HAT causes over 95% of current cases (2). In eastern and southern Africa, *T.b. rhodesiense* is the predominant cause of HAT, and the disease progresses more rapidly. Invasion of the central nervous

system, which marks late stage disease, occurs in weeks to months from initial rhodesiense HAT infection. In both subtypes of HAT, infections are fatal in more than 99% of cases if untreated (3). Distribution of the two subtypes, interestingly, does not overlap although there is the potential for overlap to occur in the near future in parts of Uganda (4). Approximately 60 million people are at risk of contracting gambiense HAT and 12 million people are at risk for contracting rhodesiense HAT (5) (6). There are many challenges to preventing and controlling HAT, and current strategies focus on vector control using tsetse fly traps and insecticides and on early detection since the treatment of late stage disease is difficult.

Current Therapies

Treatment of HAT depends on the causative subspecies and staging of the disease. Early stage disease is marked by hemolymphatic infection that manifests as fever, lymphadenopathy, and pruritus (7). Early stage gambiense HAT is treated with intramuscular pentamidine, while early stage rhodesiense HAT is treated with intravenous (IV) suramin (8). However, due to the mild nature of early stage disease, it is thought that patients are not likely to seek out diagnosis and treatment until infections progress to the acute meningoencephalitic (late) stage which is more difficult to treat. The WHO recommends that all patients diagnosed with HAT undergo a lumbar puncture to examine if parasites are in the cerebral spinal fluid, marking late stage disease. A long course of IV melarsoprol, a highly toxic arsenical with a 5% mortality rate, is effective for treating late stage HAT caused by both *T. brucei* subspecies. Since 2009 late stage disease caused by gambiense HAT can also be treated with a combination of IV eflornithine and oral nifurtimox (NECT) which has

lower toxicity than melarsoprol (9). However both melarsoprol and NECT treatments still require at least 10 days of IV infusions that are inconvenient to deliver in rural endemic regions. These challenges coupled with increasing drug resistance create a need for new drugs and treatment strategies.

Polyamine metabolism in T. brucei

Eflornithine (difluoromethylornithine) is a suicide inhibitor of the polyamine biosynthetic enzyme ornithine decarboxylase (ODC) (Figure 1.1), which in combination with nifurtimox, is a front line treatment for HAT, demonstrating the importance of polyamine function for parasite growth (2). The cationic polyamines (putrescine and spermidine) are essential for growth of most eukaryotic cells and have been explored as potential targets for the treatment of both infectious disease and cancer (2,3). Spermidine has been implicated in the regulation of translation and transcription, modulation of chromatin structure and ion channel function (4,5). Uniquely in trypanosomatids, spermidine is used in the synthesis of trypanothione (N1,N8-bis(glutathionyl)spermidine), which is required to maintain intracellular thiol-redox balance (6,7).

Biosynthesis and metabolism of polyamines is tightly controlled; in mammalian cells, regulation is orchestrated by a complex array of transcriptional, translational and post-translational mechanisms (3,4) that are generally lacking in trypanosomatids. Instead these parasites have evolved a novel mechanism to control activity and expression of a key enzyme required for spermidine biosynthesis, S-adenosylmethionine decarboxylase (AdoMetDC) (2). Previously, Willert et al found that the functional trypanosomatid AdoMetDC was a

heterodimer between a catalytically impaired subunit and a catalytically dead paralog termed prozyme, both of which were essential for cell growth (8,9). Heterodimer formation between AdoMetDC and the AdoMetDC prozyme led to a 1200-fold activation of AdoMetDC activity. Furthermore, the AdoMetDC prozyme protein levels appeared to be translationally regulated, suggesting *T. brucei* modulates prozyme expression to control AdoMetDC activity and flux through the polyamine pathway (9).

A nonpathogenic model for study of T. brucei biology

The common model used to study trypanosome biology is the nonpathogenic *T.b. brucei* that infects animals. The commonly used lab strain *Tbb* Lister 427 was originally isolated in Uganda from infected sheep blood, and both the insect stage (procyclic) and mammalian blood stage (bloodstream-form) can be cultured continuously in serum-supplemented media (10,11). The genome of *Tbb* TREU 927 was fully sequenced in 2005 (12). Unlike the human pathogenic subspecies, *T.b. brucei* forms are sensitive to trypanosome lytic factor, a component of human ApoL1 that neutralizes the parasite. Furthermore, unlike the other pathogenic trypanosomatids such as *T. cruzi* and *Leishmania* spp, the bloodstream-form of *T. brucei* is an extracellular parasite and *in vitro* cultures do not require co-culturing of host cells.

The molecular tools available to study gene essentiality in *T. brucei* also contribute to their utility as a model organism. RNA interference (RNAi) was first described in *T. brucei* in 1998 when Ngo et al. were able to induce degradation of α -tubulin mRNA using dsRNA (13). Since then, RNAi has become an invaluable tool for determining and studying gene

essentiality in *T. brucei*. The parasites express both dicer and argonaute proteins, and systems have been established for generating inducible stable RNAi cell lines in both the bloodstream-form and the procyclic-form (14,15). Multiple methods for generating knockouts by allelic replacement have also been described, including the introduction of tetracycline-regulatable ectopic expression constructs for essential genes (16,17).

II. THE HYPUSINATION PATHWAY

Spermidine is essential for growth of most eukaryotic cells and has been shown to bind DNA/RNA and interact with membrane phospholipids (18-20). Perhaps its most specialized yet essential function in eukaryotic cells is to serve as a precursor for the post-translational hypusine modification of eukaryotic initiation factor 5A (eIF5A) (21). Initiation factor 5A is a highly conserved protein in archaea and eukaryotes. Archaeal and eukaryotic IF5A have both been shown to undergo addition of the 4-aminobutyl moiety from spermidine to a specific protein lysine, a process termed deoxyhypusination catalyzed by deoxyhypusine synthase (DHS) (Figure 1.2) (22). In some eukaryotes, deoxyhypusine is further hydroxylated by deoxyhypusine hydroxylase to generate hypusine. Bacteria do not have IF5A but they do encode a homolog, elongation factor P (EF-P) (23). EF-P undergoes a different post-translational modification. A lysyl-tRNA synthetase paralog modifies an EF-P lysine with R- β -lysine which can also undergo hydroxylation to form EF-P-lysyl-lysine.

The apparent universal conservation of eIF5A suggests that it has a fundamentally important role in translation. Knockout of eIF5A-1 is embryonic lethal in mice (24). In *Saccharomyces cerevisiae*, eIF5A is essential for cell growth and a lysine to arginine mutant

resistant to hypusination was unable to substitute for the wild-type gene (25). The importance of the deoxyhypusine/hypusine modification is reinforced by the observation that under limiting spermidine conditions in *S. cerevisiae*, a larger percentage of the spermidine pool is used to modify eIF5A (26). Until recently, little was known about the function of eIF5A and hypusination. It had been shown in yeast that eIF5A associates with translating ribosomes in a hypusine-dependent manner and under stress conditions, promotes stress granule assembly (27,28). In 2012, multiple groups reported that eIF5A depletion also led to a decrease in protein synthesis that affected a large subset of but not all proteins (27,29,30).

In 2013, new insights into the function of the bacterial homolog EF-P paved the way for understanding of the function of eIF5A. Doerfel et al. reported that EF-P promoted the translation of polyproline tracts (31). Using engineered constructs containing various amino acid triplets with and without consecutive prolines, they demonstrated that *E. coli* ribosomes stalled on PP sequences. EF-P was also able to alleviate stalling in an *in vitro* transcription system specifically when synthesizing PPP and PPG peptides. Furthermore, this effect was dependent on the lysinylation of EF-P lysine-34.

Based on these results, Gutierrez et al. were able to establish an analogous role for eIF5A in eukaryotic cells (32). Using a dual luciferase system, they demonstrated that decreased translation was observed with 3 or more consecutive prolines, but unlike in bacteria, not with two consecutive prolines. Similarly, it was demonstrated that the post-translational modification of eIF5A, particularly deoxyhypusine, was required to alleviate stalling. In *in vitro* assays, the stalling typically occurred on the second or third proline in a

run of polyproline. These insights into eIF5A function explain the previous observations that eIF5A is important for translation of a subset of transcripts (33). It remains to be evaluated which endogenous proteins require eIF5A for efficient translation and thus contributes to its essentiality.

Hypusination has been previously studied in trypanosomatids. In 2010, Chawla et al. identified two putative DHS homologs in *Leishmania donovani* (21). Only one of the homologs, DHS34, encoded the catalytic lysine while the other homolog, DHSL20, appeared catalytically dead. Activity assays of recombinant enzymes confirmed that DHSL20 was unable to modify recombinant eIF5A, and even though DHS34 was able to carry out the modification, the activity level was 1000-fold lower than that reported for human DHS. Nonetheless, a definitive study of the essentiality of eIF5A and hypusination had not been done in trypanosomatids and the function of the catalytically dead homolog remained unknown.

III. DISSERTATION FOCUS

In this dissertation, I sought to determine if the essentiality of hypusination is conserved in trypanosomatids. First, using the model organism *T.b. brucei*, I studied the essentiality of eIF5A for the growth of the bloodstream-form and procyclic-form of the parasites. As part of these studies, I also validated the parasite gene as a functional homolog of eIF5A. Second, to determine if deoxyhypusination is essential, I studied the essentiality of the putative modifying enzyme DHS. Third, I validated the function of the putative DHS and studied the role of the catalytically dead homolog in trypanosomatid hypusination.

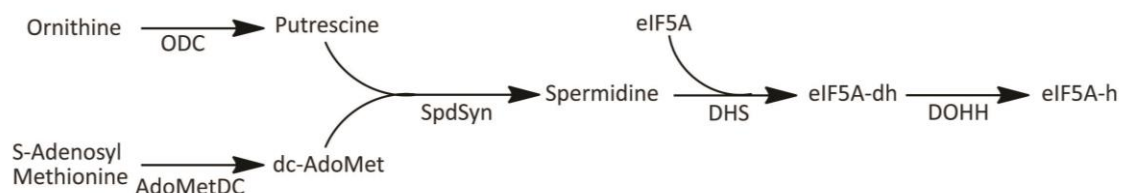


Figure 1.1. Spermidine and hypusine metabolic pathway in *T. brucei*. ODC – ornithine decarboxylase; AdoMetDC – S-adenosylmethionine decarboxylase; SpdSyn – spermidine synthase; DHS – deoxyhypusine synthase; eIF5A-dh – deoxyhypusine-modified eukaryotic initiation factor 5A; DOHH – deoxyhypusine hydroxylase; eIF5A-h – hypusine modified eIF5A.

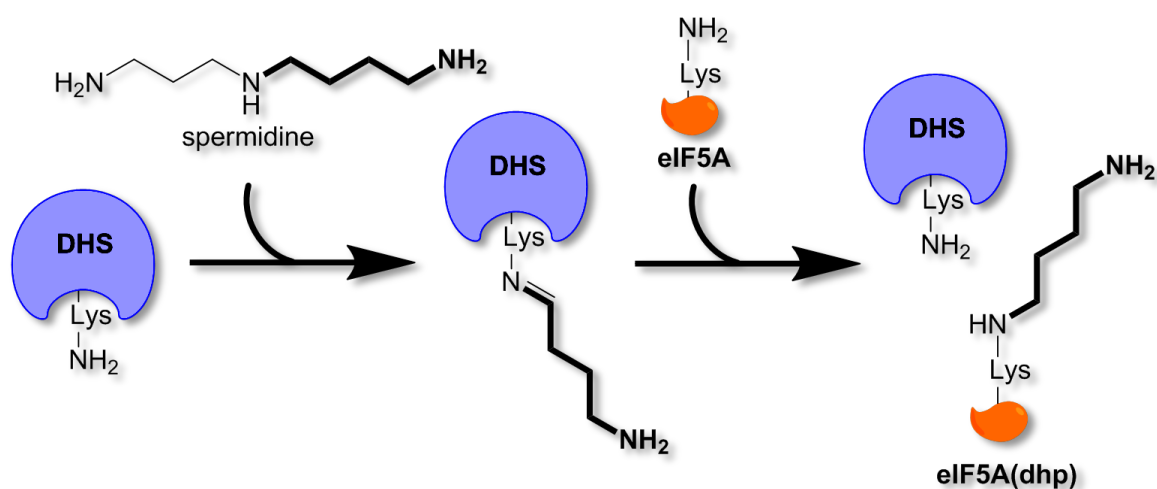


Figure 1.2. Reaction mechanism of deoxyhypusine synthase. Diagram of the transfer of the 4-aminobutyl moiety of spermidine (bolded) to a catalytic DHS lysine and subsequent transfer to the eIF5A lysine forming deoxyhypusine-eIF5A (eIF5a(dhp)).

CHAPTER TWO

Experimental Methods

Multiple sequence alignment.

DHS sequences were obtained using NCBI BLAST of the kinetoplastids with *H. sapiens* DHS (AAB02179.1) as the search query. The sequences were aligned with Clustal Omega (version 1.1.0; www.ebi.ac.uk/Tools/msa/clustalo/). The putative substrate binding sites were identified based on alignment with human DHS. Phylogenetic tree constructed with Mega5 software (www.megasoftware.net) using the neighbor-joining algorithm with Kimura-2 parameters. The analysis included the following DHS sequences: *H. sapiens* (Gene ID P49366), *Trichoplax adhaerens* (EDV28024.1), *Chlamydomonas reinhardtii* (A: EDP09680.1, B: EDP01029.1), *Acanthamoeba castellanii* (ELR12881.1), *Naegleria gruberi* (EFC43118.1), *Saccharomyces cerevisiae* (P38791), *Giardia lamblia* (EFO61259.1), *Arabidopsis thaliana* (A: AED90939.1, B: AAG53621.2, C: AED90940.1), *Perkinsus marinus* (A: EER15074.1, B: EER03596.1), *T. brucei* (TbDHSp: Tb927.1.870, TbDHSc: Tb927.10.2750), *T. cruzi* (A: Tc00.1047053511421.60, B: Tc00.1047053504119.29, C: Tc00.1047053506195.300), *L. major* (A: LmjF.20.0250, B: LmjF.34.0330), and *Entamoeba dispar* (A: EDR24093.1, B: EDR21721.1).

Generation of transgenic *T. brucei*

Cell culture.

Mammalian bloodstream-form (BSF) *T. brucei brucei* Lister strain 427 and derivatives were cultured at 37 °C with 5% CO₂ in HMI-11 supplemented with 10% heat-inactivated Tet-free fetal bovine serum (Atlanta Bio) as described (34). The ‘single marker’ cell line (SM)

expressing T7 RNA polymerase and Tet repressor were used for genetic experiments and maintained in the presence of $2.5 \mu\text{g ml}^{-1}$ G418 (Sigma) (35). Cell densities were maintained between 10^3 ml^{-1} and 10^6 ml^{-1} . Procyclic-form (PF) *T.b.b.* Lister strain 427 and derivatives were cultured in SDM-79 media supplemented with 15% FBS (36). The 29-13 cell line expression T7 RNA polymerase and Tet-repressor was used for genetic experiments and maintained in the presence of $25 \mu\text{g ml}^{-1}$ hygromycin B (Sigma) and $15 \mu\text{g ml}^{-1}$ G418. Cell densities were maintained between 10^4 ml^{-1} and 10^8 ml^{-1} .

Transfection of T. brucei.

Transfection of both forms of *T. brucei* was performed with an Amaxa Nucleofector II (37). In brief, 10^7 cells were pelleted by centrifugation ($2000 \times g$, 10 min) and resuspended in Human T Cell Nucleofector® buffer (0.1 ml, Lonza). DNA was added, the mixture was transferred to a cuvette, and transfected using preset program X-001. The mixture was immediately transferred into HMI-11 (50 ml) or SDM-79 (20 ml) accordingly. The cells were allowed to recover (BSF: 8 h, PF: 16 h) before selective antibiotics were added. A 1:10 dilution of the culture was made into media containing selective antibiotics and both cultures were plated into 24-well plates (2 ml per well). Once transfection controls died, the positive transfection wells were transferred to flasks for continued culturing. Antibiotic concentrations used for selection of BSF parasites were as follows: $2.5 \mu\text{g ml}^{-1}$ G418 (Sigma), $2.5 \mu\text{g ml}^{-1}$ phleomycin (InvivoGen), $2 \mu\text{g ml}^{-1}$ blasticidin S (Invivogen), $2.5 \mu\text{g ml}^{-1}$ hygromycin B. For PF, the following antibiotic concentrations were used: $15 \mu\text{g ml}^{-1}$ G418, $2.5 \mu\text{g ml}^{-1}$ phleomycin (InvivoGen), $10 \mu\text{g ml}^{-1}$ blasticidin (Sigma), $25 \mu\text{g ml}^{-1}$ hygromycin

B. Tet (RPI) for control of Tet-regulated gene expression was prepared in 70% ethanol (5 mg ml⁻¹) and used at a final concentration of 1 µg ml⁻¹ for BSF and 10 µg ml⁻¹ for PF.

Generation of inducible tagged DHSc and DHSp expression constructs.

The *DHSc* gene was amplified from *T. brucei* SM genomic DNA with a forward primer encoding for the AU1 tag and cloned into pCR®8/GW/TOPO® (Life Technologies). Sequence fidelity was confirmed by sequencing with the M13 primer and alignment with the *Tb* 927 sequence. The N-terminal AU1-tagged *DHSc* gene was subcloned into pLew100 using HindIII and BamHI allowing for integration into the rRNA locus and Tet-inducible expression in *T. brucei*. The *DHSp* gene was also amplified from *T. brucei* SM genomic DNA with a forward primer encoding for the FLAG tag and cloned into pCR®8/GW/TOPO®. Sequence fidelity was confirmed by sequencing with the M13 primer and alignment with the *Tb* 927 sequence. The N-terminal FLAG tagged *DHSp* gene was subcloned into pLew300 using HindIII and BamHI allowing for integration into the rRNA locus and Tet-inducible expression in *T. brucei*.

Generation of regulatable gene expression constructs and cell lines.

The *DHSc* and *DHSp* genes were amplified from *T. brucei* single marker genomic DNA, cloned into pCR®/GW/TOPO®, and sequenced with the M13 forward and reverse primers. The genes were subcloned into pLew100v5 using HindIII and BamHI, allowing for integration into the rRNA locus and Tet-inducible expression of tagless *DHSc* or *DHSp* in *T. brucei*. Similarly, human *EIF5A* was amplified from a plasmid carrying the synthetic gene (GenScript), cloned into pCR®/GW/TOPO®, and subcloned into pLew100v5-BSD using

HindIII and BamHI for usage in RNAi complementation studies. For the K52A mutant, the AAA codon was mutated to GCA by PCR mutagenesis. Mutants were confirmed by sequencing. The regulatable ectopic expression constructs (5 µg) were linearized with NotI-HF (New England Biolabs) and transfected into *T. brucei* SM or 29-13 cell line. Constructs using pLew100v5 were selected for with phleomycin and constructs using pLew100v5-BSD were selected for with blasticidin.

Generation of gene knockout constructs by PCR.

The 5' flanking region of the DHSc gene was amplified from *T. brucei* single marker genomic DNA starting 374 bases upstream of the open reading frame. The reverse primer included an overhang complementing the blasticidin resistance gene (19 bases) or hygromycin resistance gene (21 bases). The 385 base pairs of the 3' flanking region of the DHSc gene was also amplified from *T. brucei* SM genomic DNA starting directly after the annotated stop codon. The forward primer included an overhang to complement the blasticidin resistance gene (20 bases) or the hygromycin resistance gene (18 bases). Using overlapping PCR, the DHSc flanking regions were joined to the blasticidin or hygromycin resistance gene, generating a resistance marker construct for replacement of the DHSc allele. The same method was used to generate DHSp replacement constructs with 437 base pairs of the 5' flanking region and 499 base pairs of the 3' flanking region joined to the resistance genes.

Generation of DHSc and DHSp conditional knockouts.

To generate conditional knockout cell lines in *T. brucei* SM cells, the first allele of the DHSc or DHSp gene was replaced with the hygromycin resistance gene by transfection with the PCR-generated construct (0.5 µg) and selection with hygromycin B. The single knockout cells were then transfected with the regulatable gene expression construct (5 µg) and selected using phleomycin. Confirmation of ectopic expression upon Tet induction was done by Western blot using antibodies raised to recombinant *T. brucei* DHS. In the presence of Tet to maintain expression of the ectopic copy, the 2nd allele was knocked out using the blasticidin resistance gene construct (Figure 2.1). Knockouts were confirmed by PCR with primers outside the replacement region and for the specific genes. Conditional knockout cell lines were maintained in media containing Tet to maintain expression of DHSc or DHSp, and G418, hygromycin B, phleomycin, and blasticidin to maintain the selection.

Generation of stem-loop construct targeting eIF5A by RNAi.

A 451 base pair region (2-452) was identified using RNAit for targeting of the *TbEIF5A* CDS (38). The segment was PCR amplified from SM gDNA (forward primer TGTCTGACGATGAGGGACAG, reverse GCAGAAACAACAACGACCAA) and TA-cloned® into the Gateway entry vector pCR®8/GW/TOPO® (Life Technologies). The entry clone (100 ng) was combined with the destination vector pTrypRNAiGate (100ng) using Gateway® LR clonase® reaction to generate a Tet-inducible stem-loop (Life Technologies) (14). Upon transfection, the pTrypRNAiGate-TbEIF5A construct is integrated into the rDNA spacer region and allows for Tet-induced expression of the hairpin RNA.

Determination of T. brucei cell growth.

For the conditional knockouts, cells were washed with Tet-free media three times to turn off expression of the regulated expression construct. For RNAi knockdown, cells were maintained in Tet-free media and Tet ($1 \mu\text{g ml}^{-1}$) was added on day 0 of growth analysis. Cell growth of \pm Tet cultures was monitored and cell density was determined by counting with a Hausser Bright-Line hemocytometer using an Olympus CK2 inverted microscope. PF cultures were maintained between 10^3 and 5×10^7 ml. For BSF cell lines, cell cultures a density of 10^6 cells ml^{-1} were diluted 1:200 to maintain log phase growth. Parallel 250 mL cultures were grown and cells were collected for Western blot for BSF form cells. Cumulative cell number = cell density x culture volume x dilution factor.

Expression of recombinant proteins.

Gene cloning of DHS and eIF5A recombinant expression vectors.

The *T. brucei* *DHSc*, *DHSp*, and *eIF5A* genes were amplified from *T. brucei* 427 genomic DNA and cloned into BsaI-linearized pE-SUMO Kan (Life Sensors) for expression as N-terminal His₆-SUMO tagged fusion proteins. *DHSp* was also cloned into the HindIII-KpnI site of the pT7-FLAGTM-MAT-Tag®-2 vector (Sigma) for tagless coexpression with His₆-SUMO-DHSc. The expression vectors were sequenced with the T7 and reverse T7 primers to confirm sequence fidelity (Applied Biosystems Big Dye Terminator 3.1).

Gene synthesis of human DHS and eIF5A Expression Vectors.

The human *DHS* (P49366.1) and *EIF5A-1* (AAH80196.1) sequences were codon optimized for *E. coli* and synthesized by GenScript (Figure 2.2). The genes were subcloned into BsaI-linearized pE-SUMO Kan for expression as N-terminal His₆-SUMO tagged fusion proteins.

Expression and purification of yeast SUMO protease, Ulp1.

The pET28b-Ulp1 expression construct was a gift from Dr. Kim Orth (UTSW). The protein was expressed with an N-terminal His₆-tag in *E. coli BL21 (DE3)*. Protein expression was induced at A₆₀₀ of 0.5 with isopropyl β -D-1-thiogalactopyranoside (IPTG) (1 mM, Sigma) for 2h at 37 °C. Cells were harvested by centrifugation (1000 x g for 30 minutes). The pellet was resuspended in Buffer A [50 mM Hepes (pH 8), 300 mM NaCl, 50 mM Imidazole, 2 mM β -mercaptoethanol, 2 mM phenylmethylsulfonyl fluoride (PMSF)] and lysed by high pressure disruption (EmulsiFlex-C5, Avestin). Cell lysate was clarified by centrifugation (15,000 x g for 30 minutes), and protein was purified by nickel affinity chromatography (HiTrap Chelating HP column, GE Life Sciences). Protein was eluted with imidazole (250 mM). Protein concentration was estimated using Bio-Rad Protein Assay and a BSA standard curve. The Ulp1 is used to cleave the SUMO tag from fusion proteins (39).

Expression and purification of SUMO-tagged Proteins.

Expression vector was transformed into *E. coli BL21 (DE3)* cells and selected with kanamycin (50 μ g ml⁻¹). Protein expression was induced at A₆₀₀ of 0.5 with IPTG (0.25 mM) for 16 h at 16 °C. Cells were harvested by centrifugation (1000 x g for 30 minutes). The pellet was resuspended in Buffer A [50 mM Hepes (pH 8), 300 mM NaCl, 50 mM imidazole, 2 mM β -mercaptoethanol, and 2 mM phenylmethylsulfonyl fluoride (PMSF)] and lysed by

high-pressure disruption (EmulsiFlex-C5, Avestin). The cell lysate was clarified by centrifugation (15,000 x g for 30 minutes), and protein was purified by nickel affinity chromatography. Protein was eluted with a linear gradient imidazole and eluted at ~200 mM imidazole. Elution fractions were analyzed by SDS-PAGE and Coomassie staining before protein fractions were combined and concentrated (Centricon-30, Millipore). Ulp1 (10 µg) was added and incubated for 16 h at 4 °C. The sample was diluted 20-fold in Buffer A, and the cleaved protein was separated from the His₆-SUMO by nickel affinity chromatography. The flow-through fractions were analyzed by SDS-PAGE and Coomassie staining. Fractions were combined and dialyzed against DHS buffer [50 mM Tris-HCl (pH 7.5), 200 mM NaCl, 1 mM DTT]. Purified protein concentrations were calculated using the following A₆₀₀ extinction coefficient: $TbDHSc = 47.2 \text{ cm}^{-1} \text{ mM}^{-1}$, $TbDHSp = 25.4 \text{ cm}^{-1} \text{ mM}^{-1}$, $TbeIF-5A = 4.1 \text{ cm}^{-1} \text{ mM}^{-1}$.

Coexpression of DHSc:DHSp.

E. coli BL21 were transformed with the pE-SUMO-DHSc and pT7-DHSp vectors and selected for using kanamycin (50 µg ml⁻¹) and ampicillin (100 µg ml⁻¹). Protein expression was as described for SUMO-tagged proteins. After dialysis against DHS buffer, the protein was purified further by gel filtration chromatography on a Superdex 200 Prep Grade (GE Life Sciences) using DHS buffer. The eluted fractions were analyzed by SDS-PAGE and Coomassie staining. Purified protein concentrations were calculated using the following A₆₀₀ extinction coefficient: $TbDHSc$, $46.4 \text{ cm}^{-1} \text{ mM}^{-1}$; $TbDHSp$, $25.9 \text{ cm}^{-1} \text{ mM}^{-1}$; $TbDHSc:TbDHSp$, $72.3 \text{ cm}^{-1} \text{ mM}^{-1}$; $TbeIF5A$, $4.1 \text{ cm}^{-1} \text{ mM}^{-1}$; $HsDHS$, $39.9 \text{ cm}^{-1} \text{ mM}^{-1}$,

HseIF5A, $4.5 \text{ cm}^{-1} \text{ mM}^{-1}$ (computed using ProtParam, ExPASy, Swiss Institute of Bioinformatics).

Other methods for cell and protein characterization.

Deoxyhypusine synthase activity assay.

DHS activity was measured by the incorporation of tritium from [^3H]-spermidine into eIF-5A. Purified DHS was added to a reaction mix containing recombinant eIF-5A (10 μM), [^3H]-spermidine (7.5 μM), NAD^+ (1 mM), DTT (1 mM), and glycine-NaOH buffer (0.2 M, pH 9.3) for a total volume of 20 μL . The reaction was incubated in a 37 °C water bath for 1 hour and stopped by the addition of cold spermidine (10 mM in PBS, pH 7.5). The mixture was then adsorbed onto nitrocellulose for 30 minutes using the Bio-Dot® Microfiltration Apparatus (Bio-Rad), followed by filtration and washing spermidine/PBS (0.5 ml), and drying under vacuum (15 min). The nitrocellulose filter was then cut to separate the wells and each sample was added to CytoScint™ (MP Biomedicals). After incubation overnight, the samples were counted on a Beckman LS 6500 Liquid Scintillation Counter.

Antibody production.

Antibodies were raised in rabbits against purified recombinant DHSc, DHSp, and *TbeIF5A* (Covance).

Western blot analysis.

10^8 cells were harvested by centrifugation (2000 x g, 10 min). Pellets were washed twice with PBS (1 ml), resuspended in Tryp Lysis Buffer [50 mM Hepes (pH 8), 100 mM NaCl, 5 mM β -mercaptoethanol, 2 mM PMSF, 1 $\mu\text{g ml}^{-1}$ leupeptin, 2 $\mu\text{g ml}^{-1}$ antipain, 10 $\mu\text{g ml}^{-1}$

benzamidine, 1 $\mu\text{g ml}^{-1}$ pepstatin, and 1 $\mu\text{g ml}^{-1}$ chymostatin], and lysed with three freeze/thaw cycles. The lysate was clarified by centrifugation (13,000 x g, 10 min, 4 °C) and the supernatant was used. Protein concentration was estimated using the Bio-Rad Protein Assay and a bovine serum albumin standard curve. Total soluble protein (30 μg) was separated by SDS-PAGE and transferred to a PVDF membrane (iBlot®, Life Technologies). The membrane was blocked with 5% nonfat [?] milk in Tris-buffered saline (TBS) and incubated with primary antibody. The following primary antibodies were used at 1:1000: anti-DHSc (rabbit polyclonal) anti-DHSp (rabbit polyclonal), anti-FLAG/M2 (mouse monoclonal, Sigma), or anti-AU1 (mouse monoclonal, Covance). The blot was washed with TBS + 0.1% Tween-20 and incubated with the appropriate secondary antibody at 1:10,000: goat anti-rabbit antibody or goat anti-mouse antibody conjugated to alkaline phosphatase (Sigma). The protein was detected using SuperSignal West Pico Chemiluminescent Substrate (Thermo Scientific) and imaged by exposure to X-ray film or with an ImageQuant LAS 4000 (GE Healthcare).

Immunofluorescence microscopy

10^6 parasites at 10^5 ml^{-1} were pelleted and washed twice with PBSg (PBS + 50 mM glycine). Cells were resuspended in PBSg + 1% paraformaldehyde (1 mL), incubated on ice for 15 min, and then washed with PBSg. Fixed cells (0.1 ml) were spread onto Superfrost Plus (Fisherbrand) slides and allowed to dry at room temperature. Slides were blocked with 5% goat serum in PBSg for 1h at room temperature and then incubated with primary antibody (1:500) for 1h. Slides were washed with PBSg three times and then incubated with Alexa fluor 488-conjugated anti-mouse antibody (1:500) and Alexa fluor 594-conjugated anti-rabbit

antibody (1:500) for 30 minutes (Life Technologies). Slides were washed with PBSg three times before cover slips were mounted with Vectashield Hardset with DAPI (Vector Laboratories). Slides were imaged using Leica TCS SP5 microscope, and images were compiled using the ImageJ FIJI package.

Cell cycle analysis by flow cytometry.

10^6 parasites were collected and washed with PBS (1 ml). Cells were fixed in 70 % methanol/PBS (1 mL) at 4 °C for 16 h. The fixed cells were washed twice with PBS (1 ml) and resuspended in 750 μ L PBS with 7.5 μ g propidium iodide (PI) and 1 μ g RNaseA. The sample was incubated at 37 °C for 1 h prior to analysis on a FACScan flow cytometer (Becton-Dickinson). Forward scatter, side scatter, and PI fluorescence data were collected for 10,000 events per sample. PI fluorescence signal was used to quantitate DNA content and data was analyzed using FlowJo v10 (www.flowjo.com).

Immunoprecipitation from T.brucei cell lysates.

10^8 cells were harvested by centrifugation (2000 x g, 10 min). Cell pellet was washed twice with PBS (1 mL) and lysed in hypotonic buffer [10 mM Tris (pH 7.5), 2 mM PMSF, 1 μ g ml⁻¹ leupeptin, 2 μ g ml⁻¹ antipain, 10 μ g ml⁻¹ benzamidine, 1 μ g ml⁻¹ pepstatin, and 1 μ g ml⁻¹ chymostatin] on ice for 1 h. Cells were also passed through three freeze/thaw cycles and adjusted with salt buffer [10 mM Tris (pH 7.5), 400 mM NaCl] to 80 mM NaCl. Cell lysate was clarified by centrifugation (10,000 x g, 10 min, 4 °C). Protein concentration was estimated using the Bio-Rad Protein Assay and a BSA standard curve. Total soluble protein (50 μ g) was incubated with either mouse monoclonal anti-AU1 antibody (Covance), mouse

monoclonal M2 anti-FLAG antibody (Sigma), or no antibody (1:150, 12 h, 4 °C). Dynabeads® Protein A (50 µl, Life Technologies) was added and the antibody-antigen complex was captured with a magnetic stand. The beads were washed three times with TBS and the antibody-antigen complex was eluted with 40 µl citrate buffer (pH 3). The eluent was neutralized with 5 µl 0.1 M NaOH before separation by SDS-PAGE and transfer to PVDF. For coimmunoprecipitation experiments, proteins were detected by Western blot analysis as described above. For eIF5A radiolabelling experiments, the membrane was exposed on a phosphor storage screen and imaged with the phosphoscanner.

Putrescine labeling of trypanosomes.

For polyamine experiments, culturing media was supplemented with chicken serum (Gemini Bio-Products) instead of FBS to avoid amine oxidase-mediated toxicity. Log phase cells were cultured in media supplemented with 50 µM ¹⁴C-putrescine for 6-12 h before cells (BSF: 10⁶, PF: 10⁷) were pelleted and washed with PBS (1 mL) three times. Immunoprecipitation proceeded as above with 30 µg of soluble lysate and anti-TbeIF5A antibody (1:200).

Crystallization of TbDHS heterotetramer

NeXtal Tubes Cryos, PEGs II, and Protein Complex suites (Qiagen) were used to screen for crystallization conditions. Purified DHSc-DHSp (10 mg ml⁻¹ or 25 mg ml⁻¹) was incubated with 200 µM GC7 and 2 mM NAD⁺ for 12 h at 4 °C prior to addition to screening solution (1:1, 2 µL) for sitting drop vapor diffusion crystallization in a 24-well plate. Plates were

incubated at 22 °C and periodically assessed for crystals by microscopy. Drops were also set up in the presence and absence of 1 mM DTT.

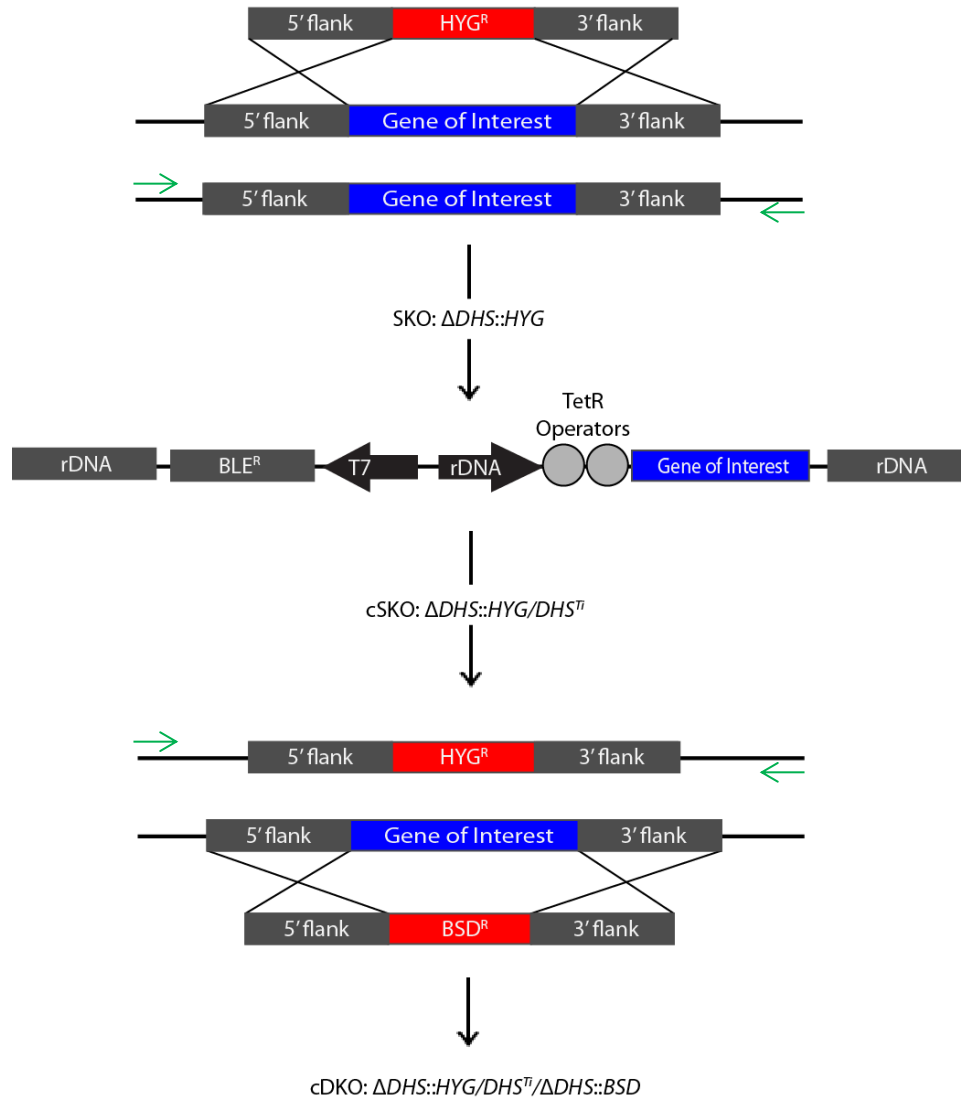


Figure 2.1. Schematic of generation of conditional knockout cell lines. First, one allele is replaced with the hygromycin resistance marker. Second, a Tet-regulatable copy of DHS was introduced to generate conditional single knockouts. Finally, the remaining endogenous allele was replaced with the blasticidin resistance marker to generate the conditional knockout. Replacement of endogenous alleles was monitored by PCR amplification of the locus using primers flanking the recombination regions (green arrows) and sequencing.

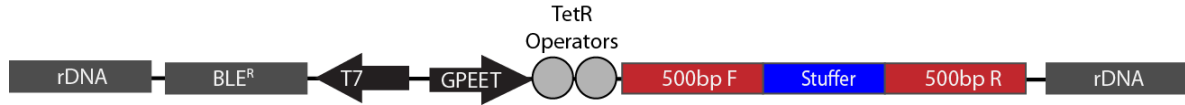


Figure 2.2. Schematic of RNAi stem-loop construct. Construct design for expression of dsRNA (red) as a stem-loop (red-blue-red) under regulation by Tet-repression. Homologous regions to rDNA allow for recombination into rDNA spacer region and selection is mediated by T7-driven expression of the bleomycin resistant gene (BLE^R).

CHAPTER THREE:

eIF5A is an essential protein in *T. brucei*

I. INTRODUCTION

The essentiality of eIF5A has been shown in *S. cerevisiae* and multicellular eukaryotes (24,40-42). Together with the highly conserved nature of eIF5A in eukaryotes, it is thought that eIF5A is fundamentally essential in all eukaryotes. Previous work on trypanosomatid eIF5A has focused on the structure and phosphorylation of the *Leishmania* protein. The structure of the *Leishmania* eIF5A was solved by the Structural Genomics of Pathogenic Protozoa Consortium in 2004 (PDB code 1X60) and was used for modeling of other eukaryotic eIF5A (43,44). The eIF5A homologs all share two domains – an N-terminal domain with an exposed loop on which hypusination occurs and a C-terminal domain with an S1-like RNA-binding domain. More recent studies of *Leishmania* eIF5A identified two phosphorylation sites, serine-2 and tyrosine-21, and overexpression of a serine-2 to aspartate mutant increased the rate of cell growth (45). The essentiality of trypanosomatid eIF5A however has not been previously determined.

We hypothesized that in both the bloodstream-form and procyclic-form *T. brucei*, eIF5A and its hypusination are essential for cell growth. We generated stable cell lines in bloodstream-form and procyclic-form cells that expressed dsRNA targeting *EIF5A* mRNA for knockdown and then monitored cell growth as eIF5A mRNA and protein was depleted. The knockdown cell lines were complemented with RNAi-resistant human *EIF5A* and a

hypusination-resistant lysine mutant to validate the phenotype and determine the essentiality of the hypusine modification for eIF5A function.

II. IDENTIFICATION OF *T. brucei* EIF5A

Based on sequence homology with *S. cerevisiae* eIF5A, a single putative *T. brucei* eIF5A was identified (Tb11.03.0410). Unlike *S. cerevisiae* and other multicellular eukaryotes that encode multiple eIF5A homologs, *T. brucei* and the other trypanosomatids only encode a single eIF5A. The *T. brucei* EIF5A gene encodes a 166 amino acid protein that retains good homology with other eukaryotic eIF5As (43% sequence identity with human eIF5A). In particular, the N-terminal hypusination motif and the C-terminal S1-like RNA-binding domain are well conserved. The ten residues surrounding the hypusinated lysine (lysine-50) of human eIF5A are fully conserved with the *T. brucei* eIF5A and as such, sequence alignment predicts that the *T. brucei* eIF5A lysine-52 is post-translationally hypusinated.

III. PUTRESCINE-DEPENDENT MODIFICATION OF EIF5A

Hypusination occurs via two enzymatic steps. In the first step, deoxyhypusine synthase (DHS) transfers the 4-aminobutyl moiety of spermidine to a specific lysine on eIF5A forming deoxyhypusine. This is then hydroxylated by deoxyhypusine hydroxylase (DOHH) to form hypusine. Spermidine is formed from putrescine and decarboxylated S-adenosylmethionine by spermidine synthase. *T. brucei* generates putrescine from ornithine, but it is also able import putrescine from the growth medium (46). We cultured trypanosomes in ¹⁴C-putrescine for 48 hours, lysed the cells, and then immunoprecipitated eIF5A using an antibody raised against recombinant *T. brucei* eIF5A. The immunoprecipitated protein was

separated by SDS-PAGE, transferred to PVDF membrane, and visualized using a phosphor storage screen. A single band was detected in the cell lysates that was between 15 and 20 kD (Figure 3.1). Immunoprecipitation with anti-eIF5A antibody also yielded the same solitary band whereas a parallel immunoprecipitation without anti-eIF5A antibody did not yield any radiolabeled bands. This shows that the ^{14}C -putrescine is incorporated into *Tb*eIF5A, and supports the existence of deoxyhypusination, at the very least, in *T. brucei*.

IV. ESSENTIALITY OF EIF5A

RNAi knockdown of TbEIF5A

To determine the essentiality of eIF5A in these parasites, we employed RNAi by generating stable inducible cell lines expressing a stem loop dsRNA targeting *EIF5A* for knockdown. The GPEET procyclin promoter is used to drive expression of the stem loop and regulation is provided by Tet repressor elements. The transfected constructs are integrated into the rDNA spacer region by homologous recombination and phleomycin resistance is used as the selection marker.

RNAi knockdown of TbEIF5A in bloodstream-form trypanosomes

The RNAi construct was transfected into the bloodstream-form *Tbb* ‘single marker’ (SM) cell line constitutively expressing T7 RNA polymerase and Tet and is hitherto referred to as BSF *EIF5A* RNAi. Induction of *EIF5A* knockdown by daily addition of Tet resulted in a reduction in *EIF5A* RNA by 74-85% as measured by qRT-PCR and a growth defect by day 2 (Figure 3.2). Western blot analysis of soluble cell lysates using an antibody to *T.b.* eIF5A showed a decrease in eIF5A one day after induction and barely detectable protein levels by

day 2. Four clonal lines were established by limited dilution and the growth rates were monitored. They all consistently showed a growth defect by day 2. In three of the four clonal lines, the induced parasite cultures cleared completely and cells were not visible by microscopy after 8 days of induction. One clonal line (BSF *EIF5A* RNAi Clone 2) entered growth arrest on day 2 but resumed growth by day 8. Western blot analysis and qRT-PCR revealed that eIF5A protein and mRNA levels returned to normal on day 8 suggesting a loss of Tet regulation. This phenomenon has been previously described for Tet repression systems in trypanosomes (35,47). The growth arrest upon induction of RNAi demonstrates that *EIF5A* is essential for bloodstream-form parasite growth *in vitro*.

Disruption of eIF5a or hypusination has been associated with a cell cycle block in cultured mammalian cells (48). To determine if this is also true in *T. brucei*, we examined the phenotypic consequences of eIF5A loss by microscopy. The cells were stained with 1-(4-amidinophenyl)-1H-indole-6-carboxamide (DAPI) which binds DNA and fluoresces upon excitation with UV light, allowing for visualization of the nucleus and kinetoplast. The number of nuclei and kinetoplast per cell were counted for 100 cells from each condition. In uninduced cells, 60% of the cells contained a single nucleus and kinetoplast (1N1K), indicative of G₁-phase cells (Figure 3.3). A second kinetoplast, the first DAPI-detectable indicator of S-phase, was visible in 14% of cells (1N2K). In 22% of cells, double DNA content was observed (2N2K), indicative of cells that duplicated their DNA and are undergoing mitosis. In RNAi-induced cells, the percentage of 1N1K cells decreased to 32%

2N2K cells decreased to 5% on day 2. An increase in aberrant (>2N2K) cells were observed, suggesting that eIF5A is required for normal cell division.

To quantify the change in proportion of dividing cells, nucleic acid content was measured by flow cytometry. Fixed and permeabilized cells were treated with RNase A and stained with propidium iodide, which intercalates into nucleic acids and is detectable by fluorescence. Compared to manual counting of DAPI-stained cells, this method rapidly quantifies the DNA content of a greater number of cells (10,000). The DNA content distribution of uninduced cells was similar to that observed before. Interestingly, the RNAi induced population did not show a decrease in 2N2K cells but a slight increase in intermediate cells from 13% to 30% (Figure 3.3). Intermediate cells have not fully duplicated their DNA and an increase in this population suggests stalling in S-phase which would lead to failed entry into G2/M-phase. The analysis discards higher nucleic content aberrant cells. Treatment with puromycin, a global translation inhibitor, resulted in a decrease of intermediate cells and increase in 2N2K cells, consistent with the known ability of puromycin to block cell division (49). Thus, while small scale analysis suggested a potential cell cycle block with eIF5A depletion, cell cycle analysis by flow cytometry shows no significant cell cycle block.

Validation of RNAi phenotype

To validate the phenotype, the BSF *EIF5A* RNAi cell lines were complemented with human eIF5A. A codon optimized sequence for expression of human eIF5A was synthesized by Genscript and nucleotide sequence alignment of *T.b.* and the synthesized *H.s.* sequences

revealed no stretches of homology greater than 12 nucleotides, predictive that the human sequence will be resistant to the *TbEIF5A*-directed stem loop. The *HsEIF5A* gene was introduced into the rDNA spacer region under control of the rDNA promoter and Tet-repressor elements. Upon addition of Tet, both human eIF5A expression was induced and *TbEIF5A* mRNA was knocked down, as confirmed by Western (Figure 3.4). Expression of human eIF5A was able to rescue to the growth phenotype due to loss of endogenous eIF5A in bloodstream-form parasites. Taken together with the rescue with RNAi-resistant *TbEIF5A*, these data validate that eIF5A is essential in cultured bloodstream-form trypanosomes. Moreover, the ability of human eIF5A to complement confirms that the two proteins are functional homologs.

Essentiality of eIF5A Hypusination

To determine if the post-translationally formed hypusine residue of eIF5A is essential in *T. brucei*, the BSF *EIF5A* RNAi cell line was complemented with a lysine-50 to alanine mutant of human eIF5A which cannot be hypusinated. Using the same complementation strategy as before, the *HseIF5A*^{K50A} mutant was expressed in the context of knockdown of endogenous *TbEIF5A*. Unlike wildtype human eIF5A, *HseIF5A*^{K50A} was unable to rescue the growth defect caused by loss of eIF5A (Figure 3.6). To determine if the growth defect is due to a dominant negative effect of the *HseIF5A*^{K50A} mutant, the mutant was also overexpressed in wildtype ‘single marker’ cells. Overexpression of the *HseIF5A*^{K50A} did not cause a change in growth rate of the bloodstream-form trypanosomes (Figure 3.7). Thus, the inability of this

mutant to rescue the RNAi phenotype supports the essentiality the hypusine modification of eIF5A for cell growth.

RNAi knockdown of T.b. EIF5A in procyclic-form trypanosomes

During the lifecycle of *T. brucei*, it undergoes a proliferative stage in the fly midgut as the procyclic-form parasite. To determine if eIF5A is also essential for growth in the procyclic-form, the *EIF5A* RNAi construct was also transfected into procyclic-form *Tbb* strain 29-13 to generate stable inducible cell lines hitherto referred to as PF *EIF5A* RNAi. Induction of *EIF5A* knockdown resulted in 64-72% decrease in RNA as determined by qRT-PCR and decreased protein as assessed by Western blot (Figure 3.8). Similar to bloodstream-form cells, the induced cells entered growth arrest on day 2. By contrast, while bloodstream-form cells proceeded to cell lysis and death, as long as induction was maintained with daily Tet addition, the procyclic-cells remained in growth arrest but otherwise appeared motile and alive. Removal of Tet on day 6 permitted the cells to resume growth by day 8. A small number of cells in growth arrest (~20%) on day 4 appeared contracted; the cytoplasmic volume appeared decreased, and the curvature of the cell body around the nucleus became more prominent (Figure 3.9). Cell cycle analysis of the cells entering growth arrest did not reveal any difference in the percentage of cycling cells (Figure 3.10). This suggests that many but not all cells enter growth arrest.

Analogous to the complementation experiments in bloodstream-form trypanosomes, the PF *EIF5A* RNAi cells were complemented with *HseIF5A*. As observed with bloodstream-form trypanosomes, wild type human eIF5A is able to rescue the growth defect

due to the loss of endogenous eIF5A (Figure 3.11). As before, the *HseIF5A*^{K50A} mutant is unable to rescue the growth arrest caused by loss of endogenous eIF5A (Figure 3.13). We confirmed that the lysine mutant does not affect cell growth of procyclic-form parasites as well (Figure 3.14). These results are consistent with the essential nature for general eukaryotic cell growth of both eIF5A expression and its hypusination.

V. DISCUSSION

While the essentiality of eIF5A in trypanosomatids was not controversial, it had yet to be directly demonstrated. In these experiments, we were able to determine the essentiality of eIF5A and the hypusine modification in *T. brucei*. Since the first report of RNAi in trypanosomes in 1998, it has become an invaluable tool for determining gene essentiality in *T. brucei* (13). Here, we have used RNAi technology to show that knockdown of *EIF5A* RNA disrupts cell growth of cultured *T. brucei*, causing cell death in bloodstream-form parasites and reversible growth arrest in procyclic-form parasites. RNAi relies upon the recognition of mRNA by complementarity to argonaute-bound small RNA. As such, there is the possibility for off-target effects due to nonspecific knockdown of other mRNAs. We confirmed that the observed phenotype was due to specific knockdown of *EIF5A* by complementing the cell lines with RNAi-resistant human eIF5A. The ability of *Hs* eIF5A to rescue the growth defect validates the essential phenotype of eIF5A and furthermore, demonstrates that human and trypanosome eIF5A are functionally homologous.

Perhaps the most fascinating aspect of eIF5A is that it is the only known protein to undergo hypusination, and as with eIF5A itself, deoxyhypusine synthase (DHS), the enzyme

responsible for the first step of this modification, is highly conserved in eukaryotes (50). Previous work evaluating the essentiality of the hypusine modification for eIF5A function relied on chemical inhibition of deoxyhypusine synthase using a spermidine analog, N1-guanyl-1,7-diaminoheptane (GC7) (51). To more directly address the essentiality of hypusination, we complemented the RNAi cell lines with a lysine-50 to alanine mutant of *Hs* eIF5A that cannot be hypusinated. This mutant is unable to rescue the growth defect, highlighting the importance of modifying lysine-50 with hypusine for the essential function of eIF5A. It has not been established whether complete modification to hypusine is required or if deoxyhypusine can be sufficient. In *S. cerevisiae* and *S. pombe*, modification of the lysine to deoxyhypusine is required but subsequent hydroxylation to hypusine is not essential, as it is in multicellular eukaryotes. Fundamentally, despite its early divergence in eukaryotic evolution, *T. brucei* is similar to other eukaryotes in its requirement for eIF5A and modification of a highly specific lysine (*TbeIF5A* lysine-52) for normal cell growth.

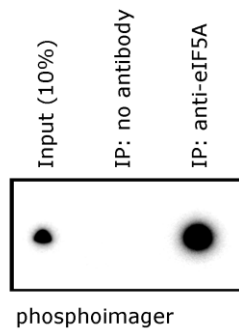


Figure 3.1. ^{14}C -Putrescine labeling and immunoprecipitation of eIF5A from procyclic-form cells. Cell lysates of cells incubated with ^{14}C -putrescine were immunoprecipitated (IP) with no antibody or anti-eIF5A antibody. The proteins were separated by SDS-PAGE and transferred to PVDF membrane before exposure to a phosphor storage screen. Shown is the phosphoimager scanned image. Left lane: cell lysate, center lane: IP with no antibody, right lane: IP with anti-eIF5A antibody.

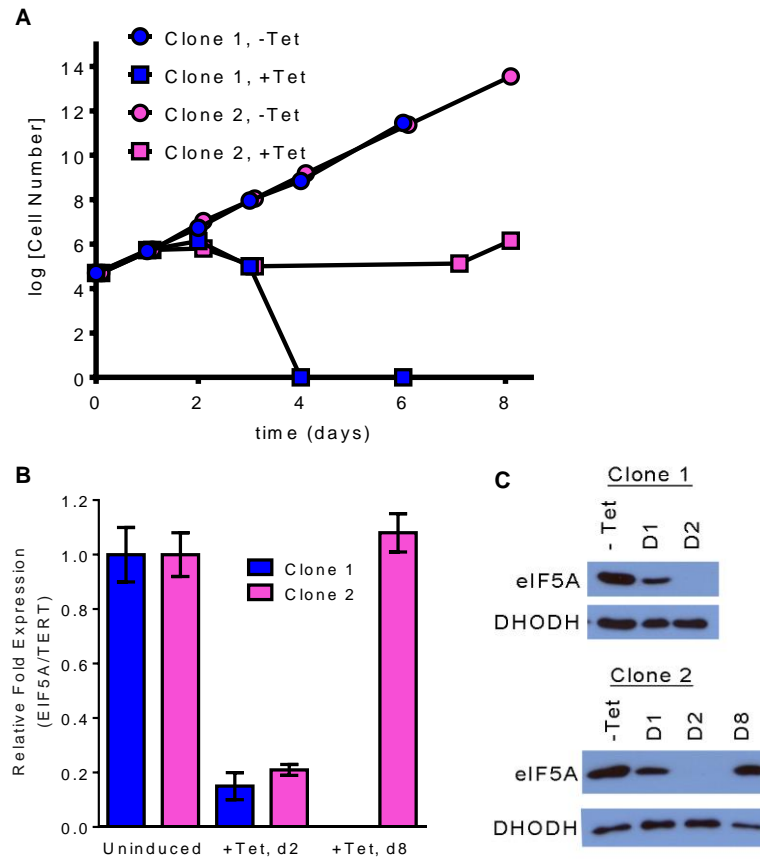


Figure 3.2. Knockdown of *EIF5A* in bloodstream-form cells. (A) The growth of BSF *EIF5A* RNAi cells in the presence (squares) and absence (circles) of Tet over time is plotted. Cell number (cell density x volume x dilution factor). (B) Quantification of eIF5A mRNA by qRT-PCR using *TERT* as reference gene and normalized to expression in uninduced cells. (C) Western blot analysis of soluble protein (20 μ g) in uninduced (-Tet) cells and cells induced with Tet for 1 (D1), 2 (D2), and 8 (D8) days. The blots were probed with anti-eIF5A antibody to determine knockdown and with anti-DHODH antibody as a loading control.

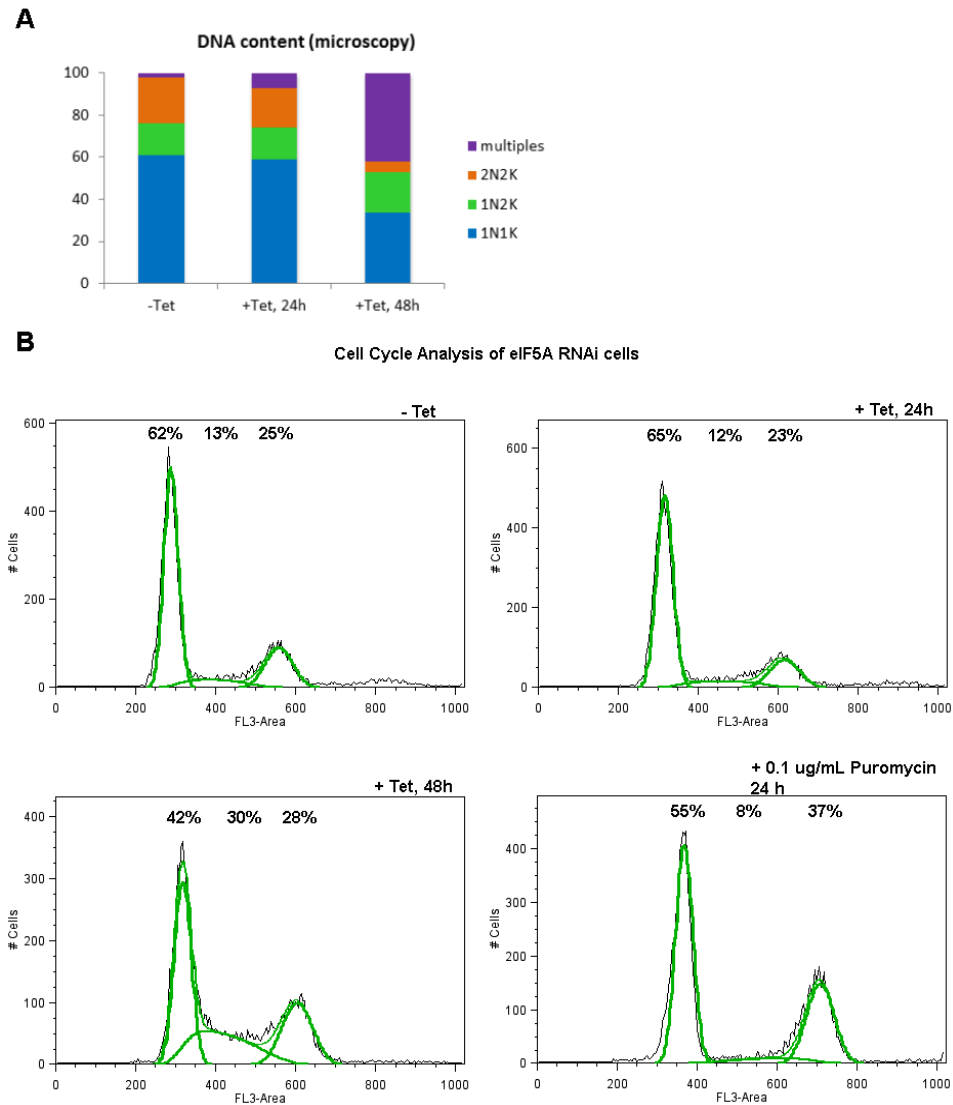


Figure 3.3. Cell cycle analysis of bloodstream-form *EIF5A* RNAi cells. (A) Percentage of cells containing 1N1K (blue), 1N2K (green), 2N2K (orange) as determined by visualization of DAPI stained cells, $n = 100/\text{timepoint}$. (B) Cell cycle analysis of propidium iodide-stained cells as counted by flow cytometry, $n=10,000/\text{sample}$.

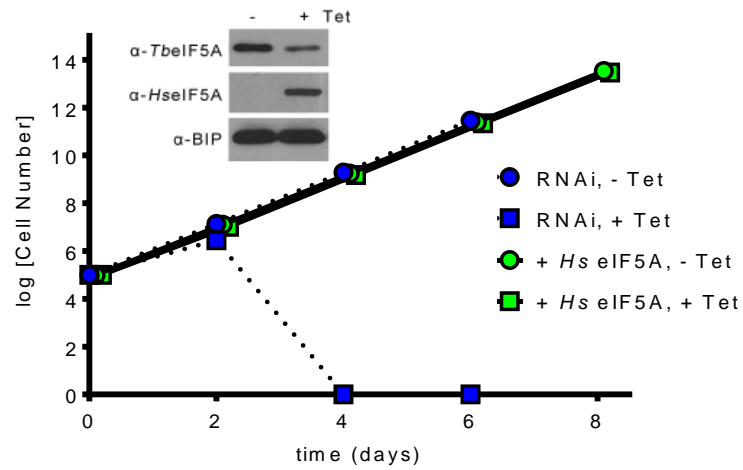


Figure 3.4. Complementation of *EIF5A* knockdown with *Hs* eIF5A in bloodstream-form cells. A growth curve of BSF *EIF5A* RNAi cells without (blue) and with (green) complementation with *Hs* eIF5A. Cell number = cell density x volume x dilution factor. (Inset) Western blot analysis soluble protein (20 μ g) from BSF *EIF5A* RNAi + *Hs* eIF5A, uninduced (- Tet) and day 2 of induction (+Tet).

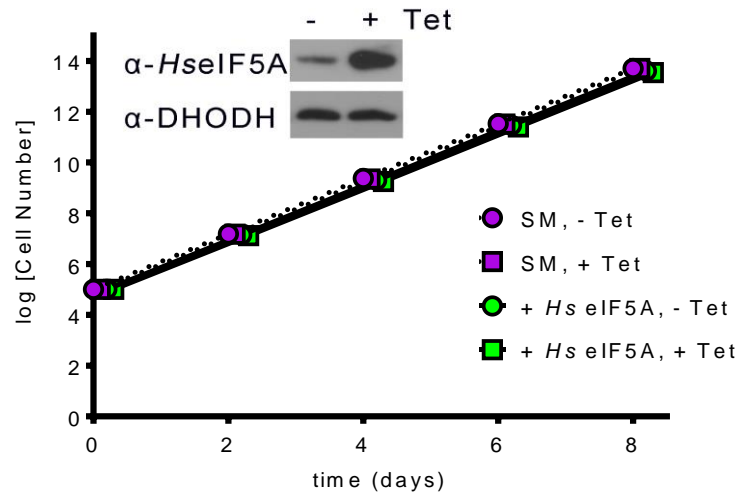


Figure 3.5. Overexpression of *Hs* eIF5A in ‘single marker’ bloodstream-form cells. A growth curve of induced (circles) and uninduced (squares) ‘single marker’ cells (SM) and SM cells overexpression *Hs* eIF5A (green). Cell number = cell density x volume x dilution factor. (Inset) Western blot analysis of soluble protein (30 μ g) from SM + *Hs* eIF5A cells, uninduced (- Tet) and day 2 of induction (+Tet).

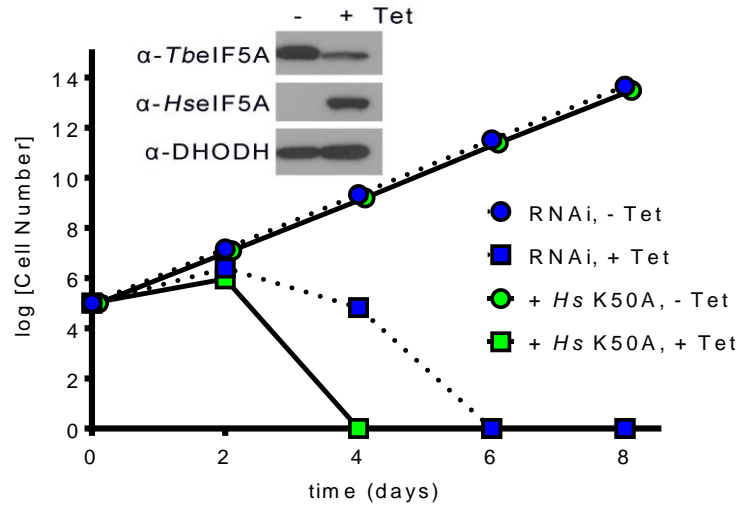


Figure 3.6. Complementation of *EIF5A* knockdown with *Hs* eIF5A^{K50A} in bloodstream-form cells. A growth curve of induced (circles) and uninduced (squares) BSF *EIF5A* RNAi cells without (blue) and with complementation with *Hs* eIF5A^{K50A} (green). Cell number = cell density x volume x dilution factor. (Inset) Western blot analysis of soluble protein (20 µg) from BSF *EIF5A* + *Hs* eIF5A^{K50A} cells, uninduced (- Tet) and day 2 of induction (+Tet).

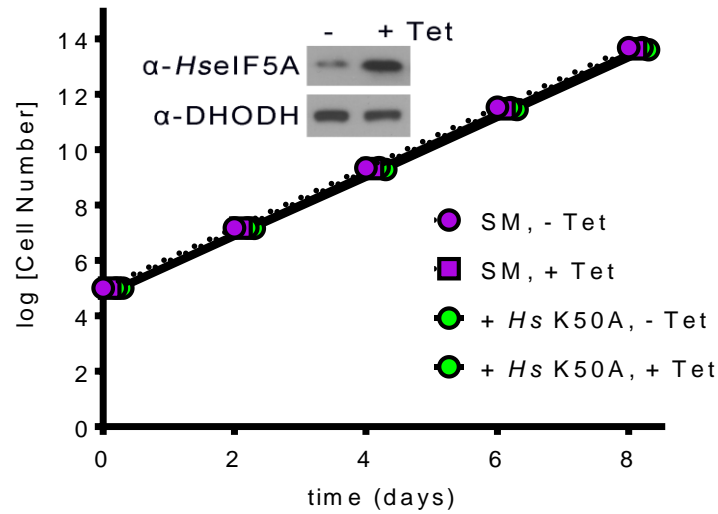


Figure 3.7. Overexpression of *Hs* eIF5A^{K50A} in 'single marker' bloodstream-form cells. A growth curve of induced (circles) and uninduced (squares) 'single marker' cells (SM) and SM cells overexpression *Hs* eIF5A^{K50A} (green). Cell number = cell density x volume x dilution factor. (Inset) Western blot analysis of soluble protein (30 μ g) from SM + *Hs* eIF5A^{K50A} cells, uninduced (- Tet) and day 2 of induction (+Tet).

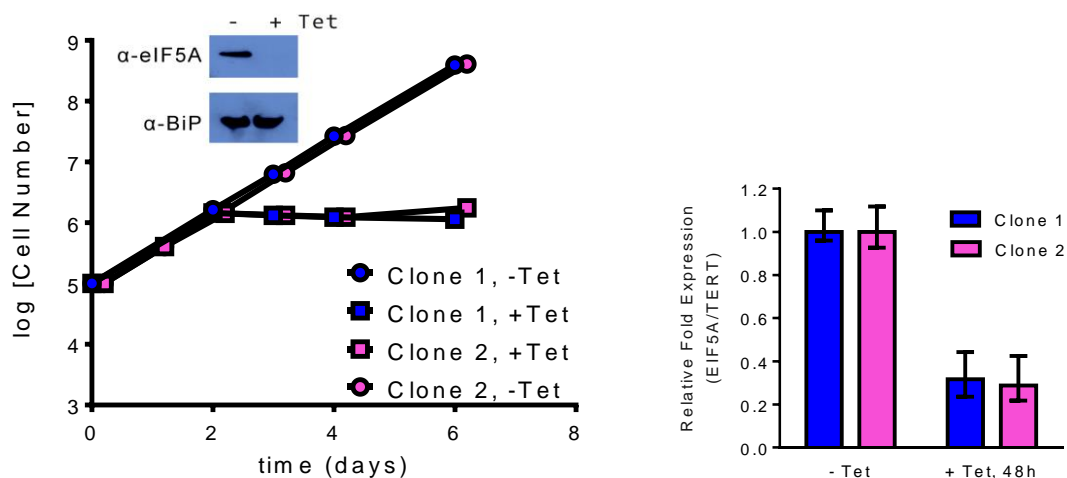


Figure 3.8. Knockdown of *EIF5A* in procyclic-form cells. (A) The growth of uninduced (circles) and induced (squares) PF *EIF5A* RNAi cells over time is plotted. Cell number (cell density x volume x dilution factor). (Inset) Western blot analysis of soluble protein (20 μ g) from uninduced (-Tet) cells and cells induced with Tet 2 days (+Tet). (B) Quantification of *eIF5A* mRNA by qRT-PCR using *TERT* as reference gene and normalized to expression in uninduced cells. The blots were probed with anti-eIF5A antibody to determine knockdown and with anti-DHODH antibody as a loading control.

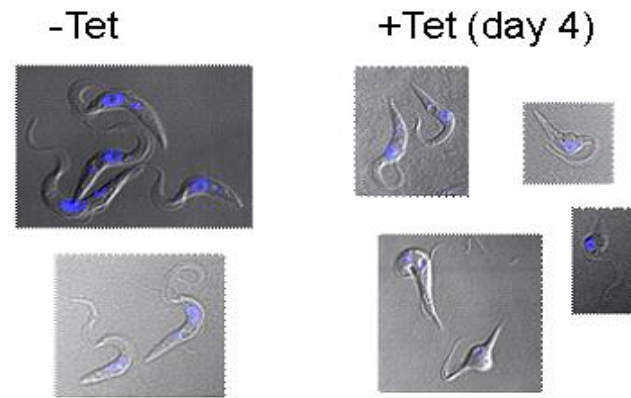


Figure 3.9. Imaging of DAPI-stained procyclic-form *EIF5A* RNAi cells. Cells were fixed and stained with DAPI prior to imaging with a confocal microscope. Shown are merged UV fluorescence and brightfield images of uninduced (-Tet) and induced (+Tet) cells.

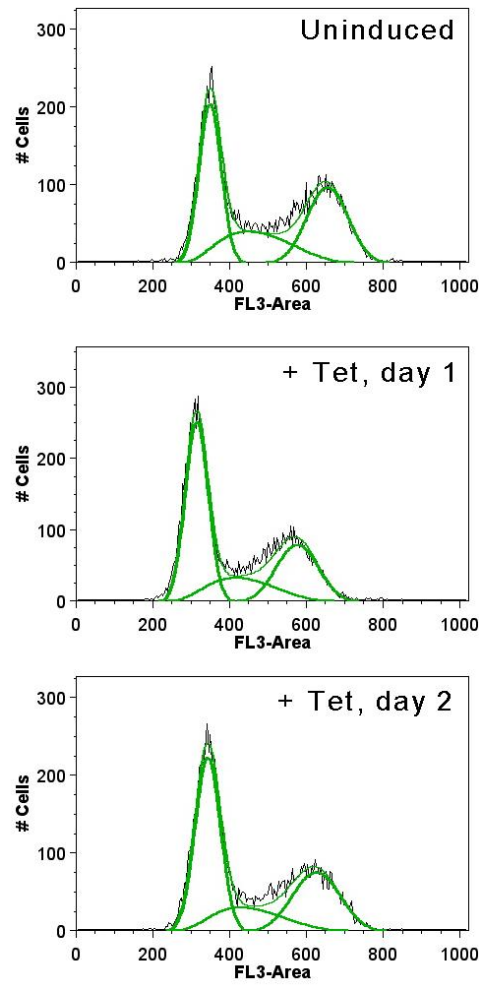


Figure 3.10. Cell cycle analysis of procyclic-form *EIF5A* RNAi cells. Cells in which knockdown was uninduced (top) or induced with Tet for 1 day (middle) or 2 days (bottom) were stained with propidium iodide and counted by flow cytometry. Cell-cycle distribution was then fitted based on PI signal using FlowJo, n=10,000/sample.

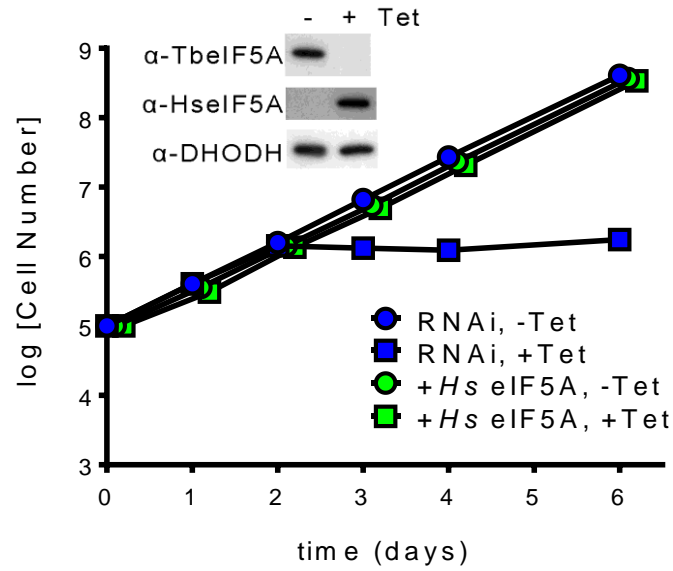


Figure 3.11. Complementation of *EIF5A* knockdown with *Hs* eIF5A in procyclic-form cells. A growth curve of PF *EIF5A* RNAi cells without (blue) and with (green) complementation with *Hs* eIF5A. Cell number = cell density x volume x dilution factor. (Inset) Western blot analysis soluble protein (20 ug) from BSF *EIF5A* RNAi + *Hs* eIF5A, uninduced (- Tet) and day 2 of induction (+Tet).

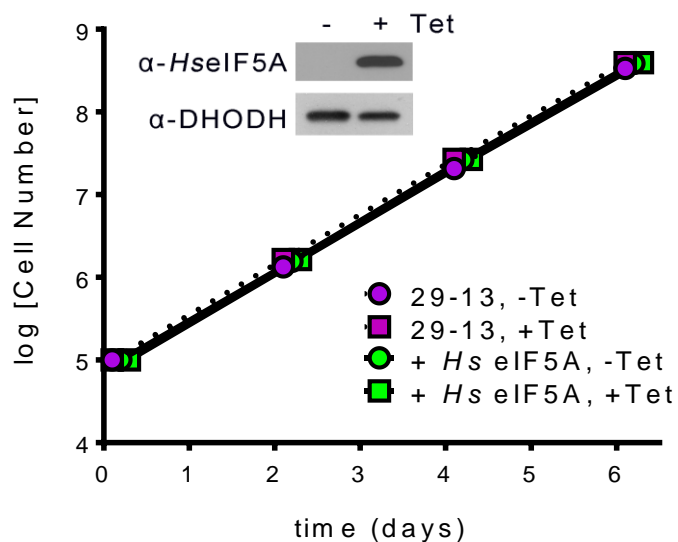


Figure 3.12. Overexpression of *Hs* eIF5A in 29-13 procyclic form cells. A growth curve of induced (circles) and uninduced (squares) “wildtype” 29-13 cells (purple) and 29-13 cells overexpression *Hs* eIF5A (green). Cell number = cell density x volume x dilution factor. (Inset) Western blot analysis of soluble protein (20 μ g) from SM + *Hs* eIF5A cells, uninduced (- Tet) and day 2 of induction (+Tet).

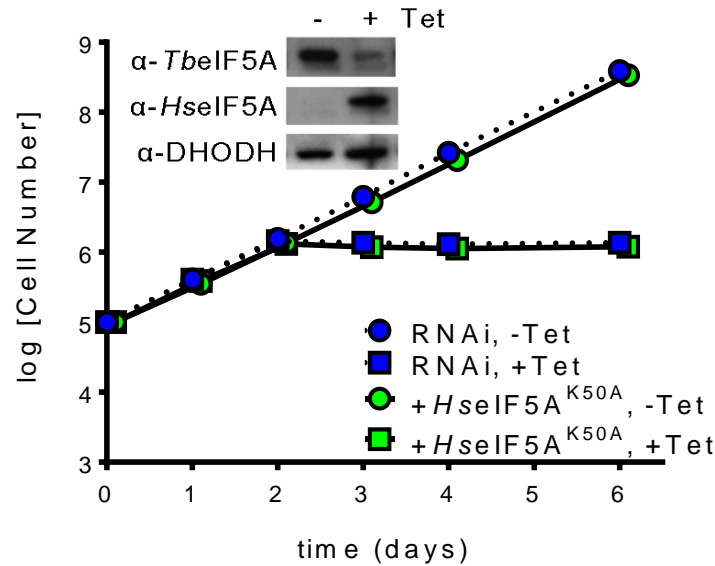


Figure 3.13. Complementation of *EIF5A* knockdown with *Hs* eIF5A^{K50A} in procyclic form cells. A growth curve of induced (circles) and uninduced (squares) PF *EIF5A* RNAi cells without (blue) and with complementation with *Hs* eIF5A^{K50A} (green). Cell number = cell density x volume x dilution factor. (Inset) Western blot analysis of soluble protein (20 μ g) from PF *EIF5A* + *Hs* eIF5A^{K50A} cells, uninduced (- Tet) and day 2 of induction (+Tet).

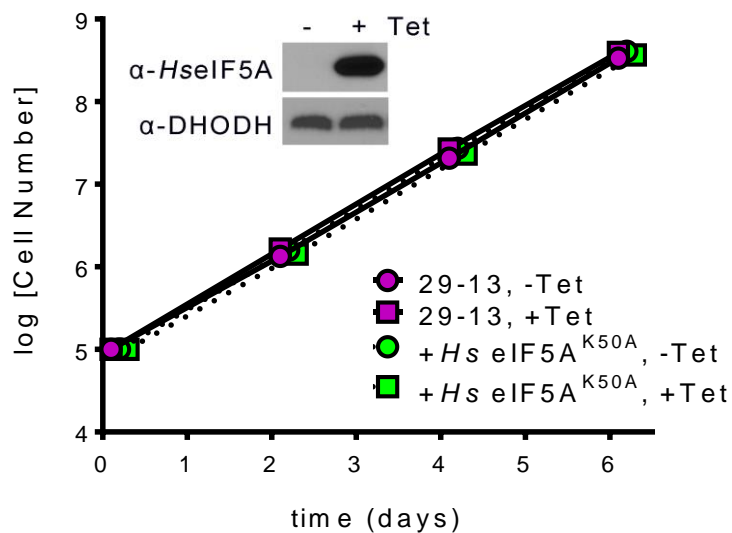


Figure 3.14. Overexpression of *Hs* eIF5A^{K50A} in 29-13 procyclic-form cells. A growth curve of induced (circles) and uninduced (squares) 29-13 procyclic-form cells (purple) and 29-13 cells overexpression *Hs* eIF5A^{K50A} (green). Cell number = cell density x volume x dilution factor. (Inset) Western blot analysis of soluble protein (30 µg) from SM + *Hs* eIF5A^{K50A} cells, uninduced (- Tet) and day 2 of induction (+Tet).

CHAPTER FOUR

Exploring the Requirement for Hypusination

I. INTRODUCTION

Last year, Doerfel et al. reported that EF-P, the bacterial homolog of IF5A, promoted the translation of polyproline stretches (31). Using engineered constructs containing various amino acid triplets with and without polyproline repeats, they demonstrated that *E. coli* ribosomes stalled on PP sequences. Addition of *Ec* EF-P to the *in vitro* transcription system was able to alleviate the stalling and the effects of EF-P are specific to PPP and PPG stalling. Furthermore, this effect was dependent on the post-translation lysinylation of EF-P lysine-34.

Based on these results, Gutierrez et al of the Dever lab were able to establish an analogous role for eIF5A in eukaryotic cells (32). Using a dual luciferase system, they demonstrated that translation of a 20 amino acid peptide containing a single proline was impaired in an eIF5A temperature sensitive mutant under restrictive conditions compared to proline-minus peptides. With regards to consecutive proline motifs, decreased translation was observed with 3 or more prolines but unlike for bacteria, not with two consecutive prolines or stretches of phenylalanine. Again, it was demonstrated that the post-translational modification of eIF5A, particularly deoxyhypusine, was required to alleviate stalling. In *in vitro* assays, the stalling typically occurred on the second or third proline in a run of polyproline. Studies prior to this discovery had implicated eIF5A in cytoskeleton maintenance because depletion of eIF5A in *S. cerevisiae* resulted in misshapen cells that were more sensitive to ethanol (52). Since then, several examples of actin-related proteins that contain polyproline tracts have been proposed to explain the phenotype (33). However, it

remains to be validated how eIF5A affects the translation of endogenous polyproline proteins are translated.

II. POLYPROLINE TRACTS IN *T. BRUCEI*

Interested in abundance of polyproline tracts in trypanosomes, with the aide of Lisa Kinch (Grishin lab, UTSW) I analyzed the *T. brucei* proteome for polyproline motifs and classified the proteins based on the number of consecutive prolines in the protein. Of the 7,835 predicted encoded proteins, only 55 were completely devoid of prolines (Figure 4.1). On average, proline comprises 5% of the peptide sequence of a protein. 1210 proteins (15%) contain consecutive proline stretches of 3 or greater (Figure 4.2). Of these, 855 (71%) are annotated as hypothetical proteins due to poor sequence homology with known proteins.

Interestingly, 19 predicted proteins contain polyproline tracts of more than 8 consecutive prolines and most of these are putative cysteine peptidases. Other polyproline proteins include *bona fide* cysteine peptidases, actin-related proteins, and zinc finger proteins. Further identification of the polyproline proteins revealed interesting trypanosome-specific proteins. An atypical variant surface glycoprotein (VSG, Tb927.9.17050) and retrotransposon hot spot protein 3 (RHSP3, Tb927.9.15810) both encode 5 consecutive prolines. One other atypical VSG and putative VSG also contain 3 consecutive prolines. The procyclin (EP) proteins are also proline-rich, but rather than encoding consecutive prolines, they encode glutamine-proline (EP) repeats, which have not yet been shown to induce ribosome stalling.

III. DISCUSSION

As a start towards understanding the implications of eIF5A function in polyproline translation, we used bioinformatics to find polyproline-containing proteins in *T. brucei*. Fifteen percent of the trypanosome proteome encoded proteins containing 3 or more consecutive prolines by comparison to 23% of human proteins (33). That so many *T. brucei* proteins contain three or more consecutive proline stretches supports the current popular hypothesis that eIF5A is a semi-global elongation factor. However, it remains a mystery if eIF5A is involved in translation of all polyproline-containing proteins or just a subset. Because proline-rich regions are known to bind SRC Homology 3 (SH3) domains that are involved in cytoskeleton organization (53), potential regulation of eIF5A could regulate cytoskeleton changes.

A potential specialized function for eIF5A is possible in the translation of the *T. brucei* surface coat proteins VSGs and EPs. VSGs are expressed in the bloodstream-form of the parasite lifecycle and form a dense surface coat. *T. brucei* contain more than 1000 VSG genes which permit antigenic variation that allows the parasite to evade the host adaptive immune system (54). During the insect stage, VSGs are silenced and the parasite expresses a dense coat of procyclins. This switch is dependent on the rapid degradation of VSGs and subsequent expression of procyclins. Interestingly, cysteine peptidases (CP) have been shown to be instrumental in the degradation of VSG during surface coat exchange (55). The trypanosomal CPs that contain more than 8 consecutive prolines may therefore be involved in the coordination of the process. In analyzing the *T. brucei* proteome, we have identified

promising candidates for the future study of eIF5A function in translation of endogenous proteins including several candidates that may lead to a specialized role or demand for eIF5A in the parasite.

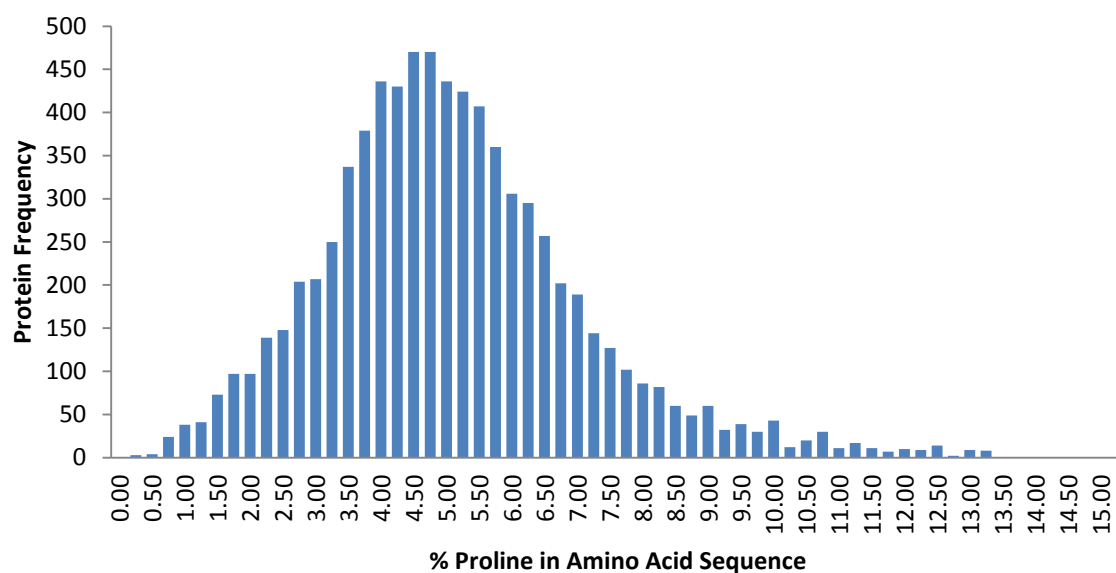


Figure 4.1. Proline composition of *T. brucei* proteins. A bar graph illustrating the distribution of percentage of prolines present in the amino acid sequences of *T. brucei* proteins. Total proteins = 7835.

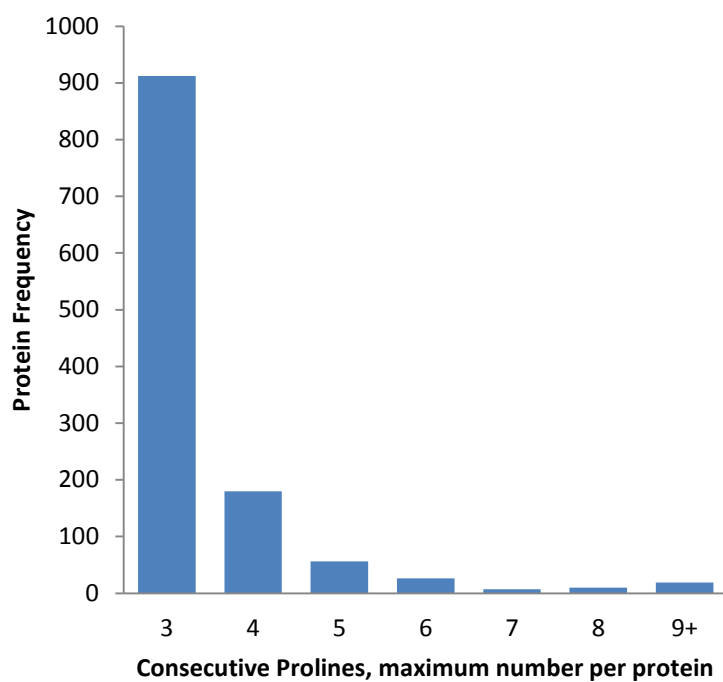


Figure 4.2. Frequency of polyproline stretches in *T. brucei* proteome Distribution of proteins containing 3 or more consecutive prolines; n = 1210.

CHAPTER FIVE

T. brucei DEOXYHYPUSINE SYNTHASE

I. INTRODUCTION

A specialized but essential function of the polyamine spermidine in eukaryotic cells is to serve as a precursor for the hypusine modification of eukaryotic initiation factor 5A (eIF5A) (50). Synthesis of hypusine requires two enzymatic reactions catalyzed by deoxyhypusine synthase (DHS) and deoxyhypusine hydroxylase. DHS catalyzes the modification of eIF5A lysine (Lys-50 of the human protein) to deoxyhypusine in a 4-step NAD^+ -dependent reaction that proceeds through two imine intermediates (Figure 5.1) (56). The reaction is highly specific; no other proteins in the cell are known to be hypusine-modified. The X-ray structure of human DHS shows the protein is a homotetramer formed from a dimer of dimers with each dimer containing two active sites at the interface between monomers (57).

Genomes of kinetoplastids such as *T. brucei* and *Leishmania* species encode two homologs of mammalian DHS. In *L. donovani*, one of these homologs was shown to be essential and to encode an active DHS (LmDHS34), though activity was significantly lower than for the mammalian enzyme (21). The functional role of the second DHS homolog was unknown. Herein we show that both DHS homologs in *T. brucei* are essential for growth *in vitro* and for survival in a mouse infection model. We further demonstrate that, analogously to AdoMetDC, the two DHS genes encode one catalytically weakly active DHS subunit and one catalytically dead subunit that associate as a heterotetramer to form the active enzyme

commensurate with a 3000-fold increase in catalytic activity. These data demonstrate that the trypanosomatids have independently evolved an analogous regulatory strategy to control activity of two key enzymes involved in polyamine synthesis and function through oligomerization with a catalytically dead paralog. Trypanosomatids represent the only known species where this regulatory strategy is used to control activity of DHS and AdoMetDC. The finding of two independent occurrences in the same pathway suggests that in the absence of transcriptional regulation the parasites are under evolutionary pressure to find novel mechanisms to control flux through essential pathways.

II. IDENTIFICATION OF DHS

A BLASTP analysis of the trypanosomatids and representative members of eukaryotic superfamilies for homologs of human DHS (NP_001921.1) revealed 2 distinct clusters of *DHS* gene products (Figure 5.2). Multiple sequence alignment and comparison of key residues showed that one cluster encodes a protein that contains the catalytic lysine that has been shown to form the imine intermediate with substrate (Figure 5.3)(50,57), while the other DHS group lacks the catalytic lysine despite containing many putative substrate-binding residues. The two gene clusters encoding these proteins are present on different chromosomes. We refer to the *T. brucei* gene products as DHSc (Tb927.10.2750, the “c” indicating the presence of the catalytic lysine), and DHSp (Tb927.1.870, the “p” for prozyme, indicating a non-catalytic function). *TbDHSc* exhibits 28% amino acid sequence identity with human DHS (*HsDHS*) but is 92 amino acids larger due to internal expansions. *TbDHSp* shares 40% identity with human DHS but only 30% identity with *TbDHSc*.

Trypanosoma cruzi, *Leishmania* species, and *Entamoeba* species also encode divergent DHS homologs (Figure 5.2). Each species encodes for one homolog of DHSc and one homolog of DHSp with the exception of *T. cruzi* which has two DHSc homologs (*TcDHS(B)* and *TcDHS(C)*) that cluster together on the tree and share 97% sequence identity. It is not clear if a single gene duplication event led to the generation of both the trypanosomatid DHSp and *Entamoeba* DHSp homologs or if they arose from independent events. The other eukaryotes queried contain either only a single *DHS* gene or closely related gene duplicates, all of which contain the catalytic lysine. The catalytic lysine-deficient DHS (DHSp) appears unique to kinetoplastids and *Entamoeba* (Figure 5.3).

III. ESSENTIALITY OF DHS PARALOGS IN *T. BRUCEI*

RNAi knockdown of TbDHS genes

The *DHSp* and *DHSc* sequences are sufficiently divergent for specific targeting of each gene by RNAi. Using the same method described for *EIF5A* knockdown, we generated Tet-inducible RNAi cell lines targeting *DHSc* or *DHSp* in bloodstream-form *T. brucei* SM cells to determine if gene knockdown was detrimental to cell growth. Induction of *DHSc* knockdown resulted in 35-45% reduction of *DHSc* mRNA and had no effect on the growth rate of the cells (Figure 5.4). Similarly, induction of DHSp knockdown only resulted in 35-40% reduction of DHSp mRNA and again, no effect on cell growth was observed over 8 days of induction (Figure 5.5). A negative result from RNAi does not address essentiality since it is possible that the remaining >50% of mRNA is sufficient to sustain production of

protein for cell growth, and as such, the results from gene knockdown were insufficient to determine the essentiality of DHSc and DHSp.

Conditional knockout mutants of TbDHS genes

We generated conditional knockout cell lines of the *DHSc* and *DHSp* genes in the *T. brucei* bloodstream-form (BSF) ‘single marker’ cells to determine if one or both of the DHS genes were essential for cell growth. Because *T. brucei* is a diploid organism, one of the two endogenous loci was replaced with the hygromycin-resistance antibiotic selection marker to generate the single knockout (SKO) cell lines, in which a Tet-regulated copy of the respective DHS genes was inserted into the rDNA spacer region to serve as a rescue copy. The second locus was then replaced with a blasticidin-resistance marker generating the final conditional double knockout (cDKO) cell lines. Two independent cDKO lines were generated for each gene.

The *DHSc* and *DHSp* cDKO lines were initially evaluated for growth defects *in vitro*. For the *DHSc* conditional knockout mutant, removal of Tet led to loss of *DHSc* expression (>90%) within 24 h, slowed growth by day 4, and complete parasite lysis by day 6 (Figure 5.6). Likewise for the *DHSp* cDKO parasites no detectable DHSp protein (>90% knockdown) was observed 24 h after Tet withdrawal and cell death occurred by day 8 (Figure 5.7). Cultures were monitored by microscopy for an additional 4 days after cell death and no live parasites were observed. These data demonstrate that both DHSc and DHSp are essential for survival of BSF *T. brucei* *in vitro*.

DHS is essential for infectivity of T. brucei in mice.

In a collaboration, the *DHSc* and *DHSp* cDKO lines were used by Alan Fairlamb's group (University of Dundee) to infect mice to determine if the gene products were essential for parasite survival *in vivo*. Mice were inoculated with *DHSc* and *DHSp* cDKO lines and with the parental SM strain. One set of animals received doxycycline (Dox) in their drinking water to maintain expression of the respective DHS proteins, while for the other set Tet was removed 24 hours prior to inoculation and mice were not administered Dox. Mice infected with the cDKO line of *DHSc* or *DHSp* that received Dox in their water succumbed to parasitemia by day 6 after inoculation and showed an identical time course to mice infected with the control parental SM cell line (Figure 5.6C and 5.7C). By contrast, in the absence of Dox, mice infected with the *DHSc* cDKO line survived to the end of the experiment (day 30), at which time they remained parasite free and were assumed to be cured (Figure 5.6C). Mice infected with the *DHSp* cDKO line showed a prolonged survival time, but eventually succumbed to parasitemia on day 24 after infection (Fig. 5.6C). The relapse of parasitemia in the *DHSp* cDKO infection suggests that a small number of parasites survived most likely through mutation in the Tet promoter, allowing re-expression of the *DHSp* protein, as previously documented for other proteins with this system (35). These data demonstrate that *DHSc* and *DHSp* are essential to sustain an *in vivo* infection of *T. brucei* in mice.

DHSc and DHSp form a complex in BSF T. brucei parasites

Further analysis of *DHSp* paralog in the cDKO cell lines was enlightening. In the *DHSc* cDKO, upon Tet removal and depletion of *DHSc*, loss of endogenous *DHSp* protein was also observed by Western blot despite no change in relative expression of *DHSp* RNA

(Figure 4.6A). DHSc protein was also lost upon Tet removal and loss of DHSp in the DHSp cDKO cell lines (Figure 5.7A). These data suggest the stability of DHSc and DHSp are dependent on one another and hint that DHSc and DHSp may form a complex within the cell.

To determine if DHSc and DHSp form a complex we generated a stable BSF cell line that co-expressed N-terminally tagged AU1-DHSc and FLAG-DHSp. Immunoprecipitation of AU1-DHSc from soluble BSF *T. brucei* lysates using monoclonal antibody to AU1 was performed followed by western blot analysis with anti-AU1 and anti-Flag antibody. Both AU1-DHSc and FLAG-DHSp were found in the immunoprecipitate (Figure 5.8A). Likewise if a monoclonal antibody to FLAG was used for immunoprecipitation both AU1-DHSc and FLAG-DHSp were detected. Thus DHSc and DHSp form a protein complex in *T. brucei* BSF cells.

IV. FUNCTIONAL CHARACTERIZATION OF *Tb*DHS

Formation of a complex between DHSc and DHSp is required for enzymatic activity.

DHSC, *DHSP*, and *eIF5A* were cloned from *T. brucei* genomic DNA into vectors for expression in *Escherichia coli*. Human DHS and human eIF5A expression vectors were also generated to serve as controls. Each protein was expressed with an N-terminal His₆-SUMO tag, purified by Ni⁺²-affinity chromatography, and digested with yeast SUMO protease, Ulp1, to generate tag-free proteins. The ability of purified recombinant DHS to catalyze hypusine modification of eIF-5A was measured with either *T. brucei* or human eIF5A as substrate using ³H-spermidine and a filter-binding assay (58,59). Multiple DHS activity assays have been published, most utilizing radiolabelled spermidine as the substrate. To

measure DHS activity, I adapted a filter binding assay. The reaction containing recombinant DHS, eIF5A and ^3H -spermidine was diluted with a cold spermidine/PBS solution, applied to nitrocellulose using a BioDot device, washed with cold spermidine/PBS, and then dried. Each dot was then separated, added to scintillation fluid, and the radioactivity was then measured using a scintillation counter. The specific activity of purified DHSc using *T. brucei* eIF5A (*TbeIF5A*) as substrate was 1000-fold lower than the activity of human DHS (Table 5.1), the latter of which was in agreement with previous reports (60,61). The low observed activity of *Tb*DHSc was similar to that reported for the *Leishmania* homolog *Lm*DHS34 (21). No activity was detectable for DHSc with human eIF5A as the substrate. Recombinant DHSp showed no activity within the limit of detection with either eIF5A substrate (Table 5.1).

In order to assess the activity of the DHSc:DHSp protein complex, tagless DHSp was co-expressed with His₆-SUMO-DHSc in *E. coli*. DHSp co-purified with DHSc during Ni⁺²-affinity chromatography (Figure 5.8). The SUMO tag was removed as described above and the tag-free DHSc:DHSp protein complex was further purified by size exclusion gel filtration column chromatography. DHSc and DHSp were present in approximately equal molar amounts in the peak fraction confirming that the two paralogs form a stable complex (Figure 5.8B). The purified complex was next analyzed by velocity sedimentation analytical ultracentrifugation. A single species of MW 175 kD was observed in this analysis consistent with the size of a heterotetrameric species (Figure 5.8C). The specific activity of the heterotetrameric complex was 0.01 s^{-1} , which was ~3000-fold higher than for the DHSc homotetramer, and comparable to the levels of human DHS (Table 5.1). The K_m^{app} for NAD⁺

and spermidine were in the 40 - 80 μM range, about 10-fold higher than reported for human DHS (61) whereas the K_m for *Tb*_eIF-5A at 0.7 μM (Table 5.2) is similar to human DHS. These data demonstrate that *in vitro* the fully functional *Tb*DHS is the heterotetrameric enzyme complex of DHSc:DHSp. Efforts to crystallize the complex and solve the protein structure have not been successful thus far.

To further characterize the enzymatic reaction we determined if we could trap the imine intermediate on the *Tb*DHS catalytic lysine and or on eIF5a. Reaction mixtures containing ^3H -spermidine were treated with sodium cyanoborohydride, TCA precipitated, and separated by SDS-PAGE. Incorporation of tritiated label was detected by exposure of the enhanced gel to X-ray film. In reactions containing DHSc:DHSp and *Tb*eIF5A, two bands were detected: a strong band corresponding in size to eIF5A and a weaker band corresponding to DHSc (Figure 5.9), consistent with the transient labeling of DHS during the reaction, followed by the transfer of the labeled substrate to eIF5A, resulting in hypusine modification. No labeling of either eIF5A or of DHS was detected for reactions containing only DHSc or DHSp as the catalyst, again showing that, on its own, DHSc is highly impaired in catalytic function, and that it becomes fully functional only in complex with DHSp.

V. INHIBITION OF DHS ACTIVITY

N1-Guanyl-1, 7-diaminoheptane (GC7) is a structural analog of spermidine and a known inhibitor of *Hs*DHS (62). GC7 inhibited the activity of recombinant DHSc:DHSp with an $\text{IC}_{50} = 1.5 \pm 0.15 \mu\text{M}$ (Figure 5.10). When bloodstream-form parasites were treated with GC7, the compound killed cells with an $\text{EC}_{50} = 8.0 \pm 1.5 \mu\text{M}$. When AU1-*Tb*DHSc or

FLAG-TbDHSp were independently over-expressed in BSF cells there was not a significant shift in the EC_{50} for GC7 ($EC_{50} = 5 - 6 \mu M$). However over-expression of AU1-DHSc and FLAG-DHSp together reduced sensitivity to GC7 ($EC_{50} = 26 \pm 3.0 \mu M$). Cell lines expressing decreased DHSc and DHSp (the SKO lines) were somewhat more sensitive ($EC_{50} = 3.8 \pm 0.4$ and 5.5 ± 0.84 , respectively). These data suggest that the mechanism of action of cell killing by GC7 is mediated by DHS inhibition, providing further evidence that DHSc:DHSp is the functional DHS species in *T. brucei*.

VI. DISCUSSION

Trypanosomatids and *Entamoeba* differ from other typical eukaryotes because they encode two distinct DHS homologs. We chose to examine the *T. brucei* DHS to better understand the essentiality and purpose of the conserved catalytically dead DHS homolog, DHSp. Conditional knockout mutants in bloodstream-form trypanosomes of each DHS gene showed loss of DHSc or DHSp led to cell death. DHSc and DHSp are also required for infectivity in mice. Studies with GC7, a known DHS inhibitor, further validated DHS as a potential drug target for treatment of HAT. In the course of our studies, we discovered that the *TbDHS* is particularly interesting because the catalytically impaired paralog, DHSc, and the dead paralog, DHSp, form a heterotetramer that is 3000-fold more active than DHSc alone, recapitulating the activation seen with AdoMetDC prozyme.

Regulation and control of gene expression, and modulation of enzyme activity are critical aspects of cellular function. Although diverse mechanisms for regulating enzyme activities are well known, we report here a new paradigm for enzyme regulation of

polyamine/hypusine biosynthesis based on activators that are catalytically dead enzyme paralogs termed prozymes. We discovered that, remarkably, parasitic trypanosomatid protozoa have independently evolved this mechanism in two different steps in the same essential biochemical pathway, the biosynthesis of spermidine and the hypusine modification of the translation led to the evolution of a novel regulatory mechanism in which one paralog retains limited catalytic function and the other has lost key catalytic residues but retained the ability to oligomerize with the impaired active paralog, thereby greatly enhancing catalytic activity. A pivotal feature of this model is that observed activation by the prozyme component is dramatically large (1,000- to 3,000-fold) and is thus likely to result from cooperative structural changes.

Inactive paralogs have been identified in a wide variety of gene families in metazoan species though they are most prevalent in the kinase, protease and RAS-like protein families, (63-65). Inactive paralogs are perfectly poised to play regulatory roles, retaining the ability to bind both ligands and regulatory molecules. It has been shown that when duplicate genes evolve complementary mutations the ability of cells to maintain both duplicates is enhanced, allowing novel function to evolve (66), and thus providing a platform for the evolution of a regulatory function. While there is still limited functional data on the roles of inactive paralogs, examples of regulation by both inhibitory and activating mechanisms have been described, though most of the examples involve inhibition or dominant negative effects. However, the sheer magnitude of the activation observed for *T. brucei* DHS and AdoMetDC

is unprecedented, and the observation that regulation is occurring in a primary metabolic pathway and for two enzymes within the same pathway is also novel.

In conclusion, the ability to regulate enzyme activity with a catalytically dead paralog provides cells with another tool for post-transcriptional regulation. Trypanosomatids represent the only known species where this regulatory strategy is used to control activity of DHS and AdoMetDC. The evolution of the prozyme mechanism in the trypanosomatids was most likely driven by the need to control polyamine synthesis and function in an organism that lacks transcriptional control of gene expression and the frame-shifting and uORF-based mechanisms employed by many other eukaryotes. The discovery of this novel regulatory control strategy first for AdoMetDC and now for DHS powerfully confirms the importance of polyamines in the parasite, first exemplified by the discovery of the role of the spermidine–glutathione conjugate trypanothione in the parasite (67). Our data suggest that the paradigm of enzyme activation by a catalytically dead paralog may be more widespread in trypanosomatids than currently known, and indeed, many additional examples of this mechanism for the regulation of enzyme function in eukaryotic cells are likely still undiscovered.

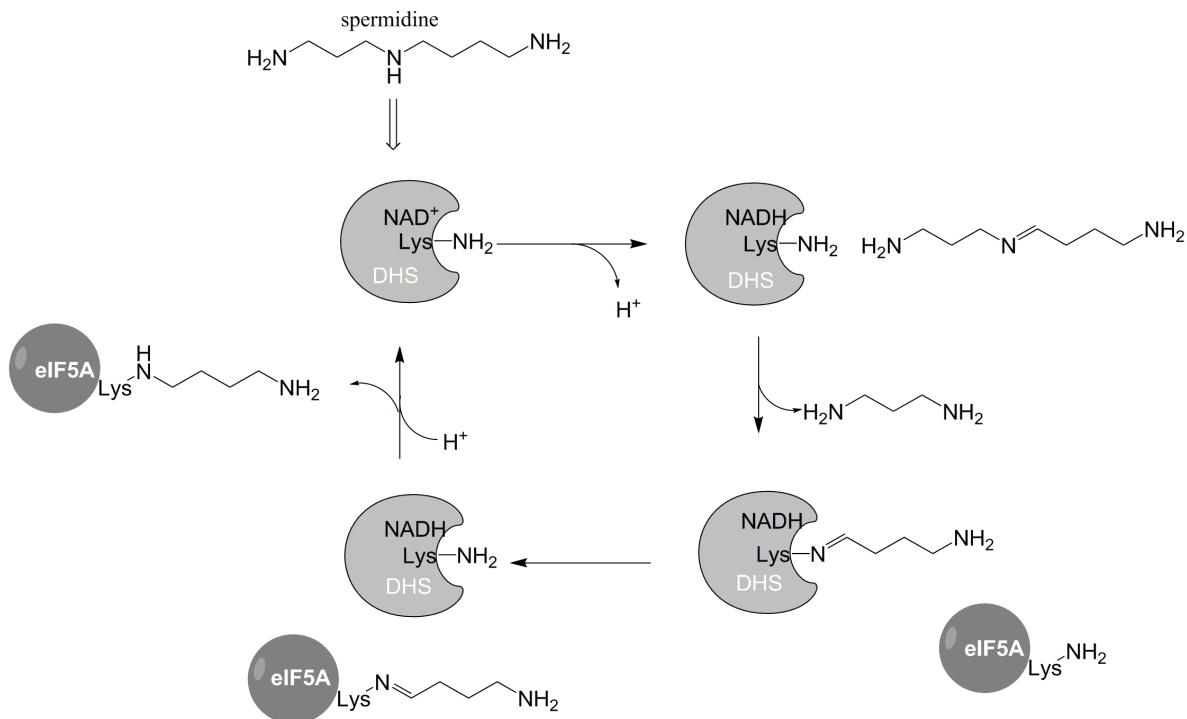


Figure 5.1. Reaction scheme for deoxyhypusine synthase. A schematic of the deoxyhypusine synthase mechanism illustrating oxidation state of the NADH cofactor, the enzyme imine intermediate, and the role of the DHS catalytic lysine.

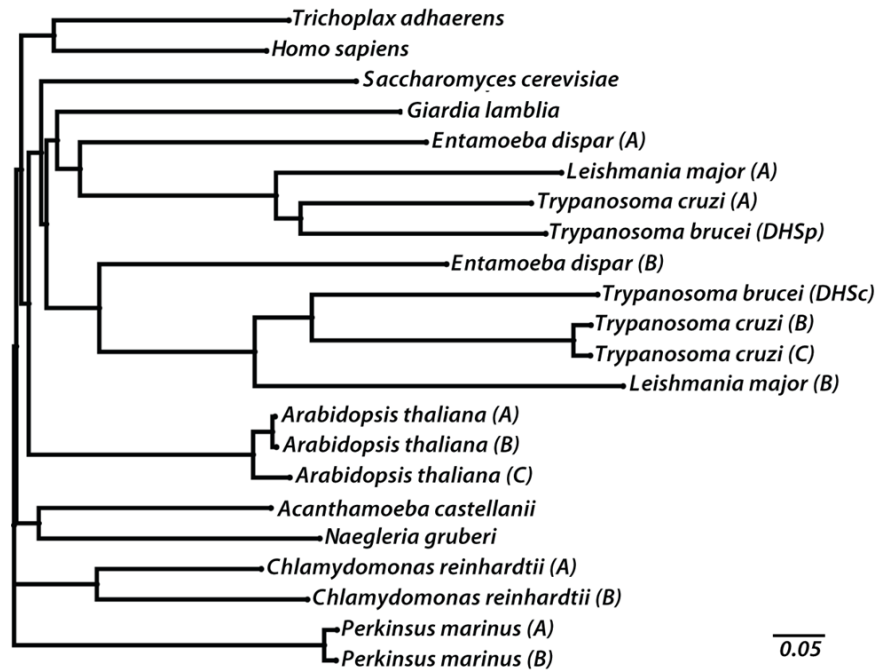


Figure 5.2. Phylogenetic analysis of DHS genes in trypanosomatids. Neighbor-Joining tree constructed with Mega5 for DHS from select eukaryotes representative of each of the major eukaryotic lineages: Opisthokonta (humans, *Trichoplax*, *Saccharomyces*), Excavata (trypanosomatids, *Giardia*, *Naegleria*), Amboezoa (*Entamoeba*, *Acanthamoeba*), Archaeplastida (*Arabidopsis* and *Chlamydomonas*) and Alveolata (*Perkinsus*). For organisms that contain more than one DHS homolog, duplicates are indicated using consecutive letters (A, B, C etc). Gene IDs are as follows: *Homo sapiens* (P49366), *Trichoplax adhaerens* (EDV28024.1), *Chlamydomonas reinhardtii* (A: EDP09680.1, B: EDP01029.1), *Acanthamoeba castellanii* (ELR12881.1), *Naegleria gruberi* (EFC43118.1), *Saccharomyces cerevisiae* (P38791), *Giardia lamblia* (EFO61259.1), *Arabidopsis thaliana* (A: AED90939.1, B: AAG53621.2, C: AED90940.1), *Perkinsus marinus* (A: EER15074.1, B: EER03596.1), *Trypanosoma brucei* (*TbDHSp*: Tb927.1.870, *TbDHSc*: Tb927.10.2750), *Trypanosoma cruzi* (A: Tc00.1047053511421.60, B: Tc00.1047053504119.29, C: Tc00.1047053506195.300), *Leishmania major* (A: LmjF.20.0250, B: LmjF.34.0330), and *Entamoeba dispar* (A: EDR24093.1, B: EDR21721.1).

<i>Homo sapiens</i>	NTAQEFDGSDSGARPDEAVSWGKIRVDAQPVKVYADASLVFP	278
<i>Trichoplax adhaerens</i>	NTANFDGSDSGARPDEAISWGKIKKTANPVKVYGEASILFP	265
<i>Chlamydomonas reinhardtii</i> (A)	NTAQEFDGSDSGARPDEAISWGKIRIDAKPVKVCGDATILFP	346
<i>Chlamydomonas reinhardtii</i> (B)	NTAQEFDGSDSGARPDEAISWGKIRVGAQPVKVYGDATVFFP	347
<i>Acanthamoeba castellanii</i>	NTGQEFDGSDSGARPDEAKSWGKIRYDASPVKMYADASMVFP	340
<i>Naegleria gruberi</i>	NTGQEFDGSDAGARCDEAVSWGKIRLGSRHTKIYAEASILFP	358
<i>Saccharomyces cerevisiae</i>	NTGQEYDGSDAGARPDEAVSWGKIKAEAKSVKLFADVTTVLP	369
<i>Giardia lamblia</i>	NTAQEYDGSDAGATCDEAVSWGKISPTARPVKLCADATLVFP	363
<i>Arabidopsis thaliana</i> (A)	NTGQEFDGSDSGARPDEAVSWGKIRGSAKTVKVCFLISSHPN	279
<i>Arabidopsis thaliana</i> (B)	NPGQEFDGSDSGARPDEAVSWGKIRGSAKTVKVYCDATIAFP	279
<i>Arabidopsis thaliana</i> (C)	NTGQEFDGSDSGARPDEAVSWGKIRGSAKTVKVCFLISSHPN	279
<i>Perkinsus marinus</i> (A)	NTAQEFDGCDSGARPDEAVSWGKIRIDAKPVKVYTEATLVLP	355
<i>Perkinsus marinus</i> (B)	NTAQEFDGCDSGARPDEAVSWGKIRIDAKPVKVYTEATLVLP	354
<i>Trypanosoma brucei</i> (TbDHSp)	TGSDADGCESSCNVMADRANGLLSPNCDDVVRVHGDAITIISP	322
<i>Trypanosoma cruzi</i> (A)	STGLEVDASPSSCNVAEDRANGVLLDNCEVVRVHGDASFVFP	327
<i>Leishmania major</i> (A)	TGLEADGCVSSGVLADDVACGLLREETETVRVQGDATVFFP	363
<i>Entamoeba dispar</i> (A)	STSIECDASDAGSEVAADRTKGFFKPECKPAKVIGDATILLP	321
<i>Trypanosoma brucei</i> (TbDHSc)	NNAQEFDGSDAGARPGEAVSWGKLRDLSTAVKVYSEVTIVFP	437
<i>Trypanosoma cruzi</i> (B)	NNGQEFDGSDSGARPDEAVSWGKIRLDGESVKVYAEVSLVFP	443
<i>Trypanosoma cruzi</i> (C)	NNGQEFDGSDSGARPDEAVSWGKIRLDGESVKVYAEVSLVFP	443
<i>Leishmania major</i> (B)	NNGQEFDGSDAGAKPEEALSWGKVRMEGAFVKVYGEVSTYLP	554
<i>Entamoeba dispar</i> (B)	NTAGDFDGSDASARPDEAVSWGKIKIESENVKVLAEASILVFP	314

Figure 5.3. Partial sequence alignment of DHS from select eukaryotes. A partial sequence alignment of DHS from human, yeast, and trypanosomatids. Highlighted in yellow are residues corresponding to the established catalytic lysine in human and yeast DHS. For organisms that contain more than one DHS homolog, duplicates are indicated using consecutive letters (A, B, C etc), except for those studied here (e.g. *T. brucei* DHSc and DHSp).

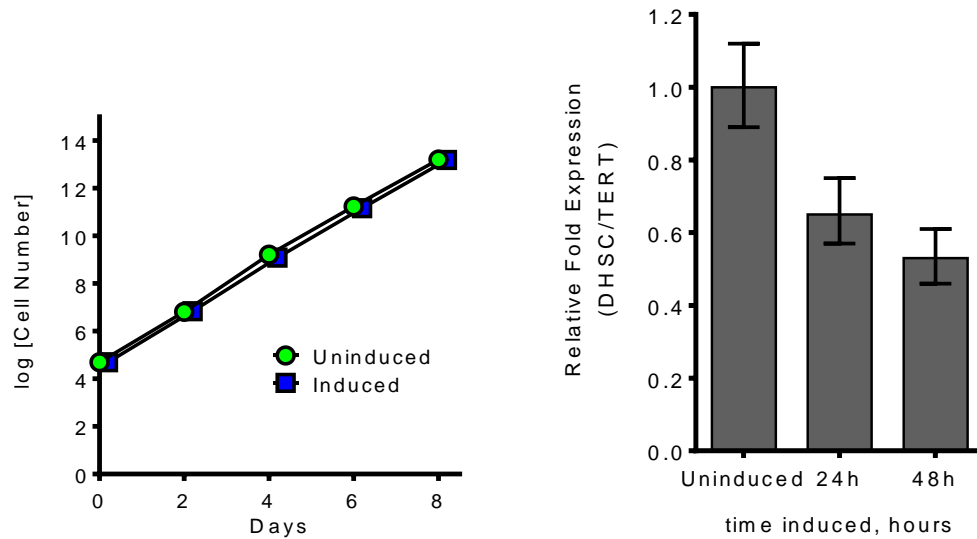


Figure 5.4. Knockdown of *DHSc* (Tb927.10.2750). (left) Growth curve of BSF *DHSc* RNAi cells with (blue) and without (green) Tet induction of gene knockdown, n=3. (right) qRT-PCR analysis of transcript levels for *DHSC* upon induction with Tet as normalized to expression in uninduced cells, n=3.

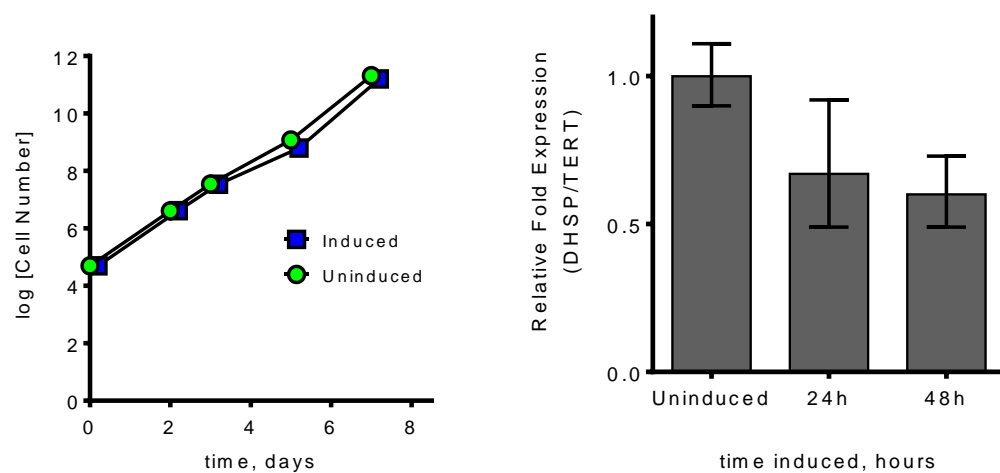


Figure 5.5. Knockdown of *DHSp* (Tb927.1.870). (left) Growth curve of BSF *DHSp* RNAi cells with (blue) and without (green) Tet induction of gene knockdown, n=3. (right) qRT-PCR analysis of transcript levels for *DHSp* upon induction with Tet as normalized to expression in uninduced cells; n=3.

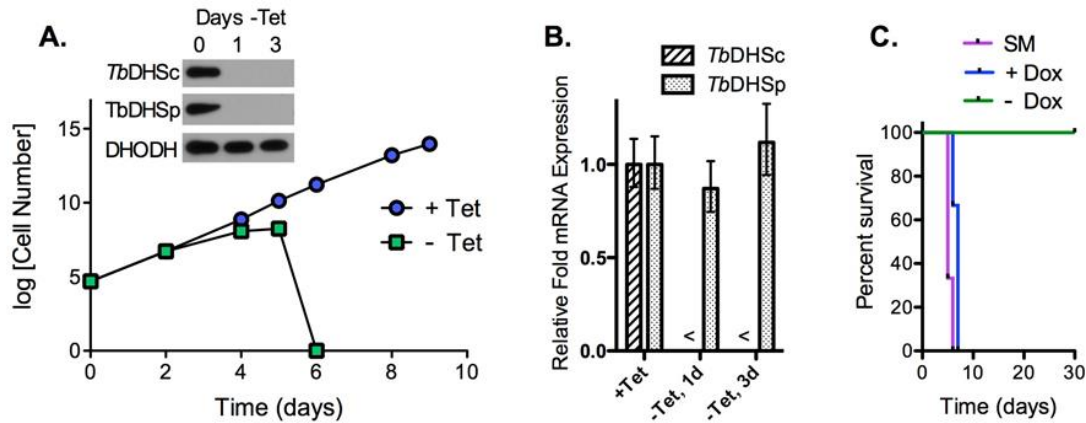


Figure 5.6. Effects of DHSc knockdown on *T. brucei* growth and survival. (A) Cell growth curve of log (cell number x dilution factor) over time. Data represent an average \pm S.E.M. for 6 independent biological replicates. Blue circle, + Tet (0.5 μ g/ml); green square, - Tet. Panel inset: representative western analysis performed with rabbit polyclonal antibodies to the indicated protein (30 μ g total protein); *TbDHODH* was detected as a loading control. (B) qPCR analysis of mRNA levels for *TbDHSc* cDKO cells. The symbol (<) indicates RNA levels were below the limit of detection. Error bars represent the standard deviation of the mean for n=3 replicates. (C) Kaplan-Meier Survival Curve of infected mice (n=3 per group); SM *T. brucei* wild-type cells (purple) and DHSc cDKO infected mice treated with (blue) or without (green) doxycycline (Dox).

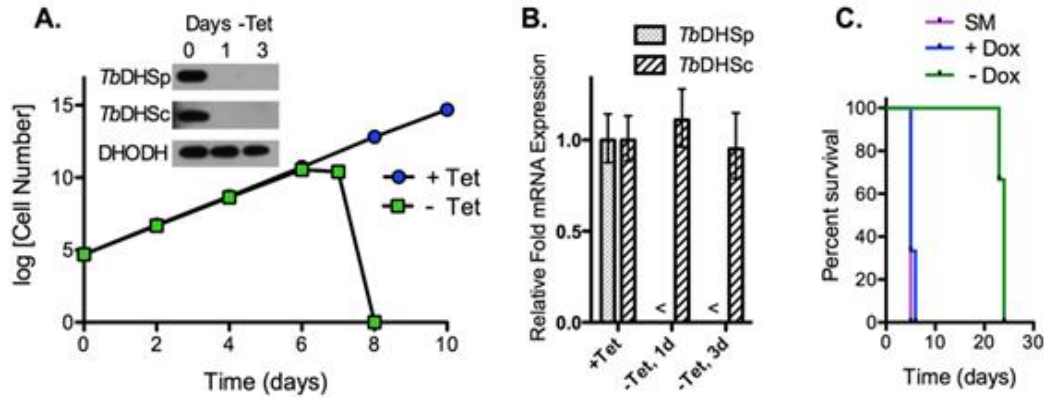


Figure 5.7. Effects of DHSp knockdown on *T. brucei* growth and survival. (A) Cell growth curve of log (cell number x dilution factor) over time. Data represent an average \pm the standard error of the mean for 3 independent biological replicates, blue circle, + Tet (0.5 μ g/ml); green square, - Tet. Panel inset: representative western analysis performed with rabbit polyclonal antibodies to the indicated protein (30 μ g total protein); *TbDHODH* was detected as a loading control. (B) qPCR analysis of mRNA levels for *TbDHSp* cDKO cells. The symbol (<) indicates RNA levels were below the limit of detection. Error bars represent the standard deviation of the mean for n=3 replicates. (C) Kaplan-Meier Survival Curve of infected mice (n=3 per group); SM *T. brucei* wild-type cells (purple) and DHSp cDKO infected mice treated with (blue) or without (green) doxycycline (Dox).

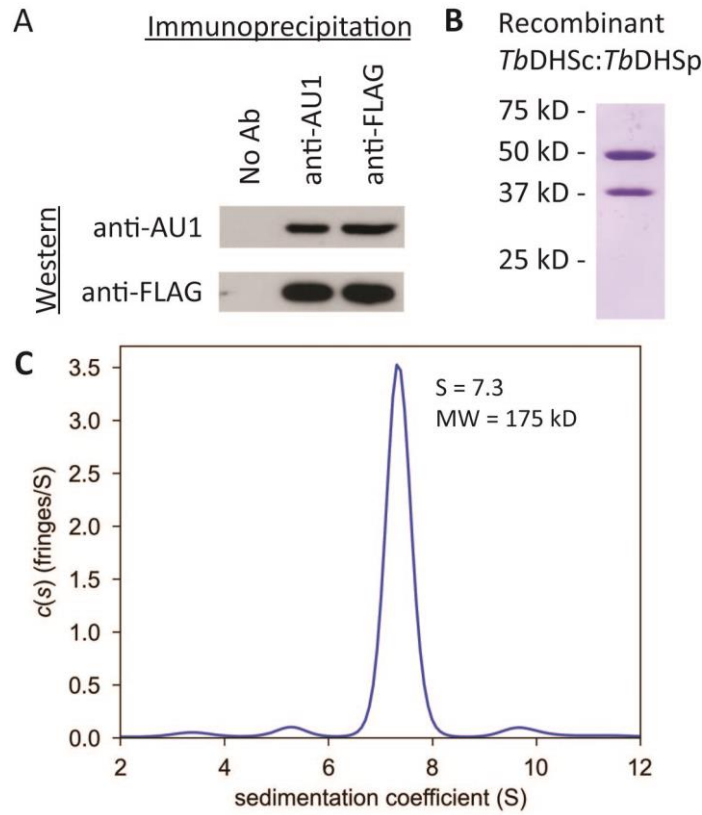


Figure 5.8. Biochemical characterization of *T. brucei* DHS. (A) Coimmunoprecipitation of AU1-*Tb*DHSc and FLAG-*Tb*DHSp from BSF *T. brucei*. Protein was immunoprecipitated with anti-AU1 or anti-FLAG antibody followed by western blot analysis. (B) SDS-PAGE analysis of *Tb*DHSc (50 kDa) and *Tb*DHSp (37 kDa) copurified by Ni^{+2} -affinity chromatography and gel filtration column chromatography. (C) Sedimentation velocity analysis of purified *Tb*DHSc:*Tb*DHSp complex. The observed $c(s)$, signal population is shown as a function of S .

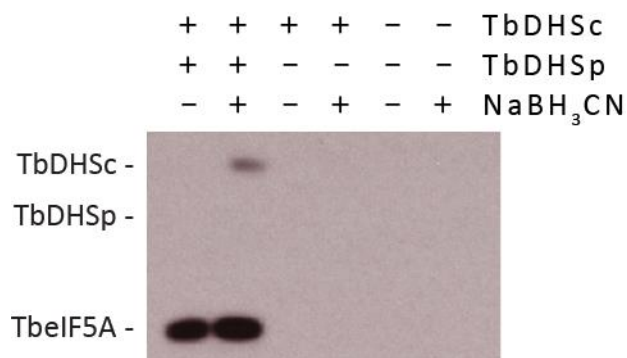


Figure 5.9. Detection of the enzyme-imine intermediate in the DHS reaction. NaBH₃CN trapping of DHS reaction intermediates for *Tb*DHSc:*Tb*DHSp (0.1 μ M) and TbeIF5A (10 μ M). Protein was separated by SDS-PAGE. ³H-spermidine labeled proteins were visualized by autoradiography.

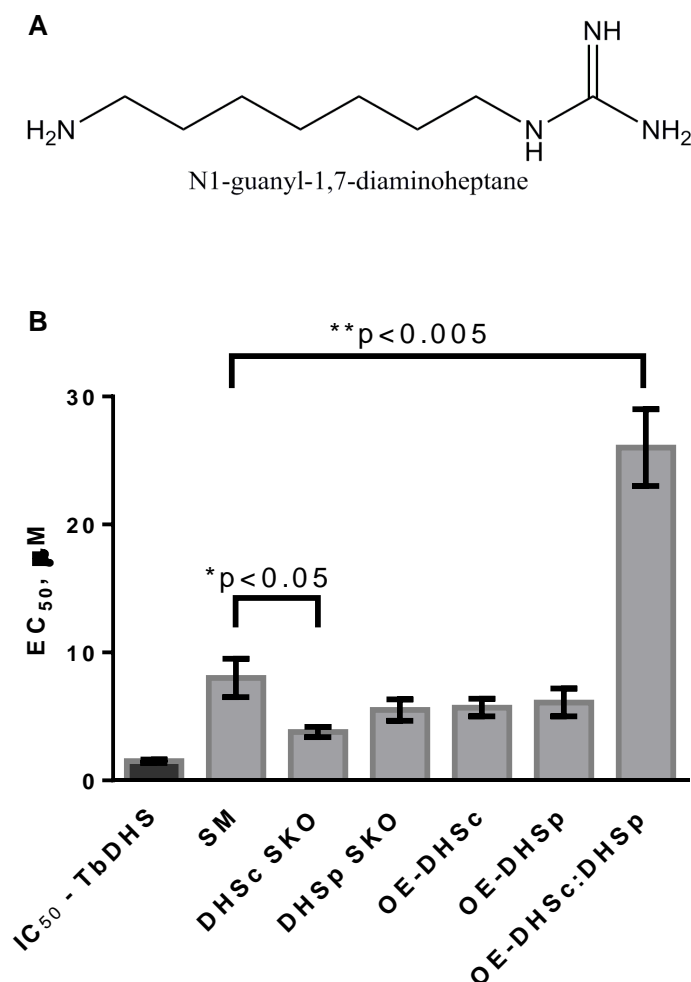


Figure 5.10. Inhibition of DHS and *T. brucei* growth by GC7. (A) Structure of GC7 (N1-guanyl-1,7-diaminoheptane), a spermidine analog. (B) Sensitivity of BSF mutants to GC7 plotted by EC₅₀ with the exception of “IC₅₀-TbDHS” which is the inhibition of recombinant enzyme; SM – single marker cell line, SKO – single knockout, OE – over expression; n = 3 and error bars represent standard deviation of the mean. P values were calculated using student t-test.

	Specific activity (s ⁻¹)	
Substrate	<i>Tb</i> eIF5A	<i>Hs</i> eIF5A
Enzyme		
<i>Hs</i> DHS	0.0029 ± 0.0001	0.016 ± 0.0003
<i>Tb</i> DHSc	1.8x10 ⁻⁶ ± 2x10 ⁻⁸	< 10 ⁻⁷
<i>Tb</i> DHSp	< 10 ⁻⁷	< 10 ⁻⁷
<i>Tb</i> DHSc: <i>Tb</i> DHSp	0.0057 ± 0.0001	0.0035 ± 0.0001

Table 5.1. Comparison of specific activity between DHS homotetramers and heterotetramers. Data were collected at fixed substrate concentrations (1 mM NAD⁺, 7.5 μM ³H-spermidine, and 10 μM eIF5A). Error represents the standard deviation of the mean for 6 replicates.

Substrate	K_m^{app} (μM)	k_{cat} s^{-1}
NAD^+	82 ± 16	0.018 ± 0.001
<i>TbeIF5A</i>	0.7 ± 0.1	0.018 ± 0.001
Spermidine	43 ± 5	0.015 ± 0.001

Table 5.2. Steady-State kinetic parameters for *T. brucei* heterotetrameric DHS.

Variable concentrations of the substrate under determination were used with fixed concentrations (1 mM NAD^+ , 100 μM *TbeIF5a* and 100 μM spermidine) of the other substrates. Error represents the standard deviation for 3 independent experiments.

CHAPTER SIX

Identification of potential prozymes

Introduction

It is critical for cells to regulate cellular processes and in turn, protein levels, which can be regulated in a number of ways including levels of transcription, mRNA stability, levels of translation, and protein turnover. Trypanosomatids do not regulate transcription using the classic RNA polymerase II (PolII) mechanisms seen in most other eukaryotic cells. Rather, PolII transcribes trypanosomatid genes as long polycistronic transcripts that can represent more than 100 genes. The transcripts then undergo *trans*-splicing to generate the individual mRNAs (68). Unlike in archaea and bacteria, however, the trypanosomatid operons do not appear to be clusters of functionally related genes (69). As such, post-transcriptional regulation becomes even more important in trypanosomatids.

Pseudoenzymes are poised to play a regulatory role in modulating enzyme activity. At first glance, these proteins contain conserved domains and or high sequence homology to known enzymes, but upon closer analysis, the proteins are unable to perform the predicted function thus earning the classification pseudoenzyme. Pseudoenzymes have several potential functions, one of which is exemplified by the regulation of mammalian ODC. The antizyme (AZ) protein is able to bind ODC and acts as a negative regulator, causing ODC to destabilize and be degraded (70). A pseudoenzyme, an inactive ODC paralog, is able to bind and inhibit AZ, earning the name antizyme inhibitor (71). We are particularly interested in prozymes, pseudoenzymes that bind to and activate their catalytically competent counterparts, and suspect that they play a regulatory role in trypanosomatids. Herein, with the

guidance of Lisa Kinch (Dept. of Biophysics, UT Southwestern), I have analyzed protein sequences to identify putative enzyme-pseudoenzyme pairs in *T. brucei*.

Homologous enzyme pairs

The discovery in our laboratory of two enzyme-prozyme pairs, AdoMetDC and DHS, served as the guide for identification of novel prozymes. Each prozyme shares 30-40% sequence identity with its catalytically competent counterpart, and BLASTp query against the *T. brucei* proteome yielded E-values less than 10^{-14} . The E-value is the number of hits that can be expected by chance within the search parameters and is an indicator of significance. We set up a search query wherein each *T. brucei* protein was BLAST against a condensed *Tbb* 927 database to find homology hits with E-values less than 0.001. The protein database was condensed so that identical multicopy genes were only counted once.

Our analysis yielded 535 protein pairs ranging from 18 to 99% identity (Figure 6.1). The 99% identity pairs typically represented multicopy proteins with 1 to 5 polymorphisms. 251 protein pairs included at least one product with an assigned putative function as determined by conserved domains and homology; the remainder were pairs of hypothetical proteins. Of these, 214 are putative enzyme pairs. The known enzyme-prozyme pairs, AdoMetDC and DHS, were both identified in our analysis.

Discussion

Pseudoenzymes that function as prozymes appear to be unique to protozoan parasites. Using bioinformatics, we were able to generate a list of 214 putative enzyme pairs from which we can begin searching for additional trypanosomatid prozymes. One of the reasons

for the seemingly high number of putative pairs is the inability to distinguish using homology between pseudoenzymes and functional isoforms. For example, 12 tRNA synthetase pairs were found, but it is known that for several of these, the mitochondrial enzyme and the cytosolic enzyme are separately encoded isoforms. Alternatively, multiple isoforms of an enzyme may exist and be differentially expressed under different conditions. The next step of analysis would be to examine the amino acid sequences of these pairs for other indicators of prozyme function such as functional multimerization, lack of catalytic residues, incomplete substrate binding domains, and evidence of co-expression. Even then, the putative pseudoenzymes may have a variety of effects on enzymatic activity. Eventually, biochemical validation will be required for definitive classification of a pseudoenzyme as a prozyme.

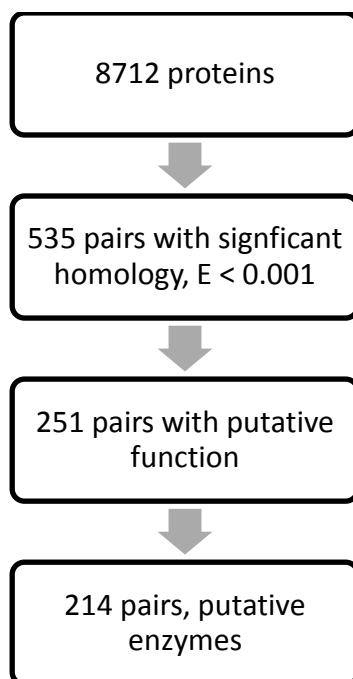


Figure 6.1. Identification of homologous enzyme pairs. The *T. brucei* proteome was queried using BLASTp to identify homologous proteins using an E-value cutoff of 0.001. The pairs were further pared based on putative functions.

CHAPTER SEVEN

Discussion and Future Direction

Translation is a complex fundamental process in all cells that requires the coordination of many RNAs and proteins. From the perspective of peptide bond formation, addition of proline to the nascent peptide carries unique challenges because of its unusual secondary amine and cyclic side chain structure. The synthesis rate of proline-rich peptides in minimal *in vitro* translation assays is slower than that measured in whole cell lysates (72). One of the key factors for overcoming ribosome stalling in translation of consecutive prolines is (deoxy)hypusinated-eIF5A in eukaryotes (32). The essentiality of DHS and eIF5A for cell proliferation has been demonstrated in several yeast and multicellular organisms (24,42,73). For my dissertation, I have studied the conservation these proteins and regulation of DHS in *T. brucei*.

T. brucei encodes a single eIF5A and two putative DHS proteins, designated DHSc and DHSp. Using radiolabelled putrescine, I indirectly showed that, at least, deoxyhypusination of eIF5A occurs in trypanosomes. In cultured BSF and PF trypanosomes, I showed that knockdown of *EIF5A* caused a growth defect and that complementation with human eIF5A was able to restore wildtype growth rates. The modified lysine of eIF5A is also required for its essential function in trypanosomes. Proteomic profiling for polyproline tracts revealed many candidate proteins, both trypanosome-specific and generally common, that may require hypusinated eIF5A for proper translation. Further evaluation of the translation of

these proteins with loss of eIF5A is needed to establish the role of eIF5A in endogenous translation.

In bloodstream-form trypanosomes, I demonstrated that both DHS paralogs are essential for cell viability by conditional gene knockouts. It is not surprising that the putative catalytically-competent DHS, DHSc, is required for parasite growth. Novel here was the discovery that DHSp, the catalytically dead paralog, is also essential for cell growth, stability of DHSc, and astonishingly, activation of DHSc activity by 3000-fold in a prozyme-like manner. Based on the size of the complex, I showed that DHSc-DHSp is a heterotetramer. While my own efforts to crystallize the complex have not been fruitful, continued work to crystallize *Tb*DHS heterotetramer and DHSc homotetramer would be very useful for determining the mechanism of this prozyme activation.

The functional significance of prozyme activation of DHS has been clearly demonstrated by our genetic studies. Based on its conservation of putative substrate binding residues, it is likely that *DHSp* arose from a gene duplication event and that both *DHSc* and *DHSp* coevolved into the modern day functional enzyme complex. We have not yet tested the activity of DHS from the related trypanosomatids *Leishmania* and *T. cruzi*; however, as was observed for AdoMetDC prozyme (AdoMetDCp) (74), the paradigm is also predicted to extend to DHS from these species. Unlike AdoMetDCp, which has only been found in trypanosomatids, a DHSp homolog was also identified by sequence homology in *Entamoeba* species. Phylogenic clustering of *Entamoeba* DHSp and DHSc with the trypanosomatid DHSp and DHSc, respectively, suggests that a gene duplication event occurred in a common

ancestor. Thus, the prozyme activation of DHS probably also extends to *Entamoeba*, which would be the first non-trypanosomatid example.

DHS and AdoMetDC are both involved in spermidine/hypusine biosynthesis. In the case of AdoMetDC, Willert et al. showed that under normal *in vitro* growth conditions AdoMetDCp levels were 5-8-fold lower than AdoMetDCc levels but in response to AdoMetDC inhibition or knockdown, AdoMetDCp protein levels increased substantially suggesting that spermidine biosynthesis could be controlled by regulation of prozyme translation (75). If DHSp levels are similarly regulated, the consequence of having two steps in the same pathway regulated by prozyme activation provides a potential dynamic range of up to 10^6 -fold (based on the combined potential enzyme activation of AdoMetDC and DHS) for regulation of the final step of hypusine modification. Trypanosomatids must also balance hypusine and trypanothione production since both require spermidine and DHSp could have a role in this regulation. In contrast, regulation of mammalian DHS has not been described and the mammalian pathway appears to be instead regulated by tissue-specific expression of two eIF5A isoforms (76).

Our discovery that trypanosomatid DHS is regulated by a prozyme mechanism adds to the list of unusual and novel mechanisms that cells have evolved to regulate polyamine metabolism. Polyamine metabolism is tightly regulated in mammals, plants and yeast (77-81). Regulation occurs through common mechanisms such as transcriptional control, but also through novel pathway specific mechanisms. In species other than trypanosomes, the intracellular turnover rate of ODC is controlled by expression of a protein inhibitor termed

antizyme that targets ODC for degradation by the proteasome. Antizyme expression is in turn initiated by translational frame-shifting of antizyme mRNA when spermidine levels are high (82), and is further regulated by antizyme inhibitor, which is itself an inactive paralog of ODC (83). AdoMetDC expression is controlled by a small ribosome stalling upstream open reading frame (uORFs) that is also sensitive to spermidine levels (84). Not only do trypanosomatids lack these mechanisms, they are uncommon in being unable to regulate RNA polymerase II transcription (85-87). The protein coding genes are intron-poor (88) and transcribed as large polycistronic clusters, which undergo 5' leader splicing (89). Regulation, instead, occurs during mRNA processing, mRNA degradation, translation, protein processing, and protein turnover (86). Furthermore, as a consequence of the mRNA trans-splicing reaction, 5'UTRs are short, and translational control by uORFs has not been observed. Thus the driving force to evolve a novel mechanism to regulate the polyamine pathway in trypanosomatids is likely to have been the paucity of other potential mechanisms. Given the large investment made by cells to control and regulate polyamine levels, and the number of novel mechanisms that have been uncovered it is clear that regulation of this pathway is a key cellular function on par with regulation of signaling pathways.

Disruption of polyamine biosynthesis is an attractive avenue for treatment of HAT. Eflornithine, one of the revolutionary drugs for treatment of late stage gambiense HAT, is a suicide inhibitor of ornithine decarboxylase. Inhibitors of the parasite AdoMetDC:AdoMetDCp complex are also being investigated as potential new drugs (90). We showed that both DHSc and the DHSp are essential for the growth of mammalian

bloodstream-form *T. brucei* and for infection of a mammalian host, and that GC7 a known inhibitor of DHS also leads to DHS-dependent cell death. These data genetically and chemically validate *T. brucei* DHS as a potential drug target. We predict that the structural differences due to the heteromeric nature of *TbDHS* compared to human DHS provide an opportunity for drug specificity against the parasite. More broadly, DHS inhibitors are being investigated as therapeutics for HIV infections (91) and different cancers (92) so it may be worthwhile to piggyback on these efforts to find compounds effective against parasite DHS.

Future work stemming from this thesis may proceed along several avenues. As previously discussed, the identification and development of DHS inhibitors as HAT therapeutics can be explored. One of the challenges to a high-throughput screen for DHS inhibitors is the lack of an easy spectrophotometric assay. Current activity assays rely on tracking of radiolabeled substrate or identification of derivatized hypusine by HPLC. To this end, RapidFire high-throughput mass spectrometry systems could be utilized. In the interest of drug development and further understanding of the prozyme regulation of DHS, a crystal structure of the trypanosome DHS heterotetramer and DHSc homodimer would also be useful. Going beyond DHS, the prozyme paradigm in trypanosomes also merits further exploration. Using bioinformatics, we have identified 214 pairs of homologous enzyme pairs, but much work remains to pare down the list to a manageable number of pseudoenzyme candidates and to characterize their functions biochemically.

In conclusion, the results of my thesis work have contributed to the understanding of hypusination and the extraordinary prozyme paradigm in *T. brucei*. I have shown by

generating genetic mutants in cultured *T. brucei* that eIF5A and two DHS paralogs are essential for cell viability. In biochemically characterizing the parasite DHS, I have also shown that the catalytically dead paralog DHSp increases the activity of DHSc by 3000-fold and is the second example of this prozyme style activation described in trypanosomes. This work, hopefully, lays the groundwork for more in-depth studies into the function of hypusination, the dynamic regulation of DHS, the development of small molecule DHS inhibitors as HAT therapeutics, and the discovery of other parasite prozymes.

APPENDICES

Appendix 1. Sequence alignment of Deoxyhypusine Synthase from representative eukaryotes. Full sequence alignment of DHS from *Homo sapiens* (P49366), *Trichoplax adhaerens* (EDV28024.1), *Chlamydomonas reinhardtii* (A: EDP09680.1, B: EDP01029.1), *Acanthamoeba castellanii* (ELR12881.1), *Naegleria gruberi* (EFC43118.1), *Saccharomyces cerevisiae* (P38791), *Giardia lamblia* (EFO61259.1), *Arabidopsis thaliana* (A: AED90939.1, B: AAG53621.2, C: AED90940.1), *Perkinsus marinus* (A: EER15074.1, B: EER03596.1), *Trypanosoma brucei* (TbDHS_p: Tb927.1.870, TbDHS_c: Tb927.10.2750), *Trypanosoma cruzi* (A: Tc00.1047053511421.60, B: Tc00.1047053504119.29, C: Tc00.1047053506195.300), *Leishmania major* (A: LmjF.20.0250, B: LmjF.34.0330), and *Entamoeba dispar* (A: EDR24093.1, B: EDR21721.1). In human DHS, K329 is the catalytic Lysine (highlighted in yellow) and H288 is a crucial proton acceptor/donor (highlighted in cyan). In red text are residues involved in NAD⁺ binding. Only residues that are conserved in these binding sites with the human enzyme are highlighted.

```

Homo sapiens          -----MEGSLEREAPAGALAAVLKHSSTLPPE--STQVRGYDF
Trichoplax adhaerens  -----MDNSTPSIAKEAVLVTSEAMPSD--AEAVKGYDF
S. cerevisiae         -----MSDINEKLPELLQDAVLKASVPIPDD--FVKVQGIDY
Giardia lamblia       -----MLVCVFIFKLLFFKGSQSMDEIQHASNNVIRASDTSCIGEKLEIHGLDL
Entamoeba dispar A    -----MSITGEEFAKVTSKVLGESKEYKGEPICIGYDF
Leishmania major A    MLASAPAPRPAKKDSAASRRKSASKSTGAAVKDDSSARVSASGAAESPEQSCQTQVHGVD
Trypanosoma cruzi A   -----METVDALDY
T. brucei (TbDHSp)    -----MSGVP----FPSRVIGDLDY
Entamoeba dispar A    -----MTTITKGYDF
T. brucei (TbDHSc)    -----MAELAKSAVLVSSCTDDLLGDAQVVGPN
Trypanosoma cruzi B   -----MAELAQKAVLIQSSDTNFQFHALGTVSGPA
Trypanosoma cruzi C   -----MAELAQKAVLIQSSDTNFQFHALGTVNGPA
Leishmania major B    -----MANIAESAVLVSSASSAQAVAKLTQVQGPT
Arabidopsis thaliana A -----MEDDRVFSVHSTVFKESESLEGG--CDKIEGYDF
Arabidopsis thaliana B -----MEDDRVFSVHSTVFKESESLEGG--CDKIEGYDF
Arabidopsis thaliana C -----MEDDRVFSVHSTVFKESESLEGG--CDKIEGYDF
Acanthamoeba castellanii -----MDAHG-----FVMVKAEPLEPG--TPIVQGYDF
Naegleria gruberi     -----MSQNTTGDIGQQAVFIKTDPIECGLLQKEVRGYDF
C. reinhardtii A      -----MAGCVDI PASQAVLVPTETIPDT---AVVRGYDF
C. reinhardtii B      -----MATTDNKQGREAVLCATDVVPST---PVVKGFDF
Perkinsus marinus A   -----MGADKSEEEESVASGQIPEIADDAVFLSSETV-DT---PVIQGYDF
Perkinsus marinus B   -----MGADKSEEE--SVASGQIPEIADDAVFLSSETV-DT---PVIQGYDF

```

```

Homo sapiens          NRG-----VNRYALLEAFGTTGFQATNFGRAVQQVNAMIEKKLEPLS-QDEDQHADLT
Trichoplax adhaerens  NNG-----INHHSLLQSFRTGFQATNFGLAIQEVNRMLELKAKPVS-EKDKNQLTLD
S. cerevisiae         SKPEATN---MRATDLIEAMKTMGFQASSVGTACEIIDSMRSWRGKHID--ELDDHEKKG
Giardia lamblia       NKPENQN---LDAILSNYARMGFSSTGFSKLCNEVNRMSWRLSDDP--YDPNRSYPE
Entamoeba dispar A    DNGVDFN-----KLMEKMKYTGFGALNLG----LCIEQVNEMR-----
Leishmania major A    QSLVHATQE-ETLRVAVSSLPPTTGLQATQIGRARQLVQQILHHR-----
Trypanosoma cruzi A   SELVALNQE-EALRRVLASYPRIGLQATELGRARRIVQRALYHK-----
T. brucei (TbDHSp)    SNLLNIGQE-EAIRCVLNAYPNIGLEATNLGRARRIVQRALNDNG-----
Entamoeba dispar A    DKG-----VNYEELVNSYVTGIIQSSNVGRAINI INKMLTWQPSEEE-----KKEY
T. brucei (TbDHSc)    QED-----LHSAEAVLNRYSTVGFQASNLARAFSICEMMLTPQSPSPSLMPTEGDQ---
Trypanosoma cruzi B   GDQ-----LQSIASLEHYAALGFQASHFSQAVAICKRMLQPQPPSVAVKQLTGSNDAN
Trypanosoma cruzi C   GDQ-----LQSIASLEHYAALGFQASHFSQAVAICKRMLQPQPPSAAVKQLTGSNDAN
Leishmania major B    SG-----FDKAQHIIIGSYSTMGFQATNYGLARSIAQRMIRKQPPSKVYQIKDGKYYLV
Arabidopsis thaliana A NQG-----VDYPKLMRSMLTGFGQASNLGAEIDVVNQMLDWRLADETTVAEDCSEEEK

```

Arabidopsis thaliana B NQG-----VDYPKLMRSM LTTG FQASNLGEAIDVVNQMLDWRLADETTVAEDCSEEEK
Arabidopsis thaliana C NQG-----VDYPKLMRSM LTTG FQASNLGEAIDVVNQMLDWRLADETTVAEDCSEEEK
Acanthamoeba castellanii N-----KGLDYEALMASL KTTG FQATSFGQAVDEVNRMLRWLSLNDEP-VTEKDDDEESR
Naegleria gruberi NNDLKDLNKPIDYNALLESYTTG FQAHNFGEAVNILNAMLRWRLSDEP-MMENEQEPYD
C. reinhardtii A NKG-----CDINGLMESML TTTG FQATTFGQAIAEVNRMINWRLSDEP-VGPATDPDHV
C. reinhardtii B ATSR-----PDLDNVMSML TTTG FQATSLGQAVNEVNR MIDWRLSDEP-VTADTPAEEA
Perkinsus marinus A NNG-----VDFNAMMDQMMYTGFQATNLGLAFKQIDAML DWSLNDEP-VADDEDEEFR
Perkinsus marinus B NNG-----VDFNAMMDQMMYTGFQATNLGLAFKQIDAML DWSLNDEP-VADDEDEEFR

Homo sapiens -----QS-RRPLTSCTIFLGYT **SNLIS**SGIRETIRYLVQH-----
Trichoplax adhaerens -----AAGSRPLSNCSIFLGYT **SNLIS**SGVRESIRYVVEH-----
S. cerevisiae -----CFDEEGYQKTTIFMGYT **SNLIS**SGVRETLRYLVQH-----
Giardia lamblia -----CPVARSKIRCKIFLGYT **SNLV**SSGLREYIRFLVQH-----
Entamoeba dispar A -----KSHAKIFLGMS **SNIV**SSGLREVIHYLVKN-----
Leishmania major A -----SPEDRVFLAYT **SNMIS**CGLRDTFTYLARE-----
Trypanosoma cruzi A -----RAGDAVFLAYT **SNLIS**SGLRDTFACLARD-----
T. brucei (TbDHSp) -----MDGNKVMLAYT **SNLIS**SGLRDTFACLARE-----
Entamoeba dispar A -----VEGDERLKRCTIYLGFT **SEM**MTSGLRDTFRYLVQH-----
T. brucei (TbDHSc) -----ASESPVMVQPTLFVGVTAN **LF**GTGCREAIRFLCTECVPLP---NGVEPATP
Trypanosoma cruzi B -----GKDASLTQVLVQPTIFLGATAN **LF**GTGCREAIRFLCKESVSLP---HGVLPAAAM
Trypanosoma cruzi C -----GKDASLTQVLVQPTIFLGATAN **LF**GTGCREAIRFLCKESVSLP---HGVLPAAAM
Leishmania major B PPDVGEDGRTLQQEHVYPNLFMGVSAN **LF**MGTGCREAVRFLVQEGVAHRSP EASAAASADG
Arabidopsis thaliana A -----NPSFRESVKCKIFLGYT **SNLV**SSGVRDTIRYLVQH-----
Arabidopsis thaliana B -----NPSFRESVKCKIFLGYT **SNLV**SSGVRDTIRYLVQH-----
Arabidopsis thaliana C -----NPSFRESVKCKIFLGYT **SNLV**SSGVRDTIRYLVQH-----
Acanthamoeba castellanii -----DPEYRKGVKCTIFLGYT **SNMIS**SGVREIRYLCQH-----
Naegleria gruberi -----DPEVRKNTKCKVFLGYT **SNMV**SSCGVREVIRFLVQH-----
C. reinhardtii A -----DPAFRANTRCMIFLGFT **SNLT**SAGVREHIRYLVQN-----
C. reinhardtii B -----DPEFRANARCIIFLGYT **SNFT**SAGTREQLRWLAQN-----
Perkinsus marinus A -----SEEARLDVRTKVWLSYT **SNII**SSGCRELIRYIAEH-----
Perkinsus marinus B -----SEEARLNVRTKVWLSYT **SNII**SSGCRELIRYIAEH-----

Homo sapiens -----NMVDVLVT **TAGG**VEEDLIKCLAPTY---
Trichoplax adhaerens -----NLVDCIVT **TAGG**IEEDFIKCLADTY---
S. cerevisiae -----KMVDAVVT **SAGG**VEEDLIKCLAPTY---
Giardia lamblia -----SLVDVIVAS **SAGG**VEEDIKCLAPTY---
Entamoeba dispar A -----KFVDAIVV **TAGG**IEEDFIKTMHPTL---
Leishmania major A -----RLVDCFISS **SAGG**IEEDVIKCGGSTL---
Trypanosoma cruzi A -----RLIDGFIS **TAGG**IEEDAICKLGKTL---
T. brucei (TbDHSp) -----NRIGAVVT **TAGG**VEEDVIKCLGDTL---
Entamoeba dispar A -----KCVDIYVT **TAG**AIETDIMKCFGNIN---
T. brucei (TbDHSc) LDDMAGIS-----CDGTGALKPS--PCDSRALIHVLVSSG **GAME**HDIRRACESYKLSR
Trypanosoma cruzi B PDEMSMPS-----CDIDDETIPLNPPFYSNALIHVLVSSG **GAME**HDIRRACEPYRITN
Trypanosoma cruzi C PDEMSMPS-----CDIDDETIPLNPPFYSNALIHVLVSSG **GAME**HDIRRACEPYRITN
Leishmania major B TDDQLMFARLKREYVETYGPPHPDEEV PRAHSFLCAIVVSSG **G**VEHDLRRACTAYTLHY
Arabidopsis thaliana A -----HMDVIVVT **TTGG**VEEDLIKCLAPTF---
Arabidopsis thaliana B -----HMDVIVVT **TTGG**VEEDLIKCLAPTF---
Arabidopsis thaliana C -----HMDVIVVT **TTGG**VEEDLIKCLAPTF---
Acanthamoeba castellanii -----KLVDVIVSS **SAGG**IEEDFIKCFAPTYC--
Naegleria gruberi -----KLVDIVVT **TCG**AIEEDIMKTMQPTY---
C. reinhardtii A -----RMVDVLVT **TAGG**IEEDFIKCMGHTY---
C. reinhardtii B -----RMVDVMVT **TAGG**IEEDFIKCMANTY---
Perkinsus marinus A -----HMAQVFIT **TAGG**IEEDFIKCLADFH---
Perkinsus marinus B -----HMAQVFIT **TAGG**IEEDFIKCLADFH---

Homo sapiens -----LGEFSLRGK-----ELRENGINRIGNLLVPNENYCKFE
Trichoplax adhaerens -----IGDFRLPGR-----QLRDKGINRIGNLLAPNDNYCKFE
S. cerevisiae -----LGEFALKGK-----SLRDQGMN RIGNLLVPNDNYCKFE
Giardia lamblia -----LGDWRADGA-----MLRKNSINRIGNLLVPNDNYCLFE
Entamoeba dispar A -----LGDYFYFKGK-----ELYPNGYNRIGNLLPNSNYCEFE
Leishmania major A -----LGQFGLDGR-----ALRRRGINRIGNLLVPNDNYCWFE
Trypanosoma cruzi A -----VGQFSLDGR-----ELRRCGVNR TGNLLVPNDNYCHFE

<i>T. brucei</i> (TbDHSp)	-----VGDFALNDH-----ALRNNGLNRVGNLLVPNDNYRNFE
<i>Entamoeba dispar</i> A	-----IGDFYMKPE-----EVQGE---RHGNMIIIPKEIIKTK
<i>T. brucei</i> (TbDHSc)	DGAEEEGEQFHHPV-----ERDRSRS-----KGTDC-H-FGNVRYNSSGVASRN
<i>Trypanosoma cruzi</i> B	YGG-FDGTFSHQ-----QRQESAT-----AGEDVARFGNISYGGSGTGTS
<i>Trypanosoma cruzi</i> C	YGS-FDGTFSHQ-----QRQESAT-----AGEDVARFGNISYGGSGTGTS
<i>Leishmania major</i> B	YASEAQGHVSSTISSEATAPLEGLQQAETPLGTGAAAGAAKPARFGNVEYPPQG-SPGS
<i>Arabidopsis thaliana</i> A	-----KGDFSLPGA-----YLRSKGLNRIGNLLVPNDNYCKFE
<i>Arabidopsis thaliana</i> B	-----KGDFSLPGA-----YLRSKGLNRIGNLLVPNDNYCKFE
<i>Arabidopsis thaliana</i> C	-----KGDFSLPGA-----YLRSKGLNRIGNLLVPNDNYCKFE
<i>Acanthamoeba castellanii</i>	-----VGDFSLDGC-----ALRLKGQNRIIGNLIIPNENYVKFE
<i>Naegleria gruberi</i>	-----LGAFDLDGK-----MLRLNGINRIGNLLIANQNYCKFE
<i>C. reinhardtii</i> A	-----LGDFQLKGS-----ELRMKGLNRIGNMVVPSNYCKFE
<i>C. reinhardtii</i> B	-----LGDFHLKGE-----ELRKQGLNRIGNMVIIPNANYCKFE
<i>Perkinsus marinus</i> A	-----LGDFALDGK-----TLRRRGLNRTGNLIVPNDNYCKFE
<i>Perkinsus marinus</i> B	-----LGDFALDGK-----TLRRRGLNRTGNLIVPNDNYCKFE

<i>Homo sapiens</i>	DWLMPILDQMVMEQNT-----EGVKWTPSKMIARLGKEINNP--
<i>Trichoplax adhaerens</i>	TWIMPILDQLVEEQNT-----HNINWTPSKIARLGKEINNC--
<i>S. cerevisiae</i>	EWIVPILDKMLEEQDEYVKKH----GADCLEANQDVDSPIWTPSKMIDRFGEINDE--
<i>Giardia lamblia</i>	DWIIPIFDECMEQQRK-----GYHWTPSRLIWKLGERINDE--
<i>Entamoeba dispar</i> A	DWMDPLLECLKQNE-----HGVHWTSPSKLVHKMGESINNE--
<i>Leishmania major</i> A	DFFTPVLESVQEAQRASR-----WKHTAPSEFIEAMGAAIAKNH-
<i>Trypanosoma cruzi</i> A	NFFMPVLKHLHELQRESR-----WETMTAPSEMAIAAIGALGCKH-
<i>T. brucei</i> (TbDHSp)	DDFVPLRLRLHEQQORDSR-----WTTKTTPSQIIAEIGAALSVR-
<i>Entamoeba dispar</i> A	QWLKEFILDIEQCQDT-----SMPFTPSQLITMMGERLNDT--
<i>T. brucei</i> (TbDHSc)	-LFSCVMRCLVKRLAEARKEKANREAAPIPEAYYDVCSWAITPSTLWYMAGLWMADIFT
<i>Trypanosoma cruzi</i> B	SIFTSVMRRLVSRLLQAAQKRRKDASTAKPIPAAHDDVCEWAFSPSTVWYMTGRWLPELFT
<i>Trypanosoma cruzi</i> C	SIFTSVMRRLVSRLLQAAQKRRKDASTAKPIPAVHGDDVCEWAFSPSTVWYMTGRWLPELFT
<i>Leishmania major</i> B	ALFDRLMRTFAQRLCARQARLRAAAMAKPIPKYDDVCSWSVTPSEVWALCGLWLVDMLA
<i>Arabidopsis thaliana</i> A	DWIIPIFDEMLKEQKE-----ENVLWTPSKLLARLGKEINNE--
<i>Arabidopsis thaliana</i> B	DWIIPIFDEMLKEQKE-----ENVLWTPSKLLARLGKEINNE--
<i>Arabidopsis thaliana</i> C	DWIIPIFDEMLKEQKE-----ENVLWTPSKLLARLGKEINNE--
<i>Acanthamoeba castellanii</i>	EWILPVLDMVLEQKE-----KGEIWSPSKMIISRFGEINNP--
<i>Naegleria gruberi</i>	DWITPVLDMLEEYQ-----KGKLWSPSLMIDRFGEKLNNE--
<i>C. reinhardtii</i> A	DWIIPIIDACLTEQNE-----QGVNWTSPSKLIDRLGKEIGHE--
<i>C. reinhardtii</i> B	DWMMPILDMLKEQNE-----QGVNWTSPSKIIARLGKEINDP--
<i>Perkinsus marinus</i> A	EWIEPIIDKMHDEQEQQ-----DGVWTPSTMIHRFGKEINDP--
<i>Perkinsus marinus</i> B	EWIEPIIDKMHDEQEQQ-----DGVWTPSTMIHRFGKEINDP--

<i>Homo sapiens</i>	-----ESVYY
<i>Trichoplax adhaerens</i>	-----NSVYY
<i>S. cerevisiae</i>	-----SSVLY
<i>Giardia lamblia</i>	-----RSIAY
<i>Entamoeba dispar</i> A	-----SSIYY
<i>Leishmania major</i> A	-----PDTCTSSLVY
<i>Trypanosoma cruzi</i> A	-----PETCSDSILY
<i>T. brucei</i> (TbDHSp)	-----PNDCGSSLIY
<i>Entamoeba dispar</i> A	-----TSVIT
<i>T. brucei</i> (TbDHSc)	EALQE-----TGEVTDEKVAS-----EEGLKRAKSTVLY
<i>Trypanosoma cruzi</i> B	EVLRE-----RSGGNMEAVA-----EEAQRRAESTVLY
<i>Trypanosoma cruzi</i> C	EVLRE-----RSGGNMEAVA-----DEAQRRAESTVLY
<i>Leishmania major</i> B	EALRAVQSCPSHLTSGSGVGTAESVTANGKGQEADRDHAIATSALYRAEALARARTTVVY
<i>Arabidopsis thaliana</i> A	-----SSYLY
<i>Arabidopsis thaliana</i> B	-----SSYLY
<i>Arabidopsis thaliana</i> C	-----SSYLY
<i>Acanthamoeba castellanii</i>	-----ESVYY
<i>Naegleria gruberi</i>	-----DSILY
<i>C. reinhardtii</i> A	-----DSIYY
<i>C. reinhardtii</i> B	-----SSIYY
<i>Perkinsus marinus</i> A	-----RSVYY
<i>Perkinsus marinus</i> B	-----RSVYY

Homo sapiens WAQKNHIPVFSALTDGSLGDMIFFHSHYKN-----
Trichoplax adhaerens WAYKNNIPVFSALTDGSLGDMIFFHSHYRN-----
S. cerevisiae WAHKNKIPIFCPSLTDGSLGDMIFFHSHYKAS-----
Giardia lamblia WAYRNKIPIFCPAITDGSIGDMIFFHSHYKN-----
Entamoeba dispar A WAAKNNIPVFSALTDGSLGDMIFFHSHYKN-----
Leishmania major A WCYRNGISVFSALTDGSMGDMIFFHSHYSH-----
Trypanosoma cruzi A WCYRNNIPVFSALTDGSLGDMIFFHSHYSK-----
T. brucei (TbDHS) WCYRNDIPVFSALTDGSMGDMIFFHSHYSR-----
Entamoeba dispar A WAAKNNITIFCPALTDGSLGDMIFFHSHYNEIN-----
T. brucei (TbDHS) WAAKNGVPIFSPSLTDGDMIFFHSHYNEIN-----
Trypanosoma cruzi B WASMNGVPIFSPSLTDGDMIFFHSHYNEIN-----
Trypanosoma cruzi C WASMNGVPIFSPSLTDGDMIFFHSHYNEIN-----
Leishmania major B WAAVQQVSLFSPSLTDGSLGDMIFFHSHYQYQ-----
Arabidopsis thaliana A WAYKNNIPVFCPLTDGSLGDMIFFHSHYFRT-----
Arabidopsis thaliana B WAYKNNIPVFCPLTDGSLGDMIFFHSHYFRT-----
Arabidopsis thaliana C WAYKNNIPVFCPLTDGSLGDMIFFHSHYFRT-----
Acanthamoeba castellanii WCWKNDIPVFCPLTDGSLGDMIFFHSHYQYQ-----
Naegleria gruberi WAHKNKIPIFCPSLTDGSLGDMIFFHSHYSYDK-----
C. reinhardtii A WAHKNKIPIFCPSLTDGSLGDMIFFHSHYSYKS-----
C. reinhardtii B WAYKNNIPVFSALTDGSLGDMIFFHSHYKKN-----
Perkinsus marinus A WCYKNNIPVFCPSLTDGSLGDMIFFHSHYSYKR-----
Perkinsus marinus B WCYKNNIPVFCPSLTDGSLGDMIFFHSHYSYKR-----

Homo sapiens -----PGLVLDIVEDLRLINTQAIFA-----KCTGMII
Trichoplax adhaerens -----PGLRIDIVEDIRRMNSQAVFA-----LNTGMLI
S. cerevisiae -----P-KQLRVDIVGDIRKINSMSMAA-----YRAGMII
Giardia lamblia -----PGLIIDVVGDIRAMNMQAVNS-----PKNGCII
Entamoeba dispar A EGLVLDLVQDVLIKIDEMAFNA-----EKVGCIL
Leishmania major A KGLVVDPLVDVRLRLKLAKE-----KGRNLAIV
Trypanosoma cruzi A KGLVLDPIVDVRLRLGCRNRRCDDSQGGNRSQNNNGRTTCIV
T. brucei (TbDHS) KGLVVDPIVDVRLRLGCRNRRCDDSQGGNRSQNNNGRTTCIV
Entamoeba dispar A PVRLVVDLVQDLRLVNSSTIHS-----VETGVII
T. brucei (TbDHS) GDTGVPLQLDLVADIHRLNRLAMRS-----RRTGMMI
Trypanosoma cruzi B EDLTTAKLKLVDVYIRLNLKAMRS-----QRSGMII
Trypanosoma cruzi C EDLTTAKLKLVDVYIRLNLKAMRS-----QRSGMII
Leishmania major B SSPTAATAVEDEPPVVERLQIDLVVDVYIRLNLKAMRS-----KKTGMII
Arabidopsis thaliana A SGLIIDVVDQDIRAMNGEAVHAN-----PKKTGMII
Arabidopsis thaliana B SGLIIDVVDQDIRAMNGEAVHAN-----PKKTGMII
Arabidopsis thaliana C SGLIIDVVDQDIRAMNGEAVHAN-----PKKTGMII
Acanthamoeba castellanii EGLIVDIAQDIRGINNKAVYA-----KKSGMII
Naegleria gruberi KGDGLVCDIVSDIRRLNGQAVRA-----KKTGMVI
C. reinhardtii A PGLRVDVVEDIRINDIAMRAT-----PRKTGMII
C. reinhardtii B PGLRVDIAEDVARMDIVLSAG-----PRKTAMLL
Perkinsus marinus A PGFIIDIAADIRKVNDES VKA-----RHTGVIV
Perkinsus marinus B PGFIVDIAADIRKVNDES VKA-----RHTGVIV

Homo sapiens LGGGVVKKHHIANANLMRNG-ADYAVYINTAQEFDGSDSGARPDEAVSWGKIRVDAQPVKV
Trichoplax adhaerens LGGGLVKKHHICNANLMRNG-ADFSVFVNTANEFDGSDSGARPDEAISWGKIKKTANPVKV
S. cerevisiae LGGGLIKHHIANACLMRNG-ADYAVYINTGQEFYDGSDAGARPDEAVSWGKIKAEAKSVKL
Giardia lamblia LGGGTIKHHILNANLFGADGADFVYINTAQEFYDGSDAGATCDEAVSWGKISPTARPVKL
Entamoeba dispar A VGAGIAKHHILNAMKRRRG-CDYACMLSTSIECDASDAGSEVAADRKTGFFKPECKPAKV
Leishmania major A LGGGLPKHHLLRNVS-----MDAVVMVTGLEADGCVSSGVLADDDVACGLLREETETVRV
Trypanosoma cruzi A LGGGLPKHHLLQNVN-----ADTVVYVSTGLEVDASPSNCNVAEDRANGVLLDNCEVVRV
T. brucei (TbDHS) LGAGLPKHHLLRNQV-----ADAVVYVSTGSDADGCESSCNVMADRANGVLLDNCEVVRV
Entamoeba dispar A LGGGVVKKHHIMNANLMRNG-ADFAVYINTAGDFDGSDASARPDEAVSWGKIKIESENVKV
T. brucei (TbDHS) LGGGVVKKHHVCNANLMRNG-ADYAVFLNNAQEFYDGSDAGARPGEAVSWGKLRLDSTAVKV
Trypanosoma cruzi B LGGGVVKKHHVCNANLMRNG-ADGAVFINNGQEFYDGSDSGARPDEAVSWGKIRLDGESVKV
Trypanosoma cruzi C LGGGVVKKHHVCNANLMRNG-ADGAVFINNGQEFYDGSDSGARPDEAVSWGKIRLDGESVKV
Leishmania major B CGGGVVKKHHVCNANLMRNG-ADFTIILNNGQEFYDGSDAGAKPEEALSWGKVRMEGAFVKV
Arabidopsis thaliana A LGGGLPKHHICNANMMRNG-ADYAVFINTGQEFYDGSDSGARPDEAVSWGKIRGSAKTVKV
Arabidopsis thaliana B LGGGLPKHHICNANMMRNG-ADYAVFINPGQEFYDGSDSGARPDEAVSWGKIRGSAKTVKV
Arabidopsis thaliana C LGGGLPKHHICNANMMRNG-ADYAVFINTGQEFYDGSDSGARPDEAVSWGKIRGSAKTVKV
Acanthamoeba castellanii LGGGLIKHHICNANLMRNG-ADYTVFINTGQEFYDGSDSGARPDEAKSWGKIRYDASPVKM

<i>Naegleria gruberi</i>	LGGGVKHHICNANLMRNG-ADFTVYINTGQEFDGSDAGARCDEAVSWGKIRLGSRHTKI
<i>C. reinhardtii</i> A	LGGGVPKHHICNANLMRNG-ADFAVYVNTAQEFDGSDSGARPDEAISWGKIRIDAKPVKV
<i>C. reinhardtii</i> B	LGGGVPKHHICNANLMRNG-ADFAVYLNTAQEFDGSDSGARPDEAISWGKIRVGAQPVKV
<i>Perkinsus marinus</i> A	IGGGVVKHHAMNANLMRNG-ADHVYVINTAQEFDGCDSGARPDEAVSWGKIRIDAKPVKV
<i>Perkinsus marinus</i> B	IGGGVVKHHAMNANLMRNG-ADHVYVINTAQEFDGCDSGARPDEAVSWGKIRIDAKPVKV
<i>Homo sapiens</i>	YADASLVFPLLVAETFAQKMDAFMHEKNED-----
<i>Trichoplax adhaerens</i>	YGEASILFPLMVAETTFAPVVEKMTADHDNKR-----
<i>S. cerevisiae</i>	FADVTTVLPLIVAATFASGKPIKKVKN-----
<i>Giardia lamblia</i>	CADATLVFPLLLHETILKKYKEDPEYWDSKKGGDPHECYWTQMESEVRESKRS----
<i>Entamoeba dispar</i> A	IGDATILLPLIVASTFAKKEETTK-----
<i>Leishmania major</i> A	QGDATVVFFPLMLI-AEKAATLEGAAA-----
<i>Trypanosoma cruzi</i> A	HGDASFVFPLLCKAETSADTHKDVA-----
<i>T. brucei</i> (TbDHSp)	HGDATIIISPLLLRSSDGKEKVGREDGN-----
<i>Entamoeba dispar</i> A	LAEASLVFPLIVSKTFVTKRFDGKI-----
<i>T. brucei</i> (TbDHSc)	YSEVTIVFPLIVVHVFAWVRMMR--SKGKENIRS-----
<i>Trypanosoma cruzi</i> B	YAEVSLVFPLLVAQVFLPFLRAARGVSLAESEFL-----
<i>Trypanosoma cruzi</i> C	YAEVSLVFPLLVAQVFLPFVRAARGVSLAKESEFL-----
<i>Leishmania major</i> B	YGEVSTYLLVADVFPVAVRQRRATDDAQPRRRQSSRGARLPQDVSGHSHLCRGE-
<i>Arabidopsis thaliana</i> A	YCDATIAFPLLVAETTFATKRDQTCEST-----
<i>Arabidopsis thaliana</i> B	YCDATIAFPLLVAETTFATKRDQTCEST-----
<i>Arabidopsis thaliana</i> C	CFLISSHPNLYLTQWF-----
<i>Acanthamoeba castellanii</i>	YADASMVFPLLVAETFVKHQLKKTKEQQQQEEGAKAQ-----
<i>Naegleria gruberi</i>	YAEASLIFPLLVAQTFVKYQ----REQEEKKLKEQQQ-----
<i>C. reinhardtii</i> A	CGDATILFPLLVSQTFVRHWP--VEPLPEKKAEQE-----
<i>C. reinhardtii</i> B	YGDATVFFPLLVSQTFVAKHFKPKGAGAPQRRPESPNTPKVSGSGPTSAGI-----
<i>Perkinsus marinus</i> A	YTEATLVPLIIGKCFAPRVASGEWERTRGDGTIRIVYNKSYTPSEHDKERRKLMVN
<i>Perkinsus marinus</i> B	YTEATLVPLIIGKCFAPRVASGEWERTRGDGTIRIVYNKSYTPSEHDKERRKLMVN

Appendix 2. Cloning primers. Restriction sites shown in **bold** and where appropriate, nucleotide number is indicated relative to A₁TG.

	FORWARD	REVERSE
Recombinant Expression		
pE-SUMO- <i>TbDHSc</i>	CCGGTCTCAAGGTATGGCTGAGTTGGC	CCTCTAGATCACGAGCGGATATTCTCC
pE-SUMO- <i>TbDHSp</i>	CCGGTCTCAAGGTATGTCAGGTGTACCTTTTCC	CCTCTAGATCAGTTCCCATCCTCCCTCA
pT7- <i>TbDHSp</i>	GGAAGCTTATGTCAGGTGTACC	GGGTACCCTAGTTCCCATCCT
pE-SUMO- <i>TbeIF5A</i>	CCGGTCTCAAGGTATGTCAGCATGAGGGA CAG	CCTCTAGATCATTATCGCTCAGCTGCAT TC
pE-SUMO- <i>HsDHS</i>	CCGGTCTCGAGGTATGGAAGGC	CCTCTAGATTAGTCTTCATTCTTTTC
pE-SUMO- <i>HseIF5A</i>	CCGGTCTCGAGGTATGGCTGACGACC	CCTCTAGATTACTTAGCCATTGCTTTG
Coimmunoprecipitation		
pLew100-AU1- <i>TbDHSc</i>	GGAAGCTTATGGACACGTACCGCTACATTAT GGCTGAGTTGGC	GGGGATCCTCACGAGCGGATATTCTCC
pLew300-FLAG- <i>TbDHSp</i>	GGAAGCTTATGGACTACAAAGACGATGACGA CAAGATGTCAGGTGTACCTTTTCC	GGGGATCCCTAGTTCCCATCCTCCCTCA
<i>In vitro</i> Regulatable Expression		
pLew100v5- <i>TbDHSc</i>	GGAAGCTTATGGCTGAGTTGGCCAAG	GGGGATCCTCACGAGCGGATATTCTCC
pLew100v5- <i>TbDHSp</i>	GGAAGCTTATGTCAGGTGTACC	GGGGATCCCTAGTTCCCATCCTCCCTCA
<i>In vitro</i> Allelic Replacement (nt number relative to ATG)		
HYG ^R	ATGAAAAGCCTGAACCTACC	CTATTCCTTTGCCCTCGG
BSD ^R	ATGGCCAAGCCTTTGTCTC	TTAGCCCTCCACACATAAC
<i>TbDHSc</i> 5' Flank + HYG ^R	(-374) GGCGGTGATATCGCATAAAT	GGTGAGTTCAGGCTTTTTTCAT (4) CCTT ATTCTCCACTTCACACG
<i>TbDHSc</i> 5' Flank + BSD ^R	(-374) GGCGGTGATATCGCATAAAT	AGACAAAGGCTTGGCCAT (4) CCTTATT CTCCACTTCACACG
<i>TbDHSc</i> 3' Flank + HYG ^R	CCGAGGGCAAAGGAATAG (1387) TTTGTTA CAACACCTGTATGAGCAT	(1771) TCGTGAGATCGGTGTAAAGG
<i>TbDHSc</i> 3' Flank + BSD ^R	GTTATGTGTGGGAGGGCTAA (1387) TTTGT TACAACACCTGTATGAGCAT	(1771) TCGTGAGATCGGTGTAAAGG
<i>TbDHSc</i> Nesting	(-3060) TTTCCCCCTCAAAGCACTA	(1750) GGCTTACACACCATTTTGCTT
<i>TbDHSp</i> 5' Flank + HYG ^R	(-437) GGTGCAGCTGCTCATTTACA	GGTGAGTTCAGGCTTTTTTCAT (-55) ACCTCAAAGAACGGATGCAG
<i>TbDHSp</i> 5' Flank + BSD ^R	(-437) GGTGCAGCTGCTCATTTACA	AGACAAAGGCTTGGCCAT (-55) ACCTCAAAGAACGGATGCAG
<i>TbDHSp</i> 3' Flank + HYG ^R	CCGAGGGCAAAGGAATAG (1030) AGTCATG TGCGGTTCTGTT	(1528) CTCAGCCCCAACATGATTT
<i>TbDHSp</i> 3' Flank + BSD ^R	GTTATGTGTGGGAGGGCTAA (1030) AGTCA TGTGCGGTTCTGTT	(1528) CTCAGCCCCAACATGATTT
<i>In vivo</i> Allelic Replacement (nt number relative to ATG)		
<i>TbDHSc</i> 5' flank	ACAGTGCGGCCCGC (-116) ACTCAGGTTGGAGTTGTCG	TGGACGGTTTAAACCTAAGCGAAGCTTC AGTGGTGTGCGGGTTC (372)
<i>TbDHSc</i> 3' flank	CGCTTAGGTTTAAACCGTCCAGGATCC (139 0) GTTACAACACCTGTATGAGC	AGTAAGCGGCCGCGTTACAAGAGGTATA TAGAGC (1888)
<i>TbDHSp</i> 5' flank	ACACGCGGCCCGC	TGGACGGTTTAAACCTAAGCGAAGCTTC

	(-508) AGAGGGATAAAGCGGATAGG	AACCGCACGACAGCAACT (-19)
<i>TbDHSp</i> 3' flank	CGCTTAGGTTTAAACCGTCCAGGATCC (1022) GCTTTGAATGTGGGTCTTAAC	ACACGCGGCCGCAGAACACTATCGCCTTCAGC (1527)
<i>In vivo</i> Regulatable Expression		
pLew100-TbDHSc	GCATCA AAGCTT CATATGGCTGAGTTGGCCA AGAG	GGTCAAGGATCCTCACGAGCGGATATTC TCC
pLew100-TbDHSp	GCATCA AAGCTT CATATGTCAGGTGTACCTT TTCC	TGCATAGGATCCCCTAGTTCCCATCCTC CC
Knockout Confirmation		
<i>TbDHSc</i> UTR/BSDR ^R	(-374) GGCGGTGATATCGCATAAAT	TTAGCCCTCCACACATAAC
<i>TbDHSc</i> UTR/HYGR ^R	(-374) GGCGGTGATATCGCATAAAT	CTATTCCTTTGCCCTCGG
<i>TbDHSc</i> UTR/DHS_C	(-374) GGCGGTGATATCGCATAAAT	GAGATTGGGGTGTGAGCATC (189)
<i>TbDHSc</i> Ectopic	TCAATTACACCAAAAAGTAAAATTCA	GAGATTGGGGTGTGAGCATC (189)
<i>TbDHSp</i> UTR/BSDR ^R	(-437) GGTGCAGCTGCTCATTTACA	TTAGCCCTCCACACATAAC
<i>TbDHSp</i> UTR/HYGR ^R	(-437) GGTGCAGCTGCTCATTTACA	CTATTCCTTTGCCCTCGG
<i>TbDHSp</i> UTR/DHS_R	(-437) GGTGCAGCTGCTCATTTACA	GCGTGATCATTGAGAGCAA (352)
<i>TbDHSp</i> Ectopic	TCAATTACACCAAAAAGTAAAATTCA	GCGTGATCATTGAGAGCAA (352)
<i>TbDHSp</i> Nesting	(-376) CCGCTTTTCCTGTGTTTGT	(1440) GAATCGGCTTCGCTTACAAC

BIBLIOGRAPHY

1. Njiokou, F., Nimpaye, H., Simo, G., Njitchouang, G. R., Asonganyi, T., Cuny, G., and Herder, S. (2010) Domestic animals as potential reservoir hosts of *Trypanosoma brucei gambiense* in sleeping sickness foci in Cameroon. *Parasite* **17**, 61-66
2. Simarro, P. P., Diarra, A., Ruiz Postigo, J. A., Franco, J. R., and Jannin, J. G. (2011) The human African trypanosomiasis control and surveillance programme of the World Health Organization 2000-2009: the way forward. *PLoS Negl Trop Dis* **5**, e1007
3. Sternberg, J. M., and Maclean, L. (2010) A spectrum of disease in human African trypanosomiasis: the host and parasite genetics of virulence. *Parasitology* **137**, 2007-2015
4. Picozzi, K., Fevre, E. M., Odiit, M., Carrington, M., Eisler, M. C., Maudlin, I., and Welburn, S. C. (2005) Sleeping sickness in Uganda: a thin line between two fatal diseases. *Bmj* **331**, 1238-1241
5. Wardrop, N. A., Atkinson, P. M., Gething, P. W., Fevre, E. M., Picozzi, K., Kakembo, A. S., and Welburn, S. C. (2010) Bayesian geostatistical analysis and prediction of Rhodesian human African trypanosomiasis. *PLoS Negl Trop Dis* **4**, e914
6. Wardrop, N. A., Fevre, E. M., Atkinson, P. M., Kakembo, A., and Welburn, S. C. (2012) An exploratory GIS-based method to identify and characterise landscapes with an elevated epidemiological risk of Rhodesian human African trypanosomiasis. *BMC infectious diseases* **12**, 316
7. Brun, R., Blum, J., Chappuis, F., and Burri, C. (2010) Human African trypanosomiasis. *Lancet* **375**, 148-159
8. Simarro, P. P., Franco, J., Diarra, A., Postigo, J. A., and Jannin, J. (2012) Update on field use of the available drugs for the chemotherapy of human African trypanosomiasis. *Parasitology* **139**, 842-846
9. Priotto, G., Kasparian, S., Mutombo, W., Ngouama, D., Ghorashian, S., Arnold, U., Ghabri, S., Baudin, E., Buard, V., Kazadi-Kyanza, S., Ilunga, M., Mutangala, W., Pohlig, G., Schmid, C., Karunakara, U., Torreele, E., and Kande, V. (2009) Nifurtimox-eflornithine combination therapy for second-stage African *Trypanosoma brucei gambiense* trypanosomiasis: a multicentre, randomised, phase III, non-inferiority trial. *Lancet* **374**, 56-64
10. Cross, G. A., and Manning, J. C. (1973) Cultivation of *Trypanosoma brucei* spp. in semi-defined and defined media. *Parasitology* **67**, 315-331
11. Hesse, F., Selzer, P. M., Muhlstadt, K., and Duszenko, M. (1995) A novel cultivation technique for long-term maintenance of bloodstream form trypanosomes in vitro. *Mol Biochem Parasitol* **70**, 157-166
12. Berriman, M., Ghedin, E., Hertz-Fowler, C., Blandin, G., Renauld, H., Bartholomeu, D. C., Lennard, N. J., Caler, E., Hamlin, N. E., Haas, B., Bohme, U., Hannick, L., Aslett, M. A., Shallom, J., Marcello, L., Hou, L., Wickstead, B., Alsmark, U. C., Arrowsmith, C., Atkin, R. J., Barron, A. J., Bringaud, F., Brooks, K., Carrington, M.,

- Cherevach, I., Chillingworth, T. J., Churcher, C., Clark, L. N., Corton, C. H., Cronin, A., Davies, R. M., Doggett, J., Djikeng, A., Feldblyum, T., Field, M. C., Fraser, A., Goodhead, I., Hance, Z., Harper, D., Harris, B. R., Hauser, H., Hostetler, J., Ivens, A., Jagels, K., Johnson, D., Johnson, J., Jones, K., Kerhornou, A. X., Koo, H., Larke, N., Landfear, S., Larkin, C., Leech, V., Line, A., Lord, A., Macleod, A., Mooney, P. J., Moule, S., Martin, D. M., Morgan, G. W., Mungall, K., Norbertczak, H., Ormond, D., Pai, G., Peacock, C. S., Peterson, J., Quail, M. A., Rabinowitsch, E., Rajandream, M. A., Reitter, C., Salzberg, S. L., Sanders, M., Schobel, S., Sharp, S., Simmonds, M., Simpson, A. J., Tallon, L., Turner, C. M., Tait, A., Tivey, A. R., Van Aken, S., Walker, D., Wanless, D., Wang, S., White, B., White, O., Whitehead, S., Woodward, J., Wortman, J., Adams, M. D., Embley, T. M., Gull, K., Ullu, E., Barry, J. D., Fairlamb, A. H., Opperdoes, F., Barrell, B. G., Donelson, J. E., Hall, N., Fraser, C. M., Melville, S. E., and El-Sayed, N. M. (2005) The genome of the African trypanosome *Trypanosoma brucei*. *Science* **309**, 416-422
13. Ngo, H., Tschudi, C., Gull, K., and Ullu, E. (1998) Double-stranded RNA induces mRNA degradation in *Trypanosoma brucei*. *Proceedings of the National Academy of Sciences of the United States of America* **95**, 14687-14692
 14. Kalidas, S., Li, Q., and Phillips, M. A. (2011) A Gateway(R) compatible vector for gene silencing in bloodstream form *Trypanosoma brucei*. *Mol Biochem Parasitol* **178**, 51-55
 15. Shi, H., Djikeng, A., Mark, T., Wirtz, E., Tschudi, C., and Ullu, E. (2000) Genetic interference in *Trypanosoma brucei* by heritable and inducible double-stranded RNA. *Rna* **6**, 1069-1076
 16. Kim, H. S., Li, Z., Boothroyd, C., and Cross, G. A. (2013) Strategies to construct null and conditional null *Trypanosoma brucei* mutants using Cre-recombinase and loxP. *Mol Biochem Parasitol* **191**, 16-19
 17. Merritt, C., and Stuart, K. (2013) Identification of essential and non-essential protein kinases by a fusion PCR method for efficient production of transgenic *Trypanosoma brucei*. *Mol Biochem Parasitol* **190**, 44-49
 18. Matthews, H. R. (1993) Polyamines, chromatin structure and transcription. *BioEssays : news and reviews in molecular, cellular and developmental biology* **15**, 561-566
 19. Schuber, F. (1989) Influence of polyamines on membrane functions. *The Biochemical journal* **260**, 1-10
 20. Wallace, H. M. (2003) Polyamines and their role in human disease--an introduction. *Biochemical Society transactions* **31**, 354-355
 21. Chawla, B., Jhingran, A., Singh, S., Tyagi, N., Park, M. H., Srinivasan, N., Roberts, S. C., and Madhubala, R. (2010) Identification and characterization of a novel deoxyhypusine synthase in *Leishmania donovani*. *J Biol Chem* **285**, 453-463
 22. Bartig, D., Lemkemeier, K., Frank, J., Lottspeich, F., and Klink, F. (1992) The archaebacterial hypusine-containing protein. Structural features suggest common ancestry with eukaryotic translation initiation factor 5A. *Eur J Biochem* **204**, 751-758

23. Bailly, M., and de Crecy-Lagard, V. (2010) Predicting the pathway involved in post-translational modification of elongation factor P in a subset of bacterial species. *Biology direct* **5**, 3
24. Nishimura, K., Lee, S. B., Park, J. H., and Park, M. H. (2012) Essential role of eIF5A-1 and deoxyhypusine synthase in mouse embryonic development. *Amino acids* **42**, 703-710
25. Schnier, J., Schwelberger, H. G., Smit-McBride, Z., Kang, H. A., and Hershey, J. W. (1991) Translation initiation factor 5A and its hypusine modification are essential for cell viability in the yeast *Saccharomyces cerevisiae*. *Molecular and cellular biology* **11**, 3105-3114
26. Chattopadhyay, M. K., Park, M. H., and Tabor, H. (2008) Hypusine modification for growth is the major function of spermidine in *Saccharomyces cerevisiae* polyamine auxotrophs grown in limiting spermidine. *Proceedings of the National Academy of Sciences of the United States of America* **105**, 6554-6559
27. Saini, P., Eyler, D. E., Green, R., and Dever, T. E. (2009) Hypusine-containing protein eIF5A promotes translation elongation. *Nature* **459**, 118-121
28. Li, C. H., Ohn, T., Ivanov, P., Tisdale, S., and Anderson, P. (2010) eIF5A promotes translation elongation, polysome disassembly and stress granule assembly. *PLoS One* **5**, e9942
29. Gregio, A. P., Cano, V. P., Avaca, J. S., Valentini, S. R., and Zanelli, C. F. (2009) eIF5A has a function in the elongation step of translation in yeast. *Biochem Biophys Res Commun* **380**, 785-790
30. Henderson, A., and Hershey, J. W. (2011) The role of eIF5A in protein synthesis. *Cell cycle* **10**, 3617-3618
31. Doerfel, L. K., Wohlgemuth, I., Kothe, C., Peske, F., Urlaub, H., and Rodnina, M. V. (2013) EF-P is essential for rapid synthesis of proteins containing consecutive proline residues. *Science* **339**, 85-88
32. Gutierrez, E., Shin, B. S., Woolstenhulme, C. J., Kim, J. R., Saini, P., Buskirk, A. R., and Dever, T. E. (2013) eIF5A promotes translation of polyproline motifs. *Molecular cell* **51**, 35-45
33. Rossi, D., Kuroshu, R., Zanelli, C. F., and Valentini, S. R. (2014) eIF5A and EF-P: two unique translation factors are now traveling the same road. *Wiley interdisciplinary reviews. RNA* **5**, 209-222
34. Hirumi, H., and Hirumi, K. (1994) Axenic culture of African trypanosome bloodstream forms. *Parasitol Today* **10**, 80-84
35. Wirtz, E., Leal, S., Ochatt, C., and Cross, G. A. (1999) A tightly regulated inducible expression system for conditional gene knock-outs and dominant-negative genetics in *Trypanosoma brucei*. *Mol Biochem Parasitol* **99**, 89-101
36. Brun, R., and Schonenberger, M. (1979) Cultivation and in vitro cloning of procyclic culture forms of *Trypanosoma brucei* in a semi-defined medium. *Acta Trop* **36**, 289-292

37. Burkard, G., Fragoso, C. M., and Roditi, I. (2007) Highly efficient stable transformation of bloodstream forms of *Trypanosoma brucei*. *Mol Biochem Parasitol* **153**, 220-223
38. Redmond, S., Vadivelu, J., and Field, M. C. (2003) RNAit: an automated web-based tool for the selection of RNAi targets in *Trypanosoma brucei*. *Mol Biochem Parasitol* **128**, 115-118
39. Kuo, D., Nie, M., and Courey, A. J. (2014) SUMO as a Solubility Tag and In Vivo Cleavage of SUMO Fusion Proteins with Ulp1. *Methods in molecular biology* **1177**, 71-80
40. Park, M. H. (2006) The post-translational synthesis of a polyamine-derived amino acid, hypusine, in the eukaryotic translation initiation factor 5A (eIF5A). *Journal of biochemistry* **139**, 161-169
41. Sugimoto, A. (2004) High-throughput RNAi in *Caenorhabditis elegans*: genome-wide screens and functional genomics. *Differentiation; research in biological diversity* **72**, 81-91
42. Patel, P. H., Costa-Mattioli, M., Schulze, K. L., and Bellen, H. J. (2009) The *Drosophila* deoxyhypusine hydroxylase homologue nero and its target eIF5A are required for cell growth and the regulation of autophagy. *The Journal of cell biology* **185**, 1181-1194
43. Costa-Neto, C. M., Parreiras, E. S. L. T., Ruller, R., Oliveira, E. B., Miranda, A., Oliveira, L., and Ward, R. J. (2006) Molecular modeling of the human eukaryotic translation initiation factor 5A (eIF5A) based on spectroscopic and computational analyses. *Biochem Biophys Res Commun* **347**, 634-640
44. Dias, C. A., Cano, V. S., Rangel, S. M., Apponi, L. H., Frigieri, M. C., Muniz, J. R., Garcia, W., Park, M. H., Garratt, R. C., Zanelli, C. F., and Valentini, S. R. (2008) Structural modeling and mutational analysis of yeast eukaryotic translation initiation factor 5A reveal new critical residues and reinforce its involvement in protein synthesis. *The FEBS journal* **275**, 1874-1888
45. Chung, J., Rocha, A. A., Tonelli, R. R., Castilho, B. A., and Schenkman, S. (2013) Eukaryotic initiation factor 5A dephosphorylation is required for translational arrest in stationary phase cells. *The Biochemical journal* **451**, 257-267
46. Phillips, M. A., and Wang, C. C. (1987) A *Trypanosoma brucei* mutant resistant to alpha-difluoromethylornithine. *Mol Biochem Parasitol* **22**, 9-17
47. Pratt, C., Nguyen, S., and Phillips, M. A. (2014) Genetic validation of *Trypanosoma brucei* glutathione synthetase as an essential enzyme. *Eukaryot Cell*
48. Maier, B., Ogihara, T., Trace, A. P., Tersey, S. A., Robbins, R. D., Chakrabarti, S. K., Nunemaker, C. S., Stull, N. D., Taylor, C. A., Thompson, J. E., Dondero, R. S., Lewis, E. C., Dinarello, C. A., Nadler, J. L., and Mirmira, R. G. (2010) The unique hypusine modification of eIF5A promotes islet beta cell inflammation and dysfunction in mice. *The Journal of clinical investigation* **120**, 2156-2170

49. Schomburg, L., Kollmus, H., Friedrichsen, S., and Bauer, K. (2000) Molecular characterization of a puromycin-insensitive leucyl-specific aminopeptidase, PILS-AP. *Eur J Biochem* **267**, 3198-3207
50. Park, M. H., Nishimura, K., Zanelli, C. F., and Valentini, S. R. (2010) Functional significance of eIF5A and its hypusine modification in eukaryotes. *Amino acids* **38**, 491-500
51. Chawla, B., Kumar, R. R., Tyagi, N., Subramanian, G., Srinivasan, N., Park, M. H., and Madhubala, R. (2012) A unique modification of the eukaryotic initiation factor 5A shows the presence of the complete hypusine pathway in *Leishmania donovani*. *PloS one* **7**, e33138
52. Chatterjee, I., Gross, S. R., Kinzy, T. G., and Chen, K. Y. (2006) Rapid depletion of mutant eukaryotic initiation factor 5A at restrictive temperature reveals connections to actin cytoskeleton and cell cycle progression. *Molecular genetics and genomics : MGG* **275**, 264-276
53. Mirey, G., Soulard, A., Orange, C., Friant, S., and Winsor, B. (2005) SH3 domain-containing proteins and the actin cytoskeleton in yeast. *Biochemical Society transactions* **33**, 1247-1249
54. Hall, J. P., Wang, H., and Barry, J. D. (2013) Mosaic VSGs and the scale of *Trypanosoma brucei* antigenic variation. *PLoS pathogens* **9**, e1003502
55. Santos, C. C., Coombs, G. H., Lima, A. P., and Mottram, J. C. (2007) Role of the *Trypanosoma brucei* natural cysteine peptidase inhibitor ICP in differentiation and virulence. *Molecular microbiology* **66**, 991-1002
56. Wolff, E. C., Wolff, J., and Park, M. H. (2000) Deoxyhypusine synthase generates and uses bound NADH in a transient hydride transfer mechanism. *J Biol Chem* **275**, 9170-9177
57. Umland, T. C., Wolff, E. C., Park, M. H., and Davies, D. R. (2004) A new crystal structure of deoxyhypusine synthase reveals the configuration of the active enzyme and of an enzyme.NAD.inhibitor ternary complex. *J Biol Chem* **279**, 28697-28705
58. Wolff, E. C., Lee, S. B., and Park, M. H. (2011) Assay of deoxyhypusine synthase activity. *Methods in molecular biology* **720**, 195-205
59. Sommer, M. N., Bevec, D., Klebl, B., Flicke, B., Holscher, K., Freudenreich, T., Hauber, I., Hauber, J., and Mett, H. (2004) Screening assay for the identification of deoxyhypusine synthase inhibitors. *J Biomol Screen* **9**, 434-438
60. Sasaki, K., Abid, M. R., and Miyazaki, M. (1996) Deoxyhypusine synthase gene is essential for cell viability in the yeast *Saccharomyces cerevisiae*. *FEBS Lett* **384**, 151-154
61. Joe, Y. A., Wolff, E. C., and Park, M. H. (1995) Cloning and expression of human deoxyhypusine synthase cDNA. Structure-function studies with the recombinant enzyme and mutant proteins. *J Biol Chem* **270**, 22386-22392
62. Lee, Y. B., Park, M. H., and Folk, J. E. (1995) Diamine and triamine analogs and derivatives as inhibitors of deoxyhypusine synthase: synthesis and biological activity. *J Med Chem* **38**, 3053-3061

63. Pils, B., and Schultz, J. (2004) Inactive enzyme-homologues find new function in regulatory processes. *J Mol Biol* **340**, 399-404
64. Adrain, C., and Freeman, M. (2012) New lives for old: evolution of pseudoenzyme function illustrated by iRhoms. *Nat Rev Mol Cell Biol* **13**, 489-498
65. Zeqiraj, E., and van Aalten, D. M. (2010) Pseudokinases-remnants of evolution or key allosteric regulators? *Curr Opin Struct Biol* **20**, 772-781
66. Force, A., Lynch, M., Pickett, F. B., Amores, A., Yan, Y. L., and Postlethwait, J. (1999) Preservation of duplicate genes by complementary, degenerative mutations. *Genetics* **151**, 1531-1545
67. Fairlamb, A. H., Blackburn, P., Chait, B. T., and Cerami, A. (1985) Trypanothione: A novel Bis(glutathionyl)spermidine cofactor for glutathione reductase in trypanosomatids. *Science (New York, N.Y)* **227**, 1485-1487
68. De Gaudenzi, J. G., Noe, G., Campo, V. A., Frasc, A. C., and Cassola, A. (2011) Gene expression regulation in trypanosomatids. *Essays in biochemistry* **51**, 31-46
69. Pi, H., Lee, L. W., and Lo, S. J. (2009) New insights into polycistronic transcripts in eukaryotes. *Chang Gung medical journal* **32**, 494-498
70. Heller, J. S., and Canellakis, E. S. (1981) Cellular control of ornithine decarboxylase activity by its antizyme. *Journal of cellular physiology* **107**, 209-217
71. Murakami, Y., Ichiba, T., Matsufuji, S., and Hayashi, S. (1996) Cloning of antizyme inhibitor, a highly homologous protein to ornithine decarboxylase. *J Biol Chem* **271**, 3340-3342
72. Pavlov, M. Y., Watts, R. E., Tan, Z., Cornish, V. W., Ehrenberg, M., and Forster, A. C. (2009) Slow peptide bond formation by proline and other N-alkylamino acids in translation. *Proceedings of the National Academy of Sciences of the United States of America* **106**, 50-54
73. Park, M. H., Joe, Y. A., and Kang, K. R. (1998) Deoxyhypusine synthase activity is essential for cell viability in the yeast *Saccharomyces cerevisiae*. *J Biol Chem* **273**, 1677-1683
74. Willert, E. K., and Phillips, M. A. (2009) Cross-species activation of trypanosome S-adenosylmethionine decarboxylase by the regulatory subunit prozyme. *Mol Biochem Parasitol* **168**, 1-6
75. Willert, E. K., and Phillips, M. A. (2008) Regulated expression of an essential allosteric activator of polyamine biosynthesis in African trypanosomes. *PLoS Pathog* **4**, e1000183
76. Caraglia, M., Park, M. H., Wolff, E. C., Marra, M., and Abbruzzese, A. (2011) eIF5A isoforms and cancer: two brothers for two functions? *Amino Acids*. 10.1007/s00726-011-1182-x
77. Pegg, A. E., and Casero, R. A., Jr. (2011) Current status of the polyamine research field. *Methods Mol Biol* **720**, 3-35
78. Nowotarski, S. L., Origanti, S., and Shantz, L. M. (2011) Posttranscriptional regulation of ornithine decarboxylase. *Methods in molecular biology* **720**, 279-292
79. Persson, L. (2009) Polyamine homeostasis. *Essays in biochemistry* **46**, 11-24

80. Pegg, A. E. (2009) Mammalian polyamine metabolism and function. *IUBMB life* **61**, 880-894
81. Casero, R. A., and Pegg, A. E. (2009) Polyamine catabolism and disease. *The Biochemical journal* **421**, 323-338
82. Kahana, C. (2009) Regulation of cellular polyamine levels and cellular proliferation by antizyme and antizyme inhibitor. *Essays in biochemistry* **46**, 47-61
83. Ivanov, I. P., Firth, A. E., and Atkins, J. F. (2010) Recurrent emergence of catalytically inactive ornithine decarboxylase homologous forms that likely have regulatory function. *J Mol Evol* **70**, 289-302
84. Ivanov, I. P., Atkins, J. F., and Michael, A. J. (2010) A profusion of upstream open reading frame mechanisms in polyamine-responsive translational regulation. *Nucleic acids research* **38**, 353-359
85. Kramer, S. (2012) Developmental regulation of gene expression in the absence of transcriptional control: the case of kinetoplastids. *Molecular and biochemical parasitology* **181**, 61-72
86. Clayton, C., and Shapira, M. (2007) Post-transcriptional regulation of gene expression in trypanosomes and leishmanias. *Mol Biochem Parasitol* **156**, 93-101
87. Gunzl, A. (2010) The pre-mRNA splicing machinery of trypanosomes: complex or simplified? *Eukaryotic cell* **9**, 1159-1170
88. El-Sayed, N. M., Myler, P. J., Blandin, G., Berriman, M., Crabtree, J., Aggarwal, G., Caler, E., Renauld, H., Worthey, E. A., Hertz-Fowler, C., Ghedin, E., Peacock, C., Bartholomeu, D. C., Haas, B. J., Tran, A. N., Wortman, J. R., Alsmark, U. C., Angiuoli, S., Anupama, A., Badger, J., Bringaud, F., Cadag, E., Carlton, J. M., Cerqueira, G. C., Creasy, T., Delcher, A. L., Djikeng, A., Embley, T. M., Hauser, C., Ivens, A. C., Kummerfeld, S. K., Pereira-Leal, J. B., Nilsson, D., Peterson, J., Salzberg, S. L., Shallom, J., Silva, J. C., Sundaram, J., Westenberger, S., White, O., Melville, S. E., Donelson, J. E., Andersson, B., Stuart, K. D., and Hall, N. (2005) Comparative genomics of trypanosomatid parasitic protozoa. *Science (New York, N.Y)* **309**, 404-409
89. Monnerat, S., Martinez-Calvillo, S., Worthey, E., Myler, P. J., Stuart, K. D., and Fasel, N. (2004) Genomic organization and gene expression in a chromosomal region of *Leishmania major*. *Mol Biochem Parasitol* **134**, 233-243
90. Barker, R. H., Jr., Liu, H., Hirth, B., Celatka, C. A., Fitzpatrick, R., Xiang, Y., Willert, E. K., Phillips, M. A., Kaiser, M., Bacchi, C. J., Rodriguez, A., Yarlett, N., Klinger, J. D., and Sybertz, E. (2009) Novel S-adenosylmethionine decarboxylase inhibitors for the treatment of human African trypanosomiasis. *Antimicrobial agents and chemotherapy* **53**, 2052-2058
91. Hauber, I., Bevec, D., Heukeshoven, J., Kratzer, F., Horn, F., Choidas, A., Harrer, T., and Hauber, J. (2005) Identification of cellular deoxyhypusine synthase as a novel target for antiretroviral therapy. *The Journal of clinical investigation* **115**, 76-85
92. Shi, X. P., Yin, K. C., Ahern, J., Davis, L. J., Stern, A. M., and Waxman, L. (1996) Effects of N1-guanyl-1,7-diaminoheptane, an inhibitor of deoxyhypusine synthase, on

the growth of tumorigenic cell lines in culture. *Biochimica et biophysica acta* **1310**, 119-126